Modelos en Nanomagnetismo

1821

Ampère's Electrodynamic Molecular Model

Contemp. Phys. 4, 113–123
(1962)

by L. PEARCE WILLIAMS
Department of History, Cornell University

Ampere, en una carta a Roux-Bordier, 21/02/1821.

You are quite right in saying that it is inconceivable that for twenty years no one tried the action of the voltaic pile upon a magnet. I believe, however, that one can assign a cause for this; it was Coulomb's hypothesis on the nature of magnetic action. People believed this hypothesis was a fact and discarded any idea of an action between electricity and the so-called magnetic wires. . . . Everyone had already decided that [interaction] was impossible.(3)

1905

J. Phys. Theor. Appl., 1905, 4 (1), pp.678-693

SUR LA THÉORIE DU MAGNÉTISME;

Par M. P. LANGEVIN.

$$\mathrm{M} = f\left(\frac{\mathrm{H}}{\mathrm{T}}\right), \quad \mathrm{M} = k\,\frac{\mathrm{H}}{\mathrm{T}};$$

$$\frac{\mathrm{MH}}{r\mathrm{T}} = a, \qquad \mathrm{I} = \mathrm{MN}\left(\frac{\mathrm{C}ha}{\mathrm{S}ha} - \frac{1}{a}\right).$$

J. Phys. Rad., 1907, 6 (1), pp.661-690

L'HYPOTHÈSE DU CHAMP MOLÉCULAIRE ET LA PROPRIÉTÉ FERROMAGNÉTIQUE;

Par M. Pierre WEISS (1).

$$\frac{I}{I_0} = \frac{cha}{sha} - \frac{1}{a}, \qquad a = \frac{\mu H}{rT}.$$

$H_m = NI$

$a = \mu H_m / rT$ → $I = a\,\frac{rT}{\mu N}$. → $I/I_0 = a\,rT/\mu N I_0$

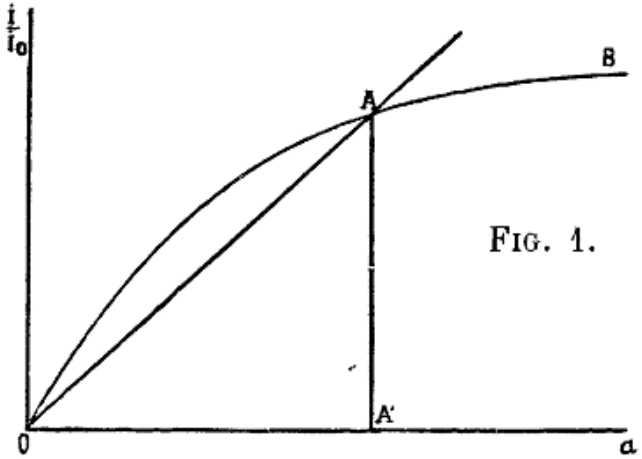

Fig. 1.

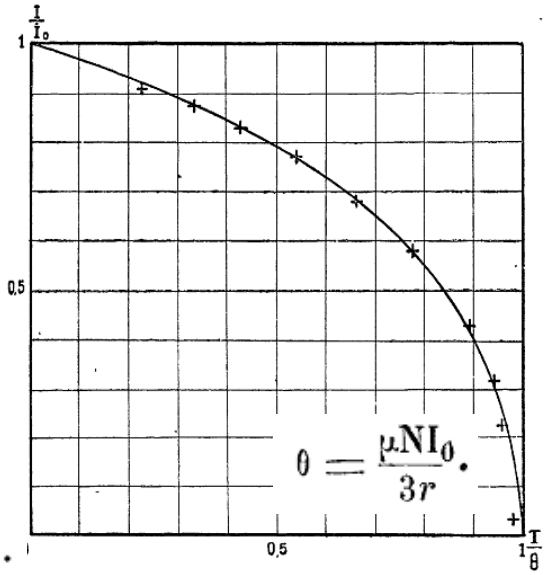

$NI = 80\,000\,000$ gauss.

1928

Zur Theorie des Ferromagnetismus.

Von **W. Heisenberg** in Leipzig.

Mit 1 Abbildung. (Eingegangen am 20. Mai 1928.)
Z. Phys. 49, 619–636

$$J_0 = \frac{1}{2}\int \psi_k^{\varkappa}\,\psi_k^{\lambda}\,\psi_l^{\varkappa}\,\psi_l^{\lambda}\left(\frac{2\,e^2}{r_{kl}} + \frac{2\,e^2}{r_{\varkappa\lambda}} - \frac{e^2}{r_{\varkappa k}} - \frac{e^2}{r_{\varkappa l}} - \frac{e^2}{r_{\lambda k}} - \frac{e^2}{r_{\lambda l}}\right) d\tau_k\, d\tau_l \quad (1)$$

$\varkappa$ und λ waren die Indizes der Atomkerne, k und l die der Elektronen.

$$\Theta = \frac{2\,J_0}{k\left(1 - \sqrt{1 - \frac{8}{z}}\right)}. \qquad J_0 \sim 10^{-13}\ \text{erg}$$

1907

P. Weiss: L'hypothese du champ moleculaire et la propriete ferromagnetique. J. de Phys. Rad. 6, 661–690

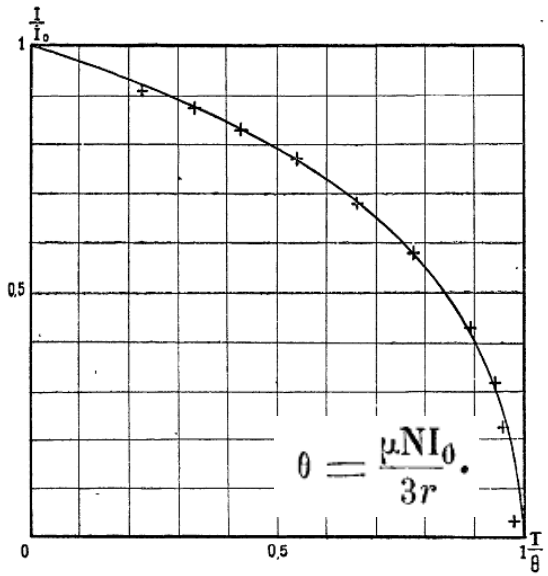

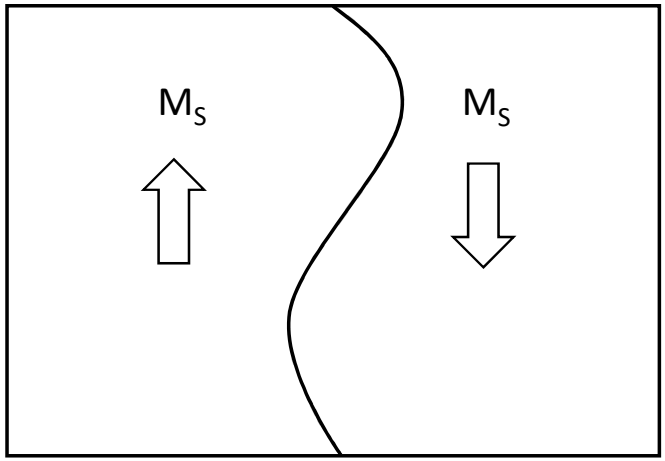

1926

P. Weiss, G. Foex: Le Magnetisme (Armand Colin, Paris)

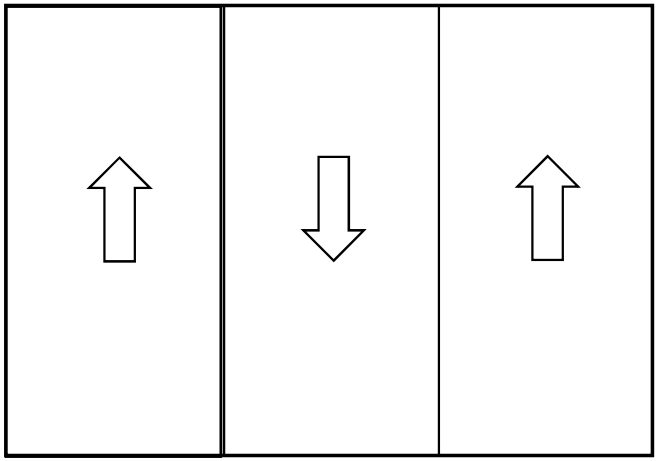

Primera mención del concepto de dominio

1919

Physik. Zeitschr. XX, 1919. 401

Zwei mit Hilfe der neuen Verstärker entdeckte Erscheinungen.

Von H. Barkhausen.

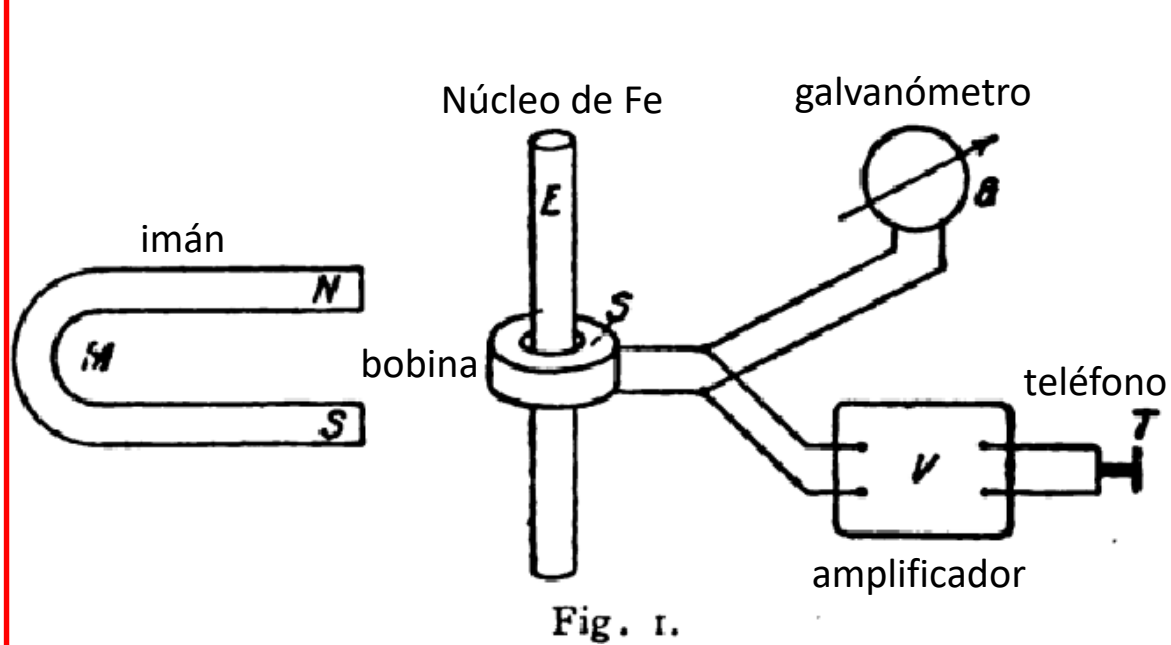

Fig. 1.

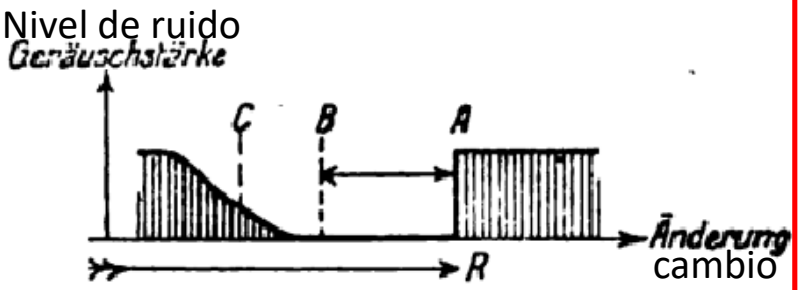

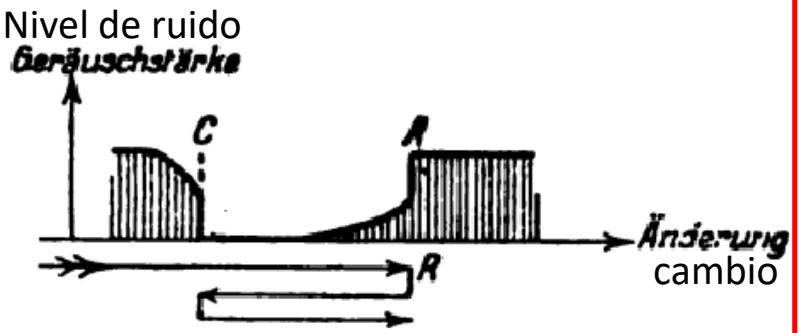

1931

APRIL 15, 1931 *PHYSICAL REVIEW* *VOLUME 37*

PROPAGATION OF LARGE BARKHAUSEN DISCONTINUITIES

By K. J. Sixtus and L. Tonks

General Electric Company, Schenectady, New York

(Received February 28, 1931)

SINCE the discovery of the Barkhausen effect, it has been a well-established fact that a great part of the change in induction in a ferromagnetic when subjected to a varying field, is made up of discontinuous changes. These ordinary discontinuities can only be observed after amplification and are not detectable by the ballistic method. Large discontinuities were first observed by Forrer[1] in 1926 in the hysteresis loop of a strained nickel wire. Later

If one tries to picture the manner in which such a magnetization discontinuity occurs, one is struck by the difficulty of accounting for a simultaneous reversal in the whole length of a fine wire. This consideration led Langmuir to predict that the magnetization first reversed at one point in the wire, forming a nucleus, and that the two boundaries which were thus formed then travelled along the wire with a finite velocity which probably depended on the magnetic field strength and the elastic strain. This prediction has been well

Concepto del experimento

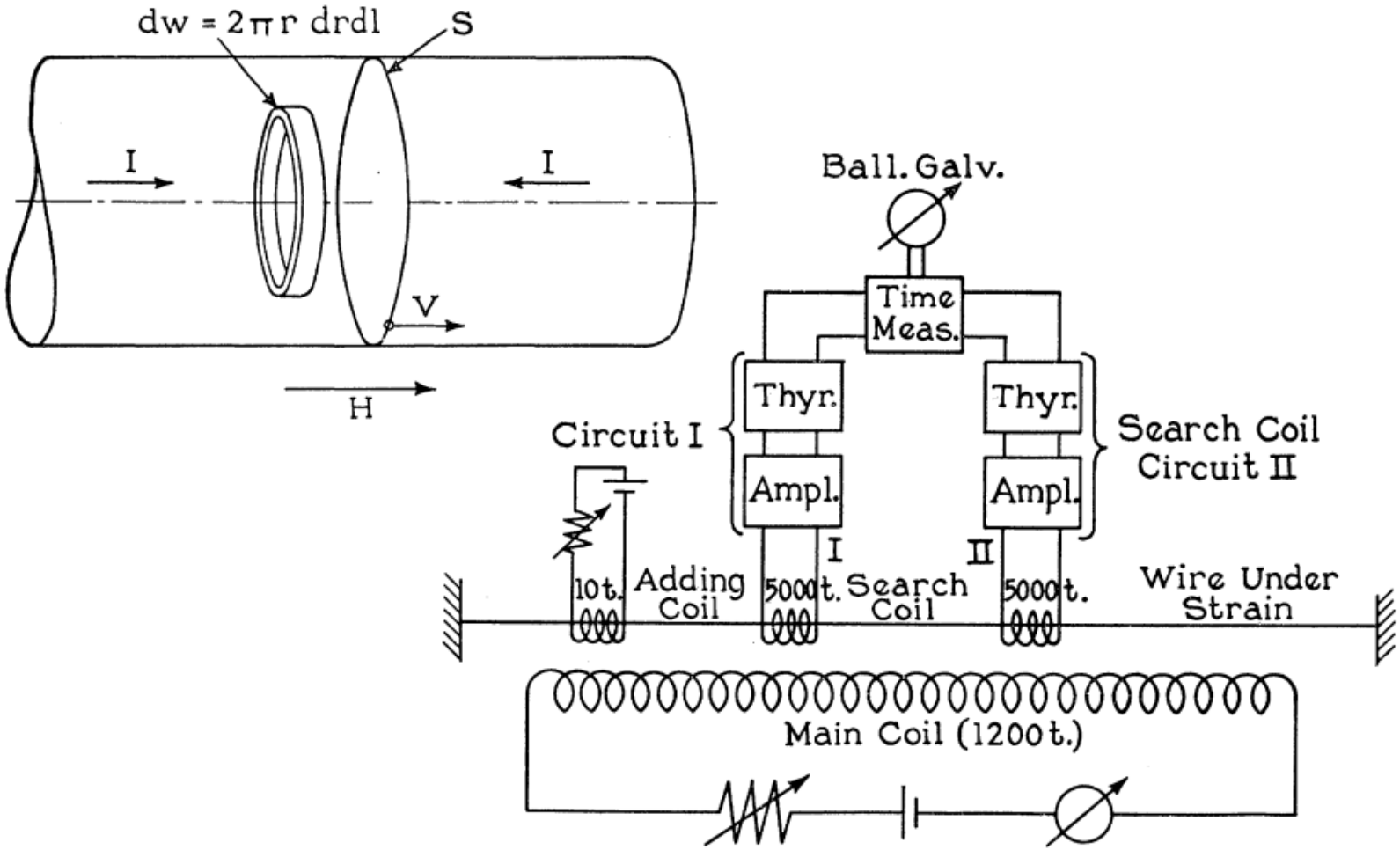

1931

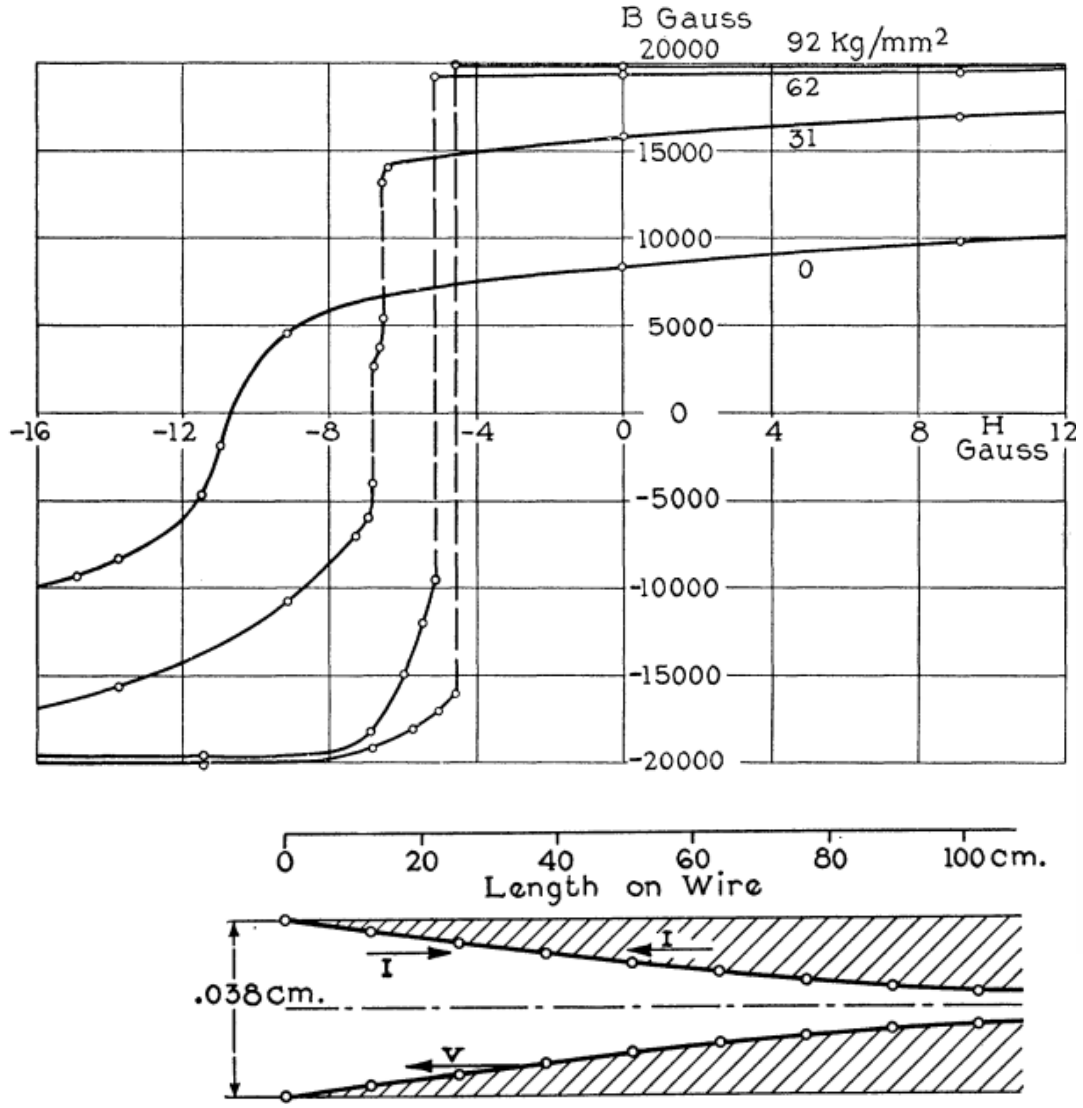
B Gauss
20000
92 Kg/mm²
62
31
0
15000
10000
5000
0
-5000
-10000
-15000
-20000
-16
-12
-8
-4
0
4
8
12
H
Gauss
0
20
40
60
80
100 cm.
Length on Wire
.038 cm.
I
I
V

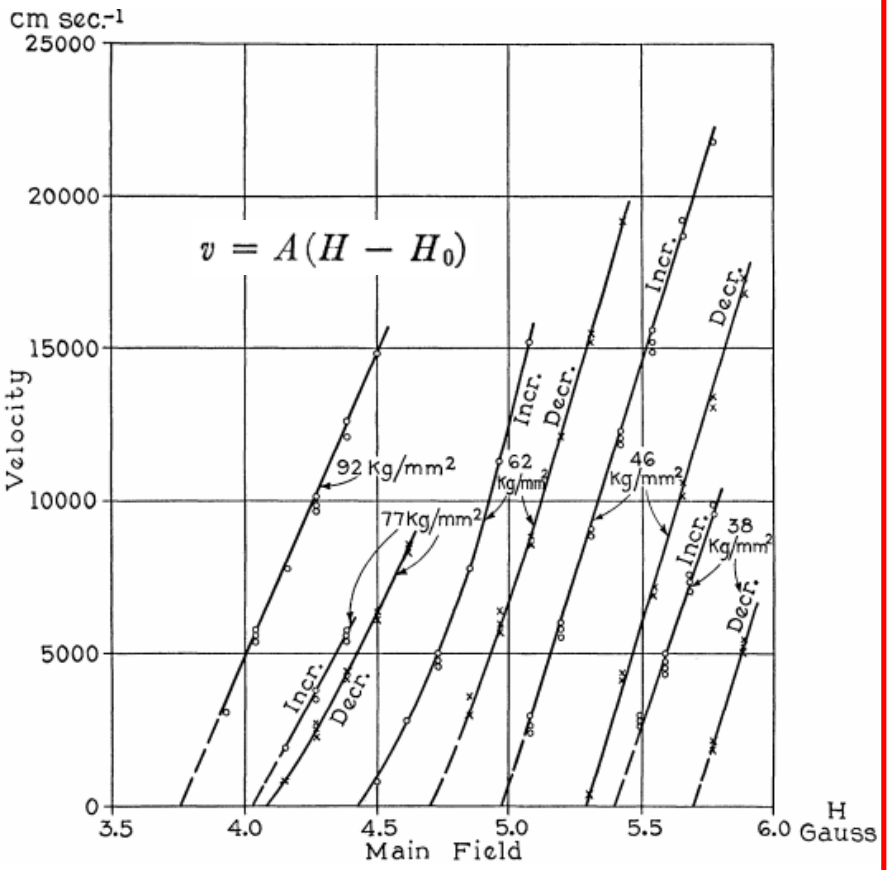
cm sec.⁻¹
25000
20000
15000
10000
5000
0
Velocity
$v = A(H - H_0)$
92 Kg/mm²
77Kg/mm²
62 Kg/mm²
46 Kg/mm²
38 Kg/mm²
Incr.
Decr.
3.5
4.0
4.5
5.0
5.5
6.0
H Gauss
Main Field

2007

Propiedades magnéticas de amorfos microestructurados con aplicaciones como sensores magnetoelásticos

Pedro Mendoza Zélis

2007

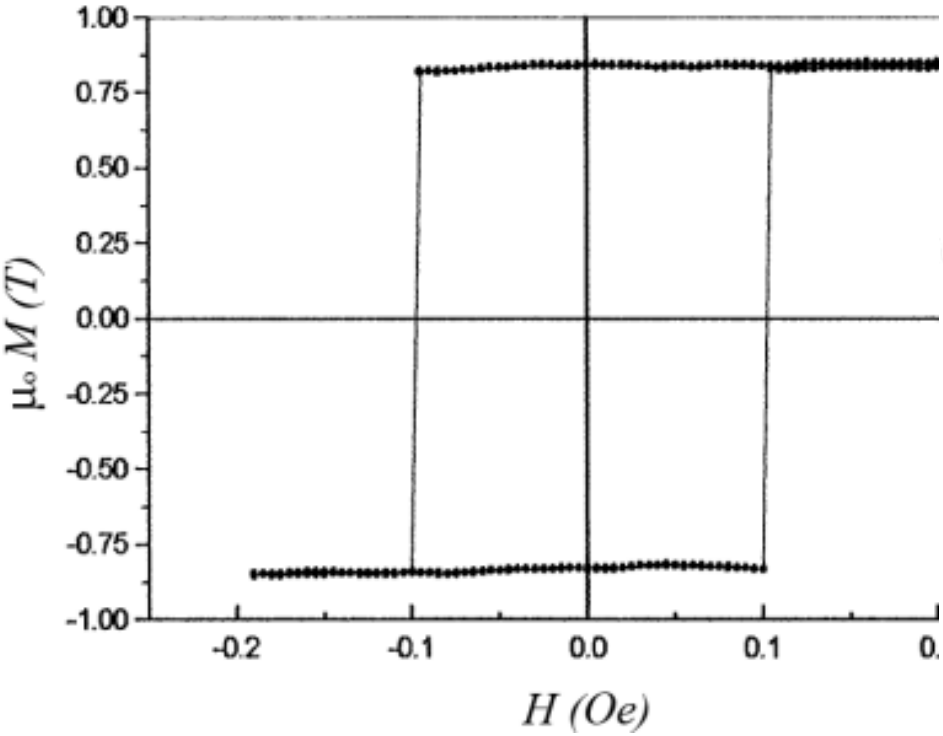
1.00
0.75
0.50
0.25
0.00
-0.25
-0.50
-0.75
-1.00
-0.2
-0.1
0.0
0.1
μ₀ M (T)
H (Oe)

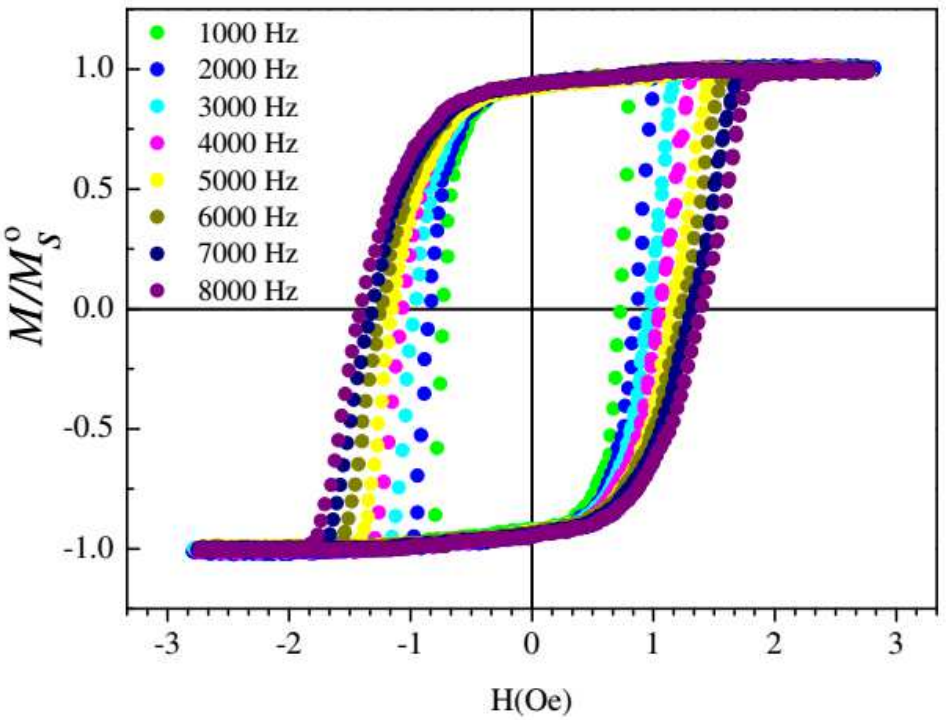
1000 Hz
2000 Hz
3000 Hz
4000 Hz
5000 Hz
6000 Hz
7000 Hz
8000 Hz
1.0
0.5
0.0
-0.5
-1.0
-3
-2
-1
0
1
2
3
M/M_S^o
H(Oe)

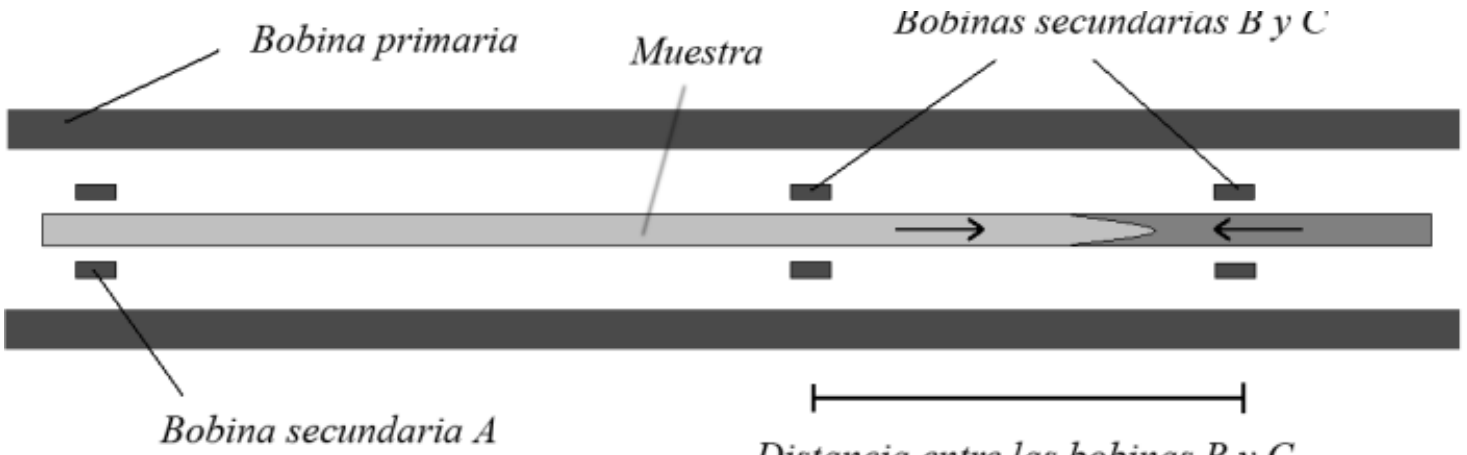

$$v = S(H - H_o),$$

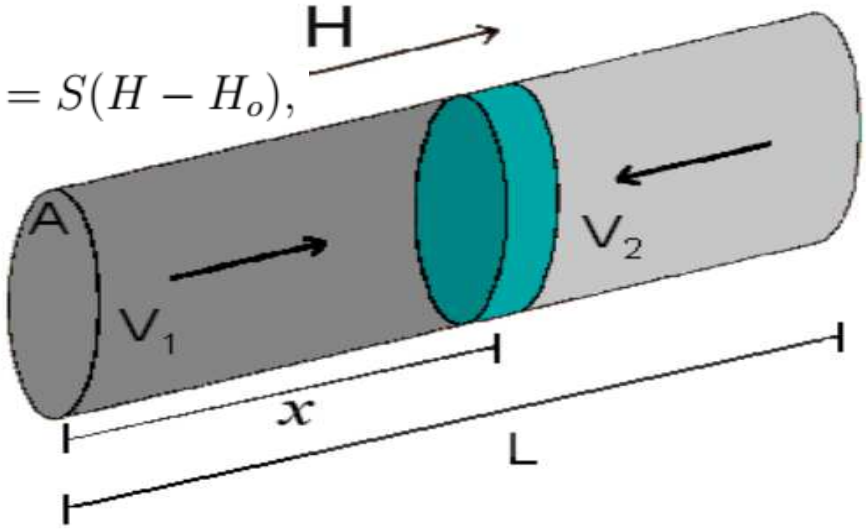

$$M \simeq M_S \frac{V_1 - V_2}{V},$$

$$x = \frac{L}{2}\left(1 - \frac{M}{M_S}\right)$$

2007

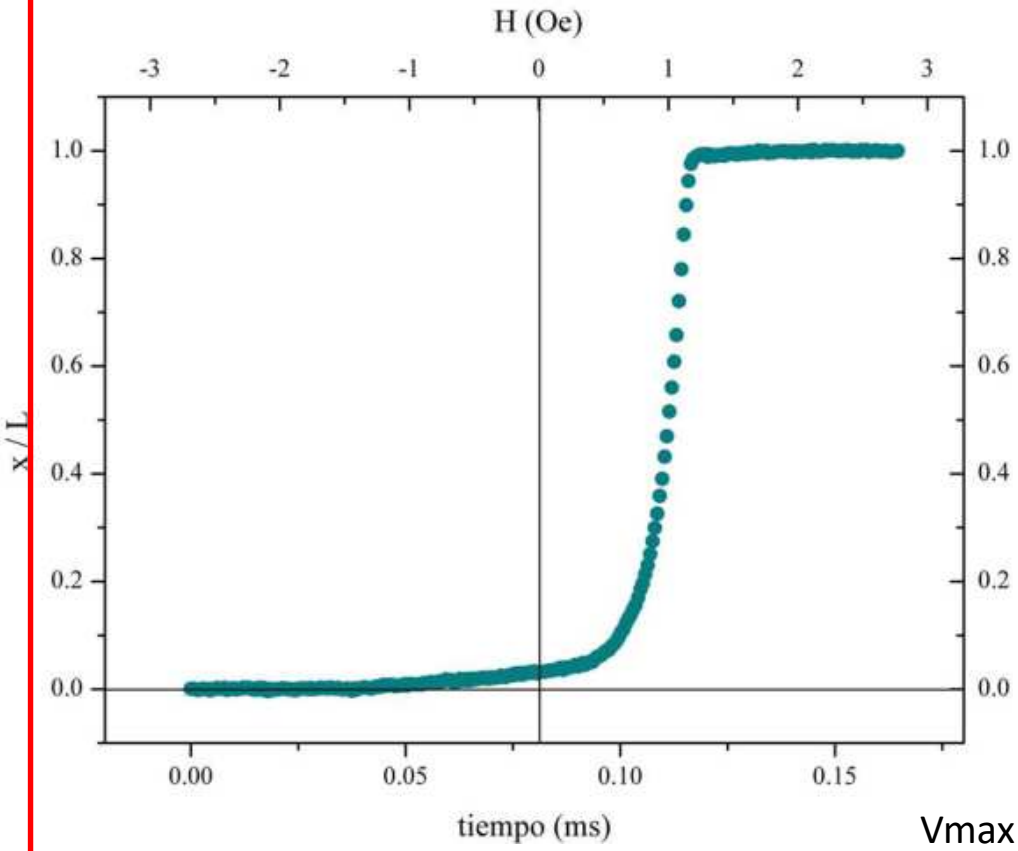

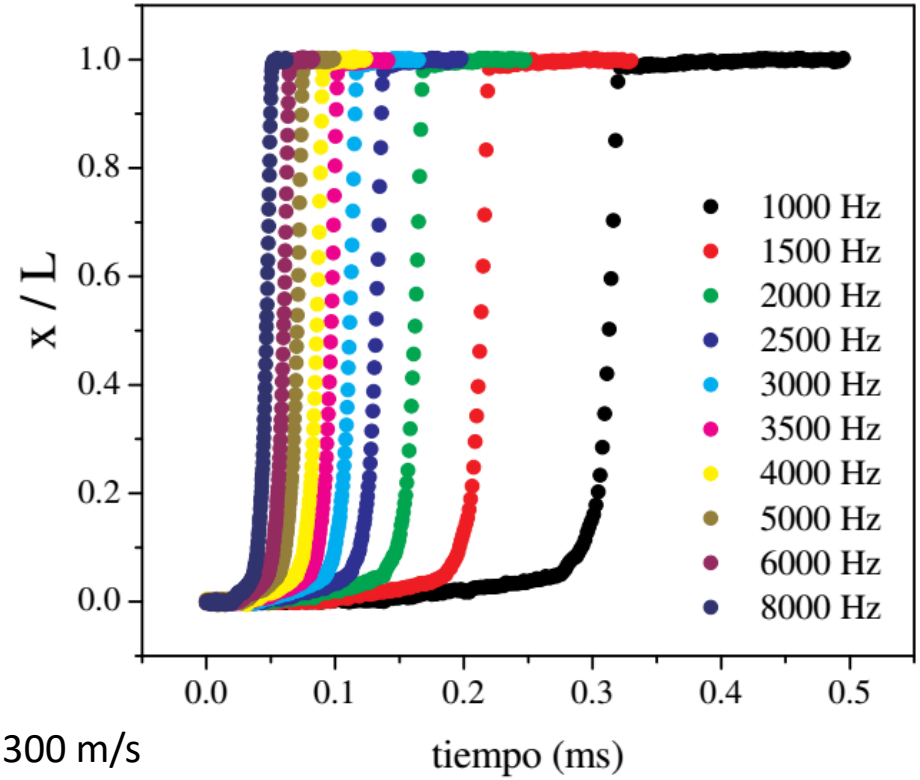

Vmax ~ 300 m/s

$$m\frac{d^2x}{dt^2} + \beta\frac{dx}{dt} + \frac{dV(x)}{dx} = F_e(t)$$

$$F_e = -\frac{dE}{dx} = 2\mu_o M_S H A.$$

1932

Zur Theorie des Austauschproblems und der Remanenzerscheinung der Ferromagnetika

Habilitationsschrift

Probleme des Atomkernbaues

Dr. phil. **Felix Bloch**

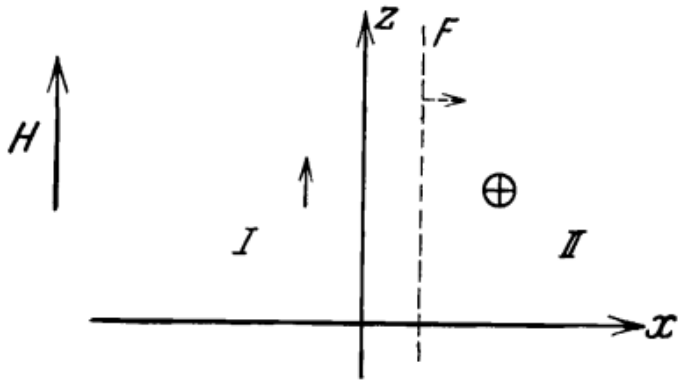

Fig. 2.

↑ = parallel zum Felde magnetisiert,
⊕ = senkrecht zum Felde magnetisiert.

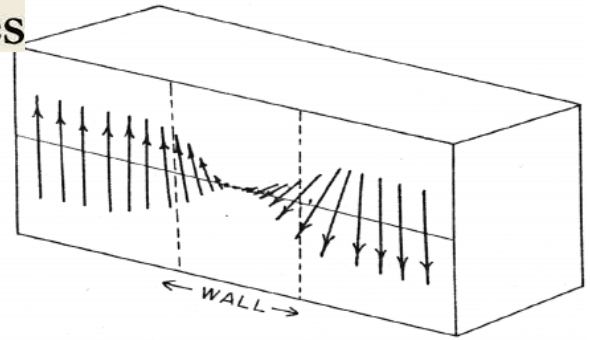

$$\delta = \frac{1}{b} = a\sqrt{\frac{J}{C}}$$

J α 1000 K, C α 1 K

⇩

$$\delta \cong a\sqrt{1000} \cong 30 \text{ Atomabstände}$$

Effects of anisotropies, magnetostriction and internal stresses

1931
1930
1926

N.S. Akulov: Zur Theorie der Magnetisierungskurve von Einkristallen. Z.Phys. 67, 794–807 (1931) (On the theory of the magnetization curve of single crystals)

R. Becker: Zur Theorie der Magnetisierungskurve. Z. Phys. 62, 253–269 (1930) (On the theory of the magnetization curve)

K. Honda, S. Kaya: On the magnetisation of single crystals of iron. Sci. Rep. Tohoku Imp. Univ. 15, 721–754 (1926)

Crystal anisotropy $\Longleftrightarrow$ spin-orbit coupling effects

Proceso de magnetización por rotación de M o desplazamiento de paredes?

La elevada permeabilidad del Fe puro se explica por el movimiento de paredes de 180°

1930
-
1932

El detalle que faltaba… aunque Frenkel&Dorfman, Bloch y Heisemberg ya lo habían percibido (1930-1932): la interacción dipolar. Por un largo tiempo permaneció ignorada, desde que Weiss había probado que era demasiado débil como para justificar el ferromagnetismo.

Heisemberg suponía que, para minimizar la energía desmagnetizante tenían que existir dominios diminutos con forma de hebra.

Bitter (también Hámos&Thiessen) mostró en 1931 y 1932 imágenes que mostraban dominios estáticos, frecuentemente periódicos y regulares y mayores de los imaginados por Heisemberg.

AUGUST 15, 1932 *PHYSICAL REVIEW* *VOLUME 41*

Experiments on the Nature of Ferromagnetism

By FRANCIS BITTER

Westinghouse Research Laboratories, East Pittsburgh, Pennsylvania

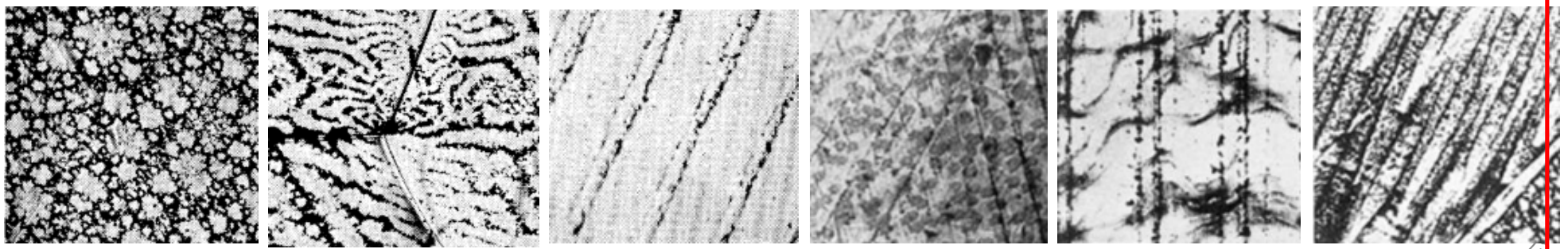

1935

Probably stimulated by such observations and by their first theoretical analysis by Bloch (see the footnote at [12 (p. 321)]), *Landau* and *Lifshitz* [22] presented the solution in 1935: domains are formed to minimize the total energy, an important part of which is the stray field energy. And the stray field energy can be avoided by *flux-closure* type domains as shown in Fig. 1.2.

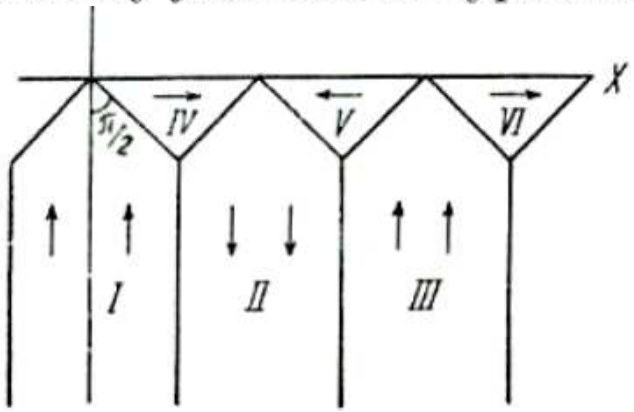

ON THE THEORY OF THE DISPERSION OF MAGNETIC PERMEABILITY IN FERROMAGNETIC BODIES

Reprinted from Phys. Zeitsch. der Sow. **8**, pp. 153–169 (1935)

L. LANDAU, E. LIFSHITS

Ukrainian Physico-Technical Institute, Academy of Sciences of the Ukrainian SSR

(Kharkov, Ukraine)

1935

Con el fin de determinar tamaños de paredes de dominio consideraron dos contribuciones a la energía

stiffness $\int \{1/2\alpha[(\nabla s_x)^2 + (\nabla s_y)^2 + (\nabla s_z)^2] +$

anisotropía $+1/2\beta(s_x^2 + s_y^2)\}dV = \min,$

s ≡ M

Para determinar tamaños y orientaciones de dominios tienen en cuenta los efectos desmagnetizantes. Hacen los cálculos para un material con anisotropía uniaxial y obtienen expresiones para la velocidad con que se mueven las Paredes de dominio y la susceptibilidad cuando se aplica un campo.

$$v = \frac{\mu_0 s}{\lambda}\sqrt{\frac{\alpha}{\beta}}h. \qquad \mu_0 = \frac{e}{mc} \qquad \alpha = A \qquad \beta = 2K \qquad \vec{h} = H\check{z}$$

$$\chi_l = \frac{\mu_0 s^2}{i\omega\lambda d}\sqrt{\frac{\alpha}{\beta}}.$$

LL sientan las bases de la teoría micromagnética.

1935

Landau&Lifschits

Macroscopically, the effect of exchange interaction can be expressed to a sufficient accuracy by a *stiffness* term, a quadratic form of the first spatial derivatives of the magnetization vector. This stiffness energy favours uniform magnetization, particularly on a microscopic scale.

Even inside domain walls the Weiss postulate of a constant value of magnetization should be valid (in contrast to Bloch's treatment who still assumed a ferromagnet to become paramagnetic in the middle of the walls). The magnetization *rotates* in passing through the wall.

Domain structures are a consequence of the finite dimensions of magnetic bodies. The domain size increases with the specimen size. A uniform infinite or toroidal body may have *no* domain structure in equilibrium.

L&L no tuvieron necesidad de introducir el término de energía dipolar en sus cálculos porque emplearon configuraciones con dominios de flujo cerrado de **M** que evitan la existencia de polos y tienen energía dipolar nula.

1949

The model of Landau and Lifshitz proved to be too simple to explain actual observations.

PHYSICAL REVIEW VOLUME 75, NUMBER 1 JANUARY 1, 1949

Magnetic Domain Patterns on Single Crystals of Silicon Iron

H. J. WILLIAMS, R. M. BOZORTH, AND W. SHOCKLEY
Bell Telephone Laboratories, Murray Hill, New Jersey

Monocristales
Pulido mecánico
Electro-pulido
Uso de coloides

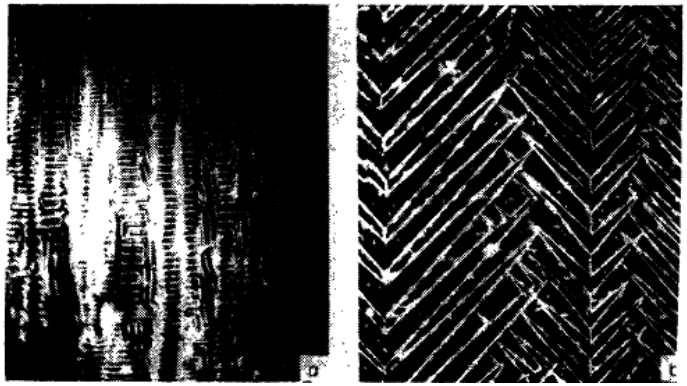

Pulido mecánico Electro-pulido

The domain patterns described below are found to conform well to this principle of "flux closure" and, consequently, they represent configurations of low magnetostatic energy.

Buen acuerdo entre los patrones observados y las predicciones teóricas basadas en el requerimiento De un flujo cerrado de **M**.

1935
-
1949

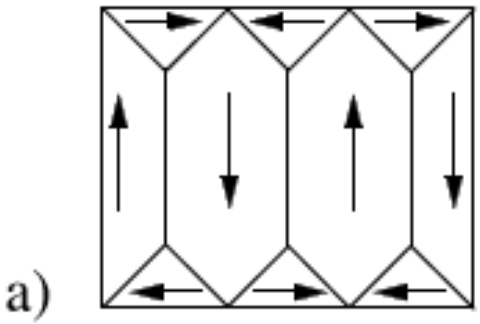

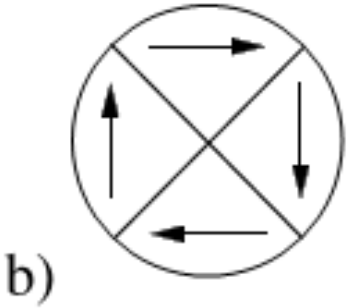

Baja anisotropía
Flujo cerrado
LL 1935
Néel 1944

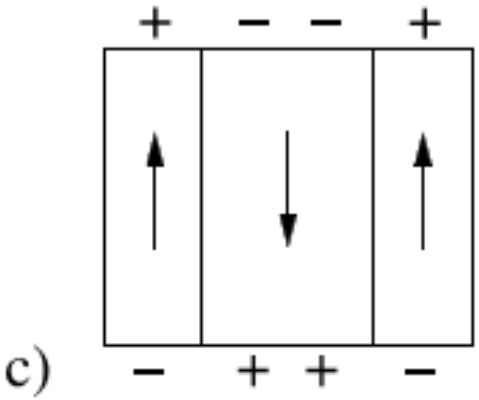

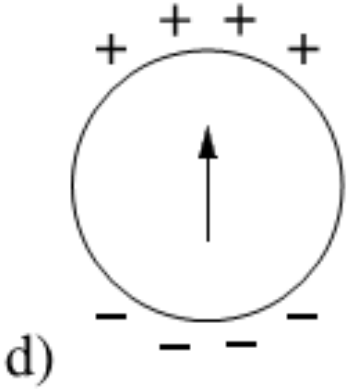

Alta anisotropía uniaxial
Flujo abierto
Kittel 1949

1944
-
1949

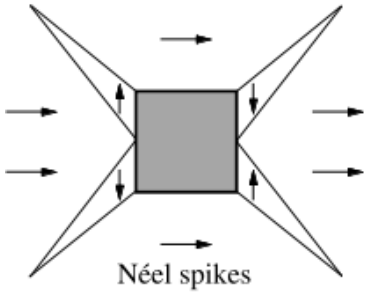

Néel 1944
predicción

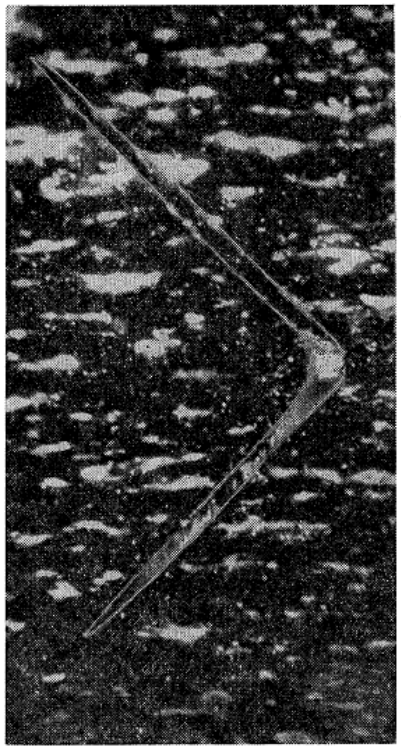

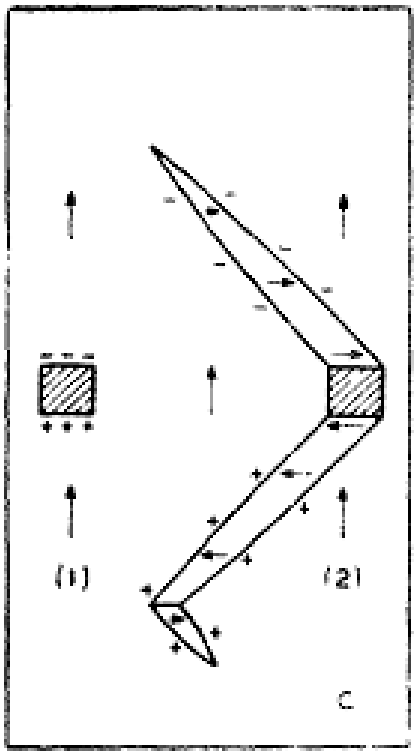

W,B & S 1949
experimental

1949

In the same year Kittel [30] reviewed domain theory and experiments, and this review became the generally accepted reference for domain research. What followed can be called *application* of the established theory,

REVIEWS OF
MODERN PHYSICS

Physical Theory of Ferromagnetic Domains

CHARLES KITTEL
Bell Telephone Laboratories, Murray Hill, New Jersey

are always the same: *domain structure has its origin in the possibility of lowering the energy of a system by going from a saturated configuration such as* (a) *with high magnetic energy to a domain configuration, such as* (c) *or* (e), *with a lower energy*. The domain structures

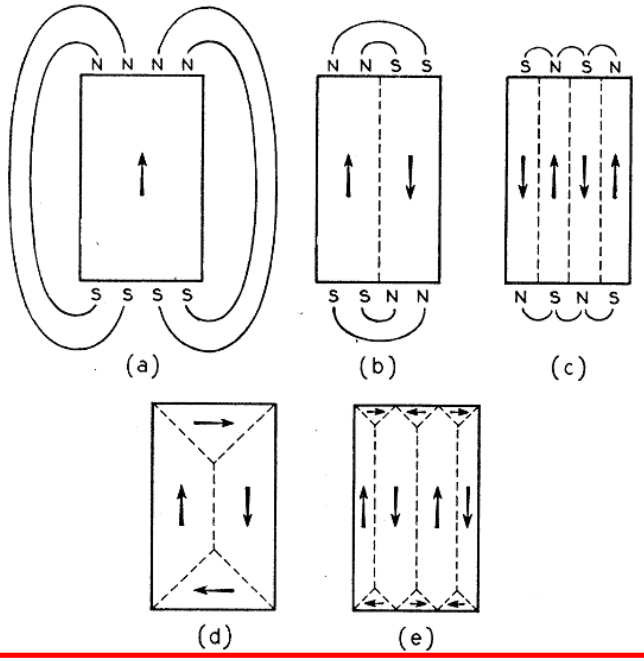

Correlación entre permeabilidad inicial y coercitividad, Kittel

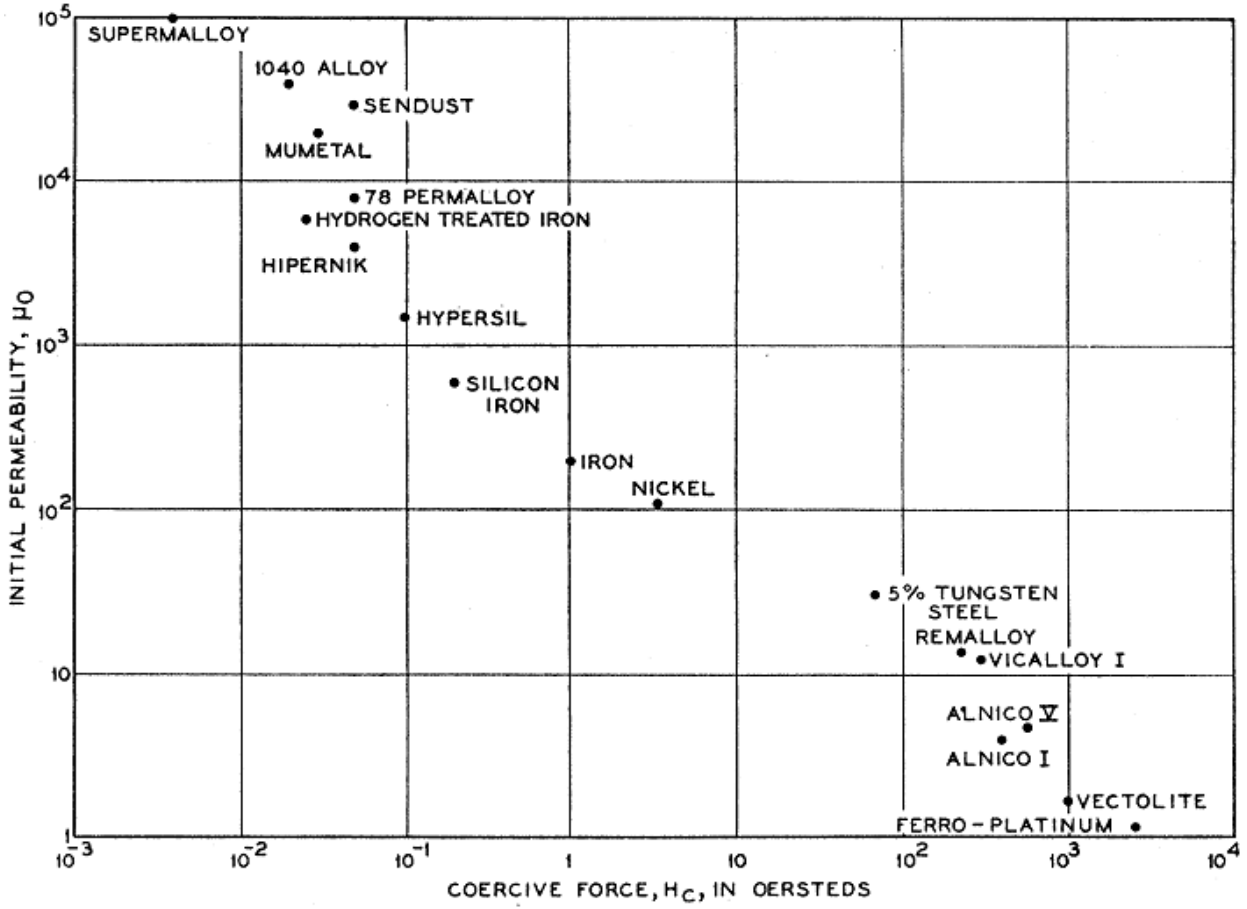

1949

$$w_{ex} = -2JS^2 \sum_{i>j} \cos\varphi_{ij}.$$

$$\Delta w_{ex} \cong JS^2 \sum \varphi_{ij}^2$$

$$\Delta w_{ex} = 2JS^2 a^2 \sum_i [(\nabla\alpha_j^x)^2 + (\nabla\alpha_j^y)^2 + (\nabla\alpha_j^z)^2]$$

$$f_{ex} = A[(\nabla\alpha_1)^2 + (\nabla\alpha_2)^2 + (\nabla\alpha_3)^2],$$

$$A = 2JS^2/a.$$

$J = 0.54kT_c$ (simple cubic; spin $\frac{1}{2}$)

$J = 0.34kT_c$ (body-centered cubic; spin $\frac{1}{2}$)

$J = 0.15kT_c$ (body-centered cubic; spin 1)

$$J = (0.15)(1043)k \cong 160k,$$

$$A = \frac{2JS^2}{a} = \frac{410k}{2.86\times10^{-8}} = 2.0\times10^{-6} \text{ ergs/cm.}$$

1949

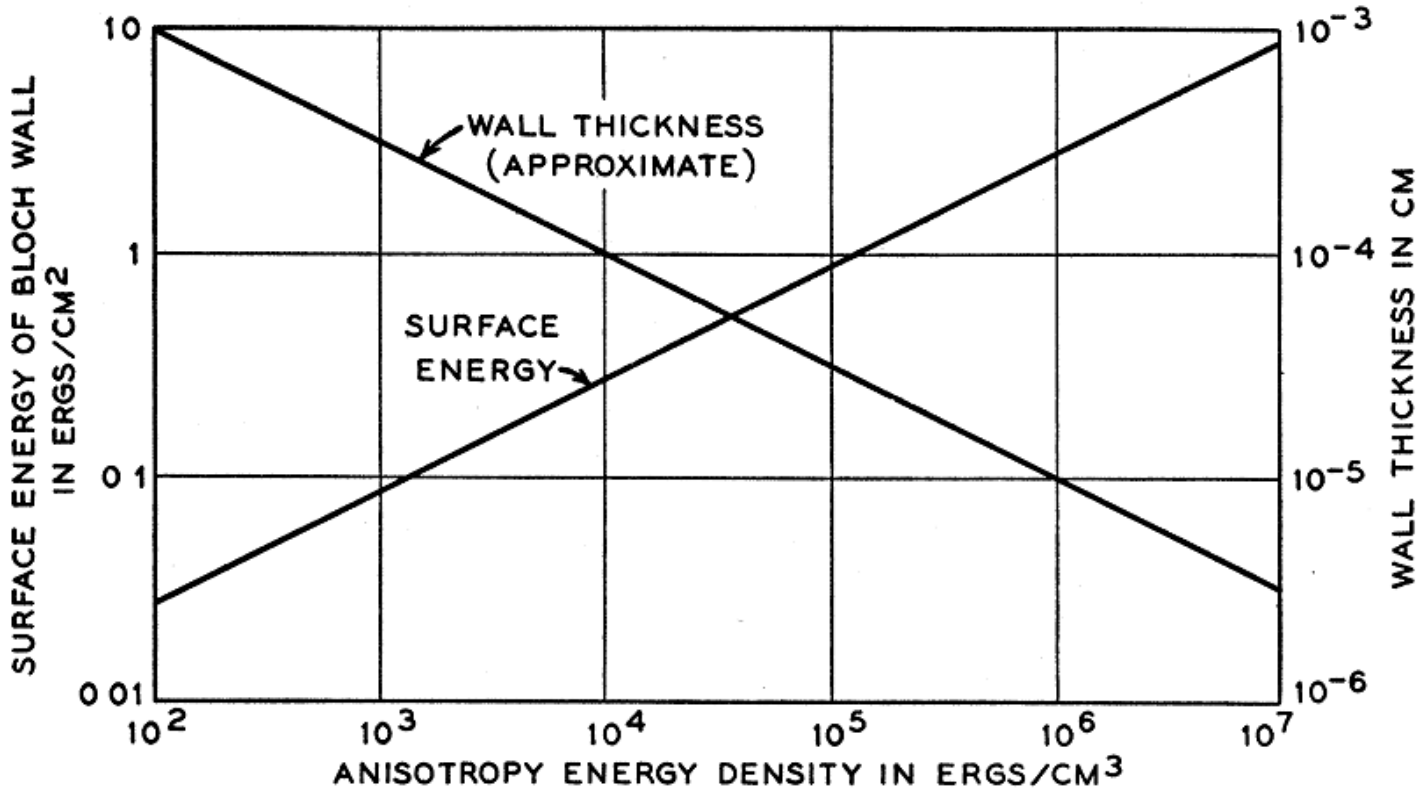
10
1
0 1
0 01
SURFACE ENERGY OF BLOCH WALL IN ERGS/CM2
WALL THICKNESS (APPROXIMATE)
SURFACE ENERGY
10-3
10-4
10-5
10-6
WALL THICKNESS IN CM
10 2
10 3
10 4
10 5
10 6
10 7
ANISOTROPY ENERGY DENSITY IN ERGS/CM3

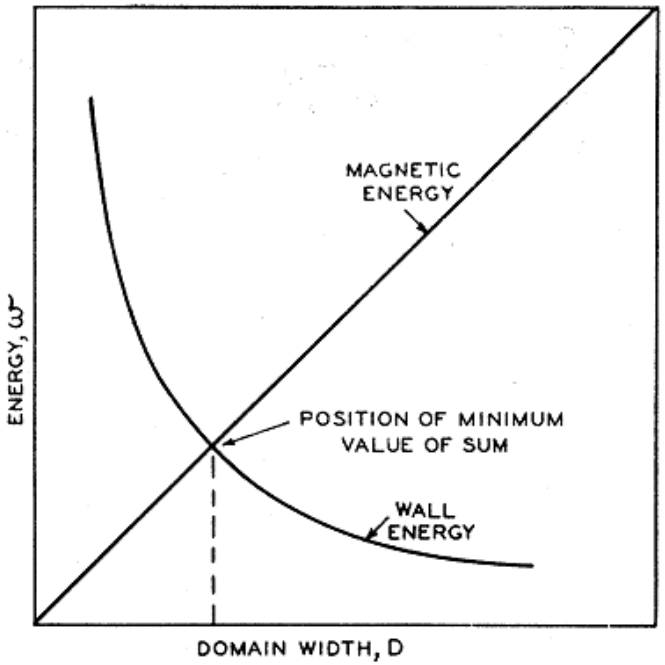

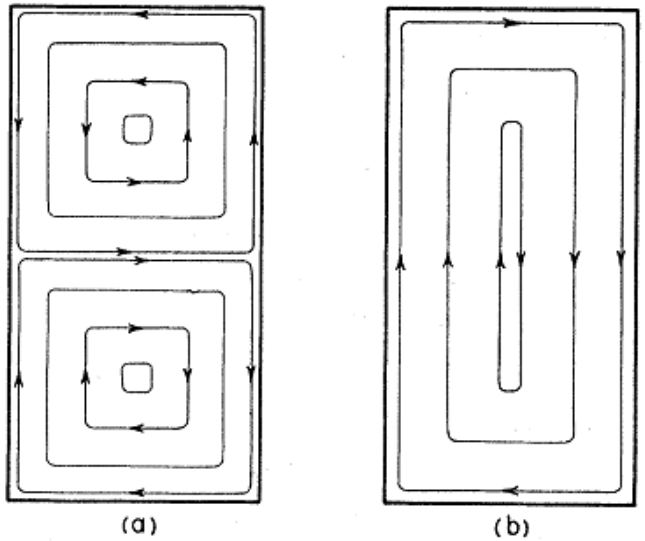

FIG. 37. Theoretical possibilities for domain structures in the limit of zero anisotropy energy.

1949

FIG. 43. Types of simple domain arrangements in a small sphere: (a) Applies for low anisotropy, (b) for high anisotropy in a cubic crystal, and (c) for high anisotropy in a uniaxial crystal.

$$(1/2)(4\pi/3)^2 R_c^3 I_s^2 = (\pi J R_c/a)[ln(2R_c/a) - 1],$$ K baja

$$R_c = (9/4\pi)(\sigma_w/I_s^2)$$ K alta, cúbica

$$R_c = 9\sigma_w/4\pi I_s^2.$$ K alta, uniaxial

1940
-
1978
Brown

Micromagnetism is the continuum theory of magnetic moments, underlying the description of magnetic microstructure. The theory of Landau and Lifshitz is based on a variational principle: it searches for magnetization distributions with the smallest total energy. This variational principle leads to a set of differential equations, the *micromagnetic equations*. They were given in [22] for one dimension. Stimulated again by experimental work [25] and its analysis, *W.F. Brown* [33, 34] extended the equations to three dimensions, including fully the stray field effects (see [35, 36]). (Brown)

The micromagnetic equations are complicated non-linear and non-local equations; they are therefore difficult to solve analytically, except in cases in which a linearization is possible. However, a number of problems in domain research needs micromagnetic methods for their adequate treatment:

To treat such problems, work on numerical solutions of the micromagnetic equations is increasingly pursued. It appears utopic, however, to apply micromagnetic methods to large-scale domain structures. The gap between the size of samples for which three-dimensional finite element calculations are possible (at most up to perhaps a micron cubed), and the scale of well defined domain patterns (often reaching millimetres and centimetres) is simply too large.

the crystal lattice sites. From the mesoscopic viewpoint of micromagnetics and domain theory it does not matter whether a material is ferromagnetic or *ferri*magnetic. In this book we consider ferrimagnets generally to be included in discussing ferromagnets for short. An interesting hybrid between atomic

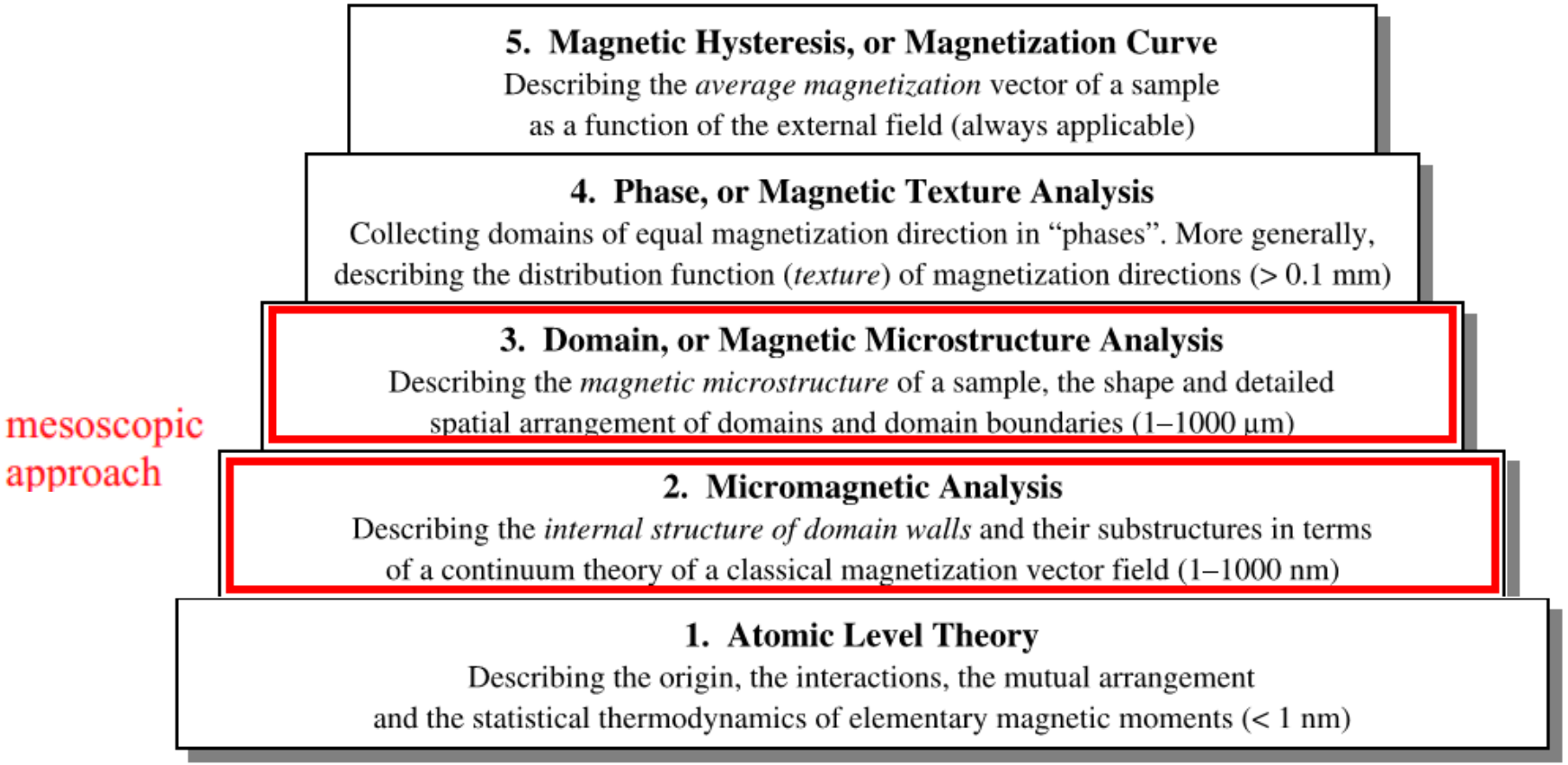

magnetic" (some recent examples are [39–41]). We stick (in agreement with still the vast majority of authors) with the classical definition of *W.F. Brown* [34], restricting the term micromagnetics to the *continuum theory of magnetically ordered materials*, to the second level in Fig. 1.5.

duce the line of arguments. In Sect. 3.2 the free energy of a magnet is presented. The principle that this energy must be a minimum leads to the micromagnetic equations and their dynamic generalizations. A discussion of the origin of domains

Micromagnetismo

duce the line of arguments. In Sect. 3.2 the free energy of a magnet is presented. The principle that this energy must be a minimum leads to the micromagnetic equations and their dynamic generalizations. A discussion of the origin of domains

(also amplifying some of the subjects of this book). The recent textbook by *Aharoni* [514] contains a careful analysis of the foundations of micromagnetics and a review with a focus on the extensive contributions of the author to this subject.

$$\boldsymbol{m}(\boldsymbol{r}) = \boldsymbol{J}(\boldsymbol{r})/J_s \qquad \boldsymbol{J} = \mu_0 \boldsymbol{M} \qquad \boldsymbol{m}^2 = 1$$

Estado de equilibrio

Minimización de la energía libre	Torque nulo sobre la magnetización	Ecuaciones micromagnéticas
$E(\boldsymbol{m}) = min$	$\boldsymbol{m} \times \boldsymbol{H}_{eff} = \boldsymbol{0}$	

Contribuciones a *E* locales y no locales

locales $E_{\mathrm{loc}} = \int f(\boldsymbol{m})\mathrm{d}V$

- Zeeman
- Anisotropía
- Magnetoelástica (con esfuerzo no-magnético)
- Intercambio

No locales: $\boldsymbol{m} \times \boldsymbol{H}_{eff}$ depende de $\boldsymbol{m}$ en toda la muestra

- Magnetostática
- Autoenergía magnetostrictiva (interacciones elásticas entre regiones magnetizadas en direcciones diferentes)

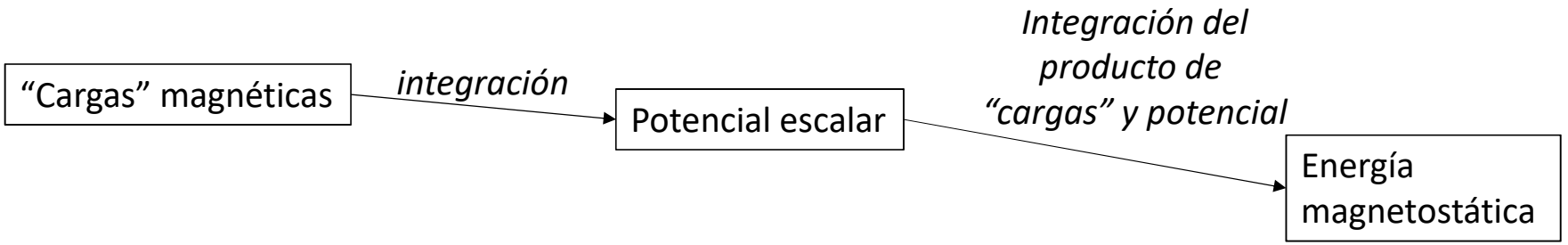

Intercambio

$$E_x = A \int (\mathbf{grad}\, \boldsymbol{m})^2 \, dV$$ Stiffness*

$A = 2JS^2/a$

$$A(0) \approx kT_c/a_L$$ (a 0 K)

parámetro de red

$$(\mathbf{grad}\, \boldsymbol{m})^2 = e_x = A[(\mathbf{grad}\, m_1)^2 + (\mathbf{grad}\, m_2)^2 + (\mathbf{grad}\, m_3)^2]$$
$$= A[m_{1,x}^2 + m_{1,y}^2 + m_{1,z}^2 + m_{2,x}^2 + m_{2,y}^2 + m_{2,z}^2$$
$$+ m_{3,x}^2 + m_{3,y}^2 + m_{3,z}^2]$$

where $m_{1,x}^2 = (\partial m_1/\partial x)^2$, etc. This formula is derived by a Taylor expansion of the isotropic Heisenberg interaction $\boldsymbol{s}_1 \cdot \boldsymbol{s}_2$ between neighbouring spins. It

Un análisis de la contribución por stiffness se puede ver en la sección 3.4, ecs. 3.32 a 3.41 del libro "micromagnetis" de W.F. Brown, (INTERSCIENCE PUBLISHERS , Wiley)

**Landau y Lifschits 1935*

Intercambio a través de una interfaz o de una interfase

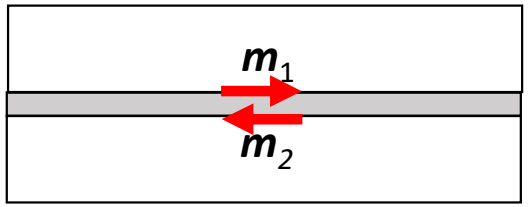

$$e_{\mathrm{coupl}} = C_{\mathrm{bl}}(1 - \boldsymbol{m}_1 \cdot \boldsymbol{m}_2) + C_{\mathrm{bq}}[1 - (\boldsymbol{m}_1 \cdot \boldsymbol{m}_2)^2]$$

Rugosidad interfacial

$C_{bl} > 0$ ⇨ 

$C_{bl} < 0$ (dominante) ⇨ 

$|C_{bl}| << |C_{bq}|$, $C_{bq} < 0$ ⇨ 

anisotropía

Incluye anisotropía magnetocristalina y anisotropía inducida debida a defectos de red o efectos de ordenamiento atómico.

No incluye efectos de forma.

Generalmente se usan los términos de menor orden de una serie en potencias pares de los cosenos directores de la magnetización. Sólo a bajas temperaturas puede ser necesario usar términos de orden mayor.

cúbica

$$e_{\mathrm{Kc}} = K_{\mathrm{c1}}\left(m_1^2 m_2^2 + m_1^2 m_3^2 + m_2^2 m_3^2\right) + K_{\mathrm{c2}} m_1^2 m_2^2 m_3^2$$

$|K_{c1}| \leq 10^4$ J/m^3

$K_{c1} > 0$ direcciones fáciles <100>

$K_{c1} < 0$ direcciones fáciles <111>

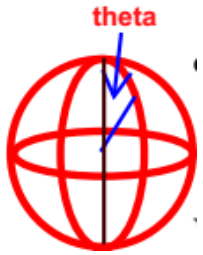

$$e_{\mathrm{Kc}} = K_{\mathrm{c1}} \cos^2\vartheta \cos^2\varphi(\cos^2\vartheta \sin^2\varphi + \sin^2\vartheta) + \tfrac{1}{4}(K_{\mathrm{c1}} + K_{\mathrm{c2}} \cos^2\vartheta \cos^2\varphi)(\cos^2\vartheta \sin^2\varphi - \sin^2\vartheta)^2$$

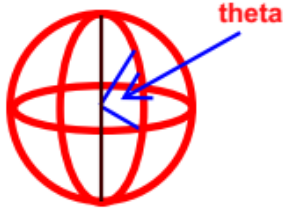

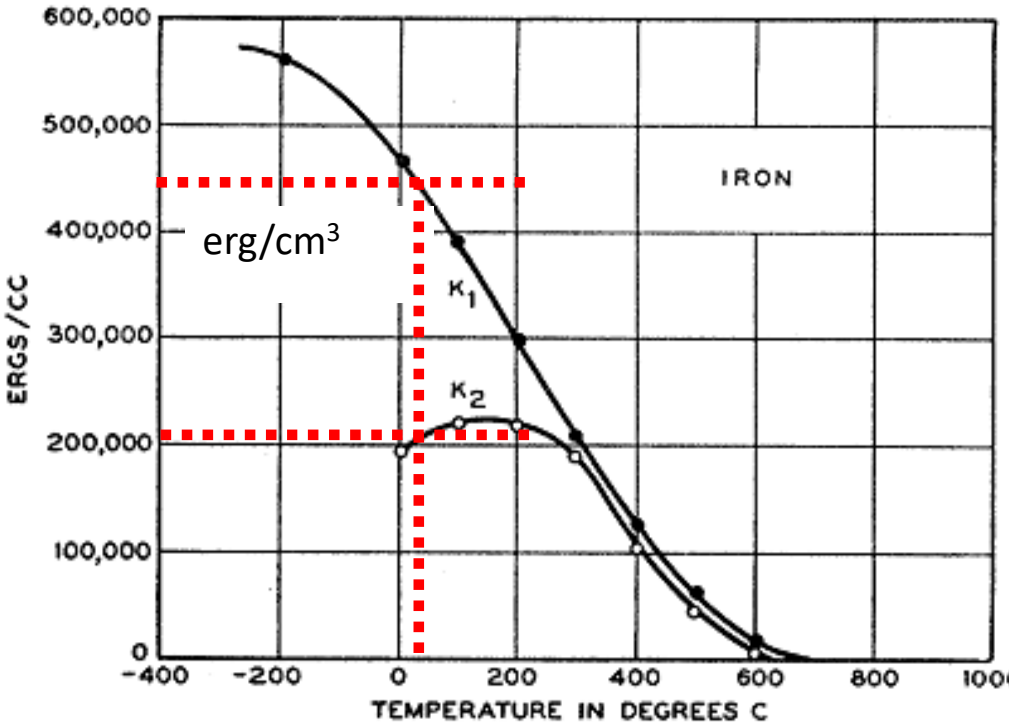
IRON
ERGS/CC
600,000
500,000
400,000
300,000
200,000
100,000
0
-400
-200
0
200
400
600
800
K1
K2
TEMPERATURE IN DEGREES C
erg/cm3

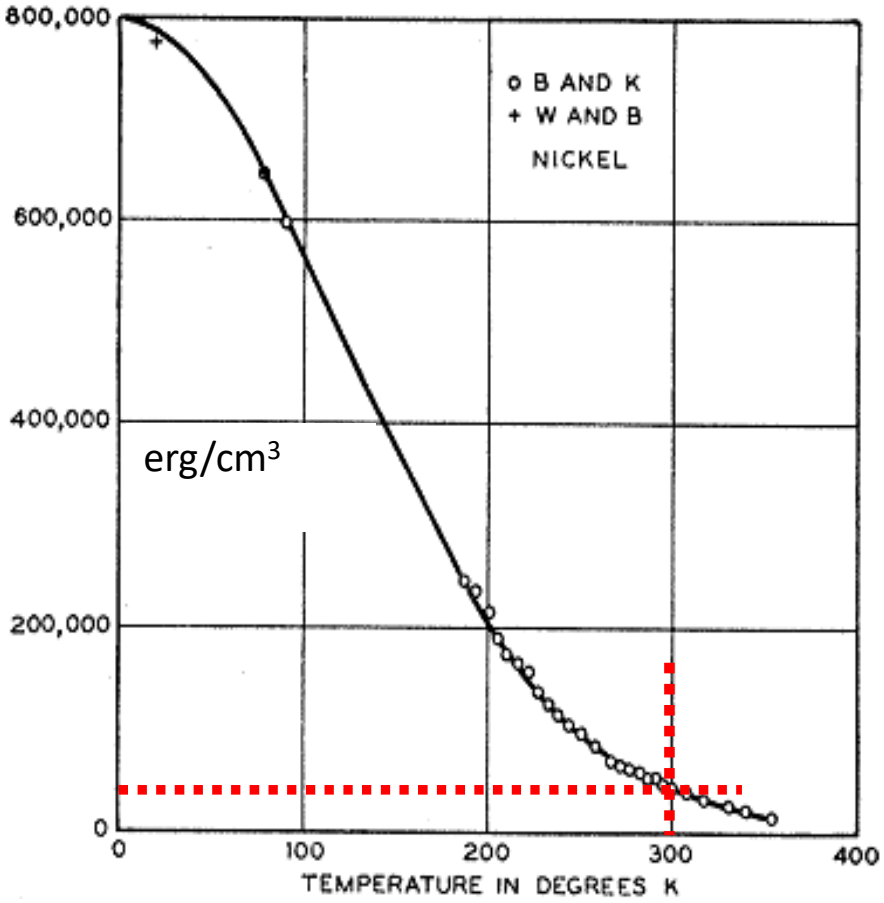
o B AND K
+ W AND B
NICKEL
800,000
600,000
400,000
200,000
0
0
100
200
300
400
TEMPERATURE IN DEGREES K
erg/cm3

44

uniaxial

$$e_{Ku} = K_{u1} \sin^2 \vartheta + K_{u2} \sin^4 \vartheta$$

$|K_{u1}| \leq 10^7$ J/m^3

$K_{u1} >> 0$ ⇨ Eje fácil en 0 - π

$K_{u1} << 0$ ⇨ Plano fácil en π/2

$0 > K_{u1}/K_{u2} > -2$ ⇨ Cono fácil en $\text{sen}^2\theta = -K_{u1} / 2K_{u2}$

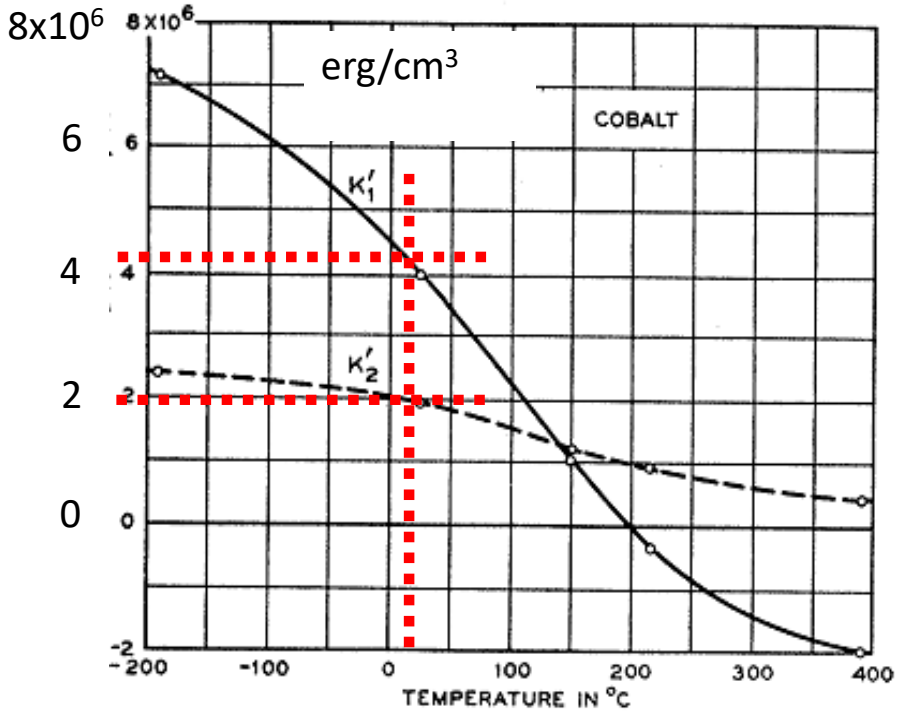

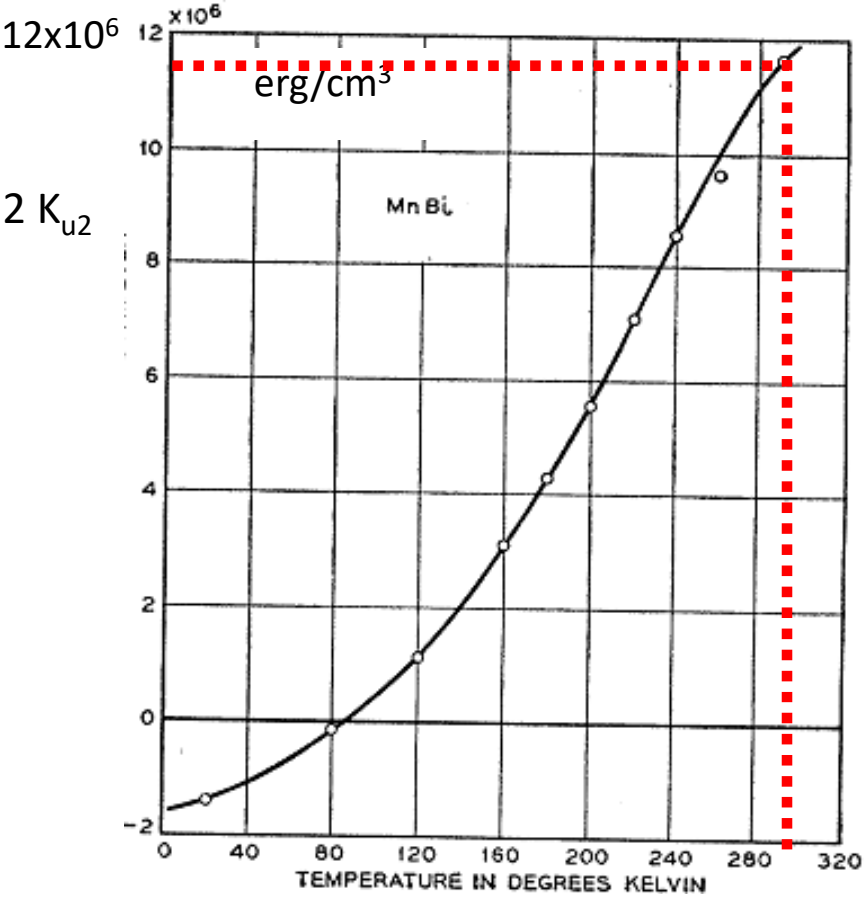

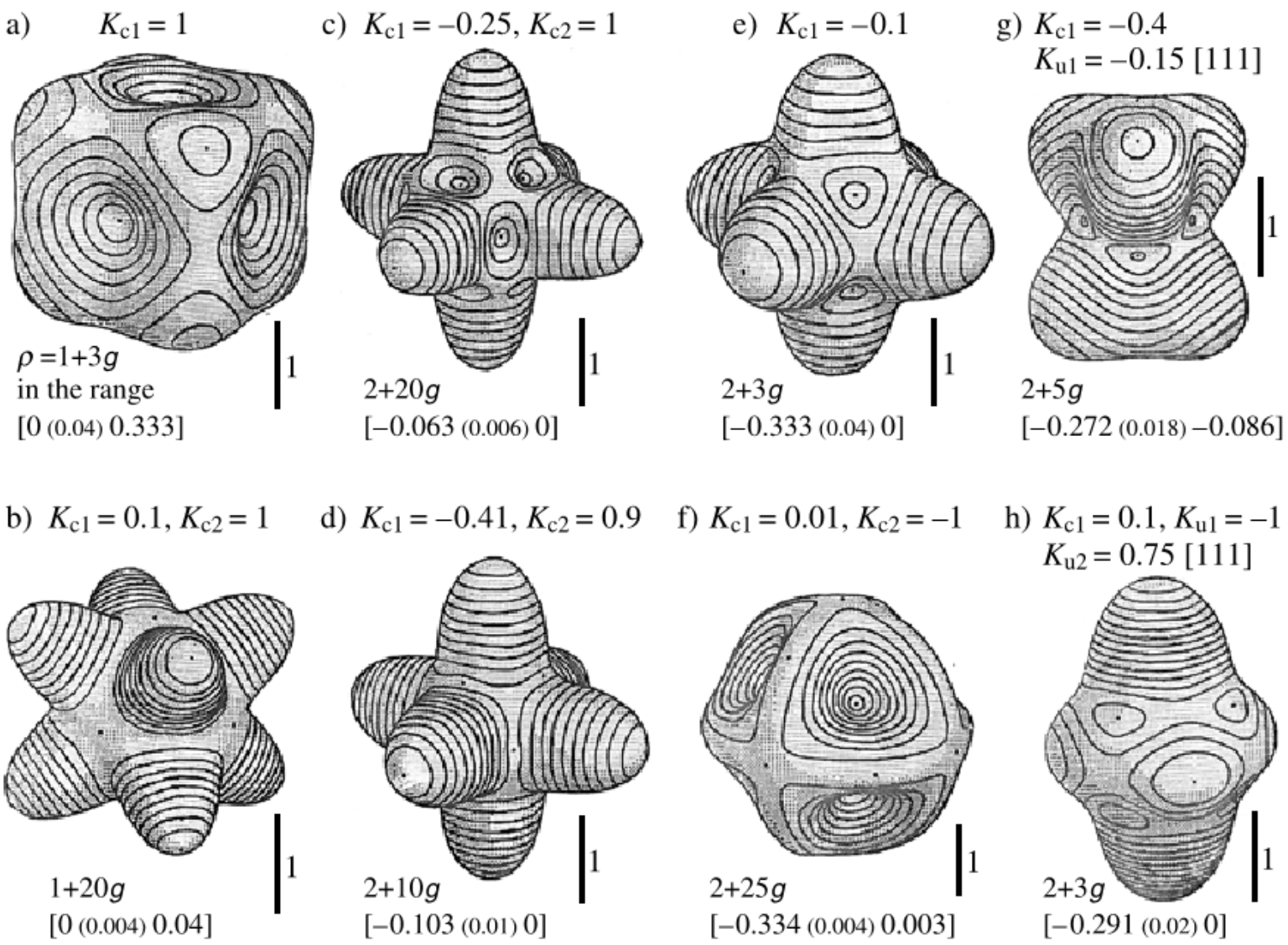
a) $K_{c1} = 1$
$\rho = 1+3g$
in the range
[0 (0.04) 0.333]
1
c) $K_{c1} = -0.25$, $K_{c2} = 1$
2+20g
[−0.063 (0.006) 0]
1
e) $K_{c1} = -0.1$
2+3g
[−0.333 (0.04) 0]
1
g) $K_{c1} = -0.4$
$K_{u1} = -0.15$ [111]
2+5g
[−0.272 (0.018) −0.086]
1
b) $K_{c1} = 0.1$, $K_{c2} = 1$
1+20g
[0 (0.004) 0.04]
1
d) $K_{c1} = -0.41$, $K_{c2} = 0.9$
2+10g
[−0.103 (0.01) 0]
1
f) $K_{c1} = 0.01$, $K_{c2} = -1$
2+25g
[−0.334 (0.004) 0.003]
1
h) $K_{c1} = 0.1$, $K_{u1} = -1$
$K_{u2} = 0.75$ [111]
2+3g
[−0.291 (0.02) 0]
1

ortorrómbica

$$e_{\mathrm{Ko}} = K_1 m_1^2 + K_2 m_2^2 + K_3 m_3^2$$

Combinación cúbica-ortorrómbica

An *induced* anisotropy in a cubic crystal can take the form of an orthorhombic anisotropy [531], as described by the second-order expression:

$$e_{\mathrm{Ki}} = F_{\mathrm{ind}}(m_1^2 a_1^2 + m_2^2 a_2^2 + m_3^2 a_3^2) + 2G_{\mathrm{ind}}(m_1 m_2 a_1 a_2 + m_1 m_3 a_1 a_3 + m_2 m_3 a_2 a_3)$$

F_{ind}, G_{ind}, parámetros del material dependientes del tiempo y la temperatura
a = (a_1, a_2, a_3) dirección de la magnetización durante el proceso de annealing.

Superficie e interface

$e_i = K_s [1 - \{(\boldsymbol{m}_1 - \boldsymbol{m}_2) \cdot \boldsymbol{n}_1\}^2]$

Cuando el medio 2 es reemplazado por el vacío:

$$e_s = K_s[1 - (\boldsymbol{m} \cdot \boldsymbol{n})^2] \qquad (1)$$

$|K_s| \sim 10^{-3} - 10^{-4}$ J/m^2

Importante en partículas pequeñas, películas delgadas y multicapas

In cubic crystals, surface anisotropy is described to first approximation by two independent quantities [34]:

$$e_s = K_{s1}(1 - m_1^2 n_1^2 - m_2^2 n_2^2 - m_3^2 n_3^2) - 2K_{s2}(m_1 m_2 n_1 n_2 + m_1 m_3 n_1 n_3 + m_2 m_3 n_2 n_3) \qquad (2)$$

Cuando $K_{s1} = K_{s2}$,(2) = (1)

Anisotropía de intercambio

$$e_{XA} = - K_{XA} \cos\theta = - \mu_0 H_{XA} M_S \cos\theta \qquad K_{XA} > 0$$

ferro soft

antiferro hard

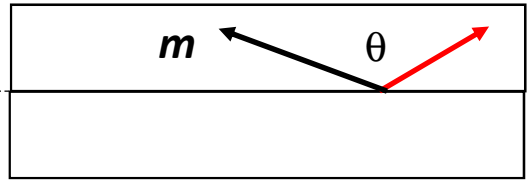

Sentido fácil

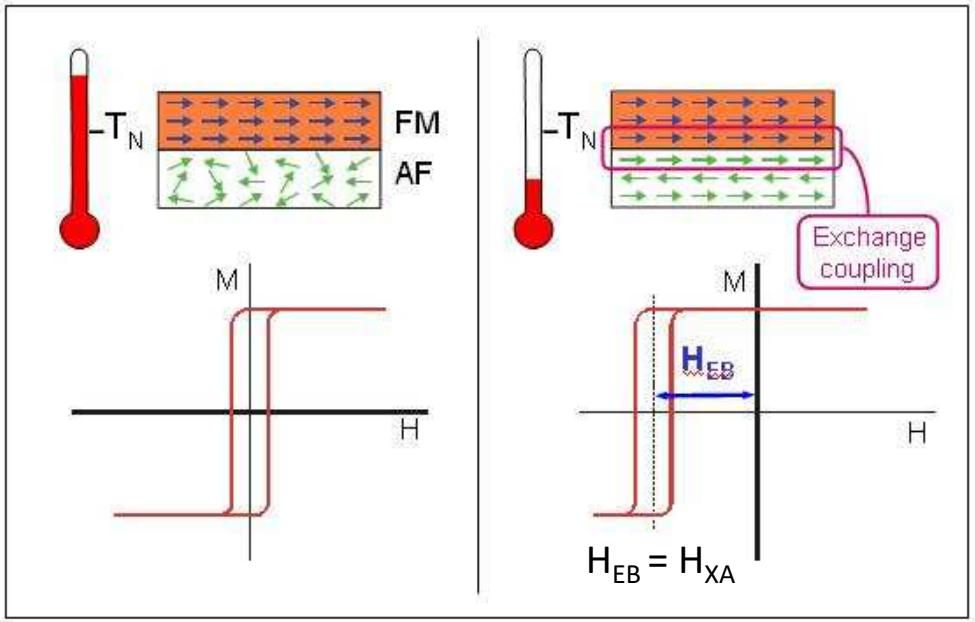

Energía Zeeman

$$E_{\mathrm{H}} = -J_{\mathrm{s}} \int \boldsymbol{H}_{\mathrm{ex}} \cdot \boldsymbol{m}\, \mathrm{d}V$$

Cuando $\boldsymbol{H}_{\mathrm{ex}}$ es constante

$$E_H = -J_S V \boldsymbol{H}_{ex} \cdot \frac{\int \boldsymbol{m} dV}{\int dV} = -V \boldsymbol{H}_{ex} \cdot \langle \boldsymbol{J} \rangle$$

Energía magnetostática
o energía de campo disperso (stray field)

Leyes de Maxwell

$$\nabla \cdot \mathbf{E} = \frac{\rho}{\varepsilon_0}$$

$$\nabla \cdot \mathbf{B} = 0$$

$$\nabla \times \mathbf{E} = -\frac{\partial \mathbf{B}}{\partial t}$$

$$\nabla \times \mathbf{B} = \mu_0 \mathbf{J} + \mu_0 \varepsilon_0 \frac{\partial \mathbf{E}}{\partial t}$$

$$\operatorname{div} \boldsymbol{B} = \operatorname{div} (\mu_0 \boldsymbol{H} + \boldsymbol{J}) = 0 \Rightarrow \operatorname{div} \boldsymbol{H}_\mathrm{d} = -\operatorname{div} (\boldsymbol{J}/\mu_0)$$

Campo generado por la magnetización

The sinks and sources of the magnetization act like positive and negative "*magnetic charges*" for the stray field. The field can be calculated like a field in electrostatics from the electrical charges. The only difference is that magnetic

$$E_\mathrm{d} = \tfrac{1}{2}\mu_0 \int_{\text{all space}} \boldsymbol{H}_\mathrm{d}^2 \, \mathrm{d}V = -\tfrac{1}{2} \int_{\text{sample}} \boldsymbol{H}_\mathrm{d} \cdot \boldsymbol{J} \, \mathrm{d}V \quad > 0$$

Energía asociada al stray field

A general solution of the stray field problem is given by potential theory.

Definimos “cargas” volúmétricas y superficiales como

$$\lambda_\mathrm{v} = -\mathrm{div}\,\boldsymbol{m}\,, \quad \sigma_\mathrm{s} = \boldsymbol{m}\cdot\boldsymbol{n}$$

volumen superficie

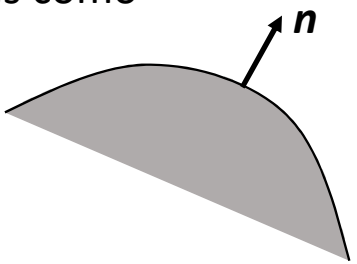

Caso de dos medios magnéticos

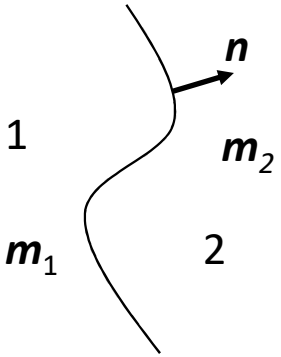

$$\sigma_\mathrm{s} = (\boldsymbol{m}_1 - \boldsymbol{m}_2)\cdot\boldsymbol{n}$$

Potencial escalar para el campo disperso

$$\Phi_\mathrm{d}(\boldsymbol{r}) = \frac{J_\mathrm{s}}{4\pi\mu_0}\left[\int \frac{\lambda_\mathrm{v}(\boldsymbol{r}')}{|\boldsymbol{r}-\boldsymbol{r}'|}\,\mathrm{d}V' + \int \frac{\sigma_\mathrm{s}(\boldsymbol{r}')}{|\boldsymbol{r}-\boldsymbol{r}'|}\,\mathrm{d}S'\right]$$

campo disperso

$$\boldsymbol{H}_\mathrm{d}(\boldsymbol{r}) = -\mathbf{grad}\;\Phi_\mathrm{d}(\boldsymbol{r})$$

Energía magnetostática

$$E_\mathrm{d} = \tfrac{1}{2}J_\mathrm{s}\left[\int \lambda_\mathrm{v}(\boldsymbol{r})\Phi_\mathrm{d}(\boldsymbol{r})\,\mathrm{d}V + \int \sigma_\mathrm{s}(\boldsymbol{r})\Phi_\mathrm{d}(\boldsymbol{r})\,\mathrm{d}S\right]$$

$$\mathbf{h}_i = \sum_j \left[-\frac{\boldsymbol{\mu}_j}{|\mathbf{r}_{ij}|^3} + \frac{3(\boldsymbol{\mu}_j \cdot \mathbf{r}_{ij})\mathbf{r}_{ij}}{|\mathbf{r}_{ij}|^5} \right]$$

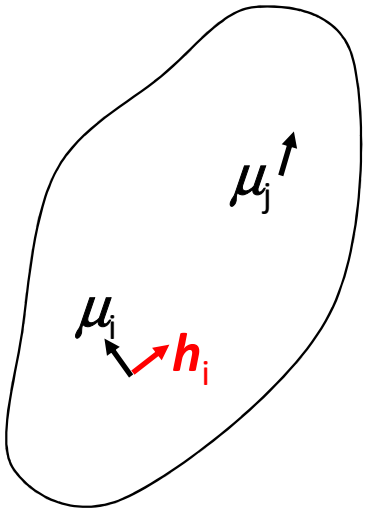

$$\mathcal{E}_M = -\frac{1}{2} \sum_i \boldsymbol{\mu}_i \cdot \mathbf{h}_i,$$

$$\mathcal{E}_M = -\frac{1}{2} \int \mathbf{M} \cdot \mathbf{H}' \, d\tau,$$

$$\nabla \cdot \mathbf{B} = 0,$$

$$\mathbf{B} = \mathbf{H} + 4\pi \mathbf{M},$$

$$\mathbf{H} = -\nabla U$$

$$\nabla^2 U_{\text{in}} = 4\pi \nabla \cdot \mathbf{M} \qquad \nabla^2 U_{\text{out}} = 0$$

$$U_{\text{in}} = U_{\text{out}}\,; \qquad \frac{\partial U_{\text{in}}}{\partial n} - \frac{\partial U_{\text{out}}}{\partial n} = 4\pi \mathbf{M} \cdot \mathbf{n}$$

$$U(\mathbf{r}) = \left(- \int \frac{\nabla' \cdot \mathbf{M}(\mathbf{r}')}{|\mathbf{r} - \mathbf{r}'|} \, d\tau' + \int \frac{\mathbf{n} \cdot \mathbf{M}(\mathbf{r}')}{|\mathbf{r} - \mathbf{r}'|} \, dS' \right)$$

$$\mathbf{H} = -\nabla U.$$

$$\int \mathbf{H}' \cdot \mathbf{B}' d\tau = -\int \mathbf{B}' \cdot \nabla U d\tau = -\int [\nabla \cdot (U\mathbf{B}') - U\nabla \cdot \mathbf{B}'] d\tau,$$

$$\nabla \cdot \mathbf{B} = 0,$$

Teorema divergencia

$$\int \mathbf{H}' \cdot \mathbf{B}' d\tau = -\int \mathbf{n} \cdot U\mathbf{B}' dS,$$

$$\int_{\text{all space}} \mathbf{H}' \cdot \mathbf{B}' d\tau = 0.$$

$$\int_{\text{all space}} \mathbf{H}' \cdot \mathbf{B}' d\tau = 0.$$

$$\mathbf{B}' = \mathbf{H}' + 4\pi \mathbf{M},$$

$$\int_{\text{all space}} \mathbf{H}' \cdot (\mathbf{H}' + 4\pi \mathbf{M}) d\tau = 0.$$

$$\frac{1}{2} \int \boldsymbol{M} \cdot \boldsymbol{H}' d\tau = \frac{1}{8\pi} \int H'^2 d\tau$$

$$\mathcal{E}_{\mathrm{M}} = \frac{1}{8\pi} \int_{\text{all space}} H'^2 \, d\tau > 0$$

ejemplo

Lámina delgada infinita

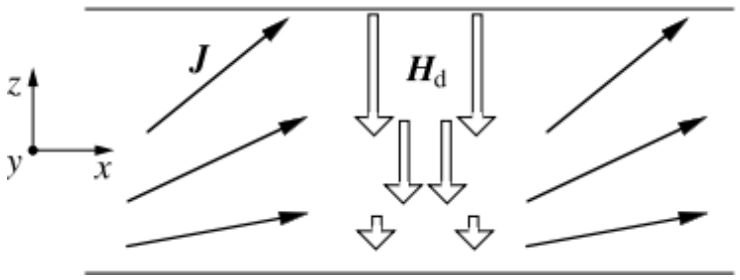

Por simetría

$$\boldsymbol{J} = \boldsymbol{J}(z) = J_S[\,\boldsymbol{m}_1(z)\boldsymbol{i} + \boldsymbol{m}_2(z)\boldsymbol{j} + \boldsymbol{m}_3(z)\boldsymbol{k}]$$

$$\mathrm{div}\boldsymbol{H}_\mathrm{d} = -\mathrm{div}\,(\boldsymbol{J}/\mu_0)$$

⇩

$$\boldsymbol{H}_\mathrm{d} = -\,(J_\mathrm{s}/\mu_0)\,m_3(z)\boldsymbol{k} + \boldsymbol{Cte}$$

⇩ ⤡ nula

$$e_\mathrm{d} = -\tfrac{1}{2}\boldsymbol{H}_\mathrm{d}\cdot\boldsymbol{J} = \left(J_\mathrm{s}^2/2\mu_0\right)m_3^2(z)$$

introduciendo

$$K_\mathrm{d} = J_\mathrm{s}^2/2\mu_0 \quad \Rightarrow \quad e_d = K_d m_3^2(z)$$

$$K_\mathrm{d} = J_\mathrm{s}^2/2\mu_0$$

environment). Even in cases where a stray field energy is much more difficult to calculate than by the simple formula (3.20), it will scale with the material parameter K_d. The quantity K_d becomes $2\pi M_\mathrm{s}^2$ in the Gaussian system; this means that if any calculation of a stray field energy presented in the old system is to be transferred to the SI system, the coefficient M_s^2 has to be replaced by $K_\mathrm{d}/2\pi$.

An often used dimensionless quantity is the ratio $Q = K/K_\mathrm{d}$, where K is an appropriate anisotropy coefficient. This material parameter plays a role in

elipsoide

The demagnetizing field of an ellipsoid is uniform and linearly related to the (average or uniform) magnetization $\boldsymbol{J}$ by the symmetrical demagnetizing tensor $\boldsymbol{N}$:

$$\boldsymbol{H}_\mathrm{d} = -\boldsymbol{N} \cdot \boldsymbol{J}/\mu_0 \,. \qquad \mathrm{tr}(\boldsymbol{N}) = 1$$

Tensor desmagnetizante

elipsoide

$$N_a = \tfrac{1}{2}abc \int_0^\infty \left[(a^2+\eta)\sqrt{(a^2+\eta)(b^2+\eta)(c^2+\eta)}\right]^{-1} d\eta$$

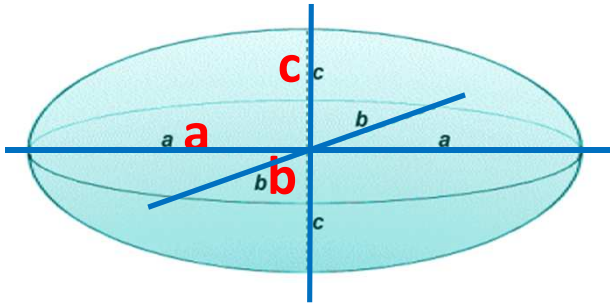

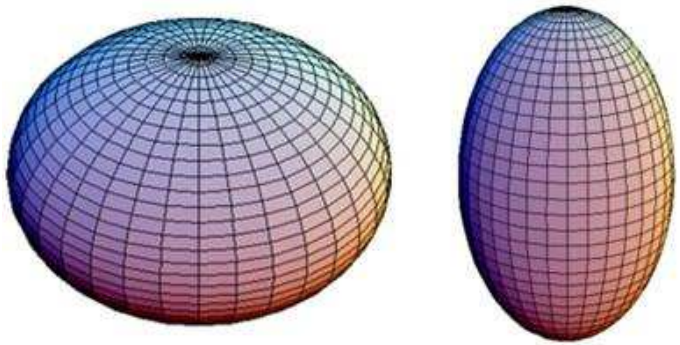

oblate spheroid *prolate spheroid*

$$\boldsymbol{H}_d = -\boldsymbol{N} \cdot \boldsymbol{J}/\mu_0 \,. \quad \text{tr}(\boldsymbol{N}) = 1$$

elipsoide

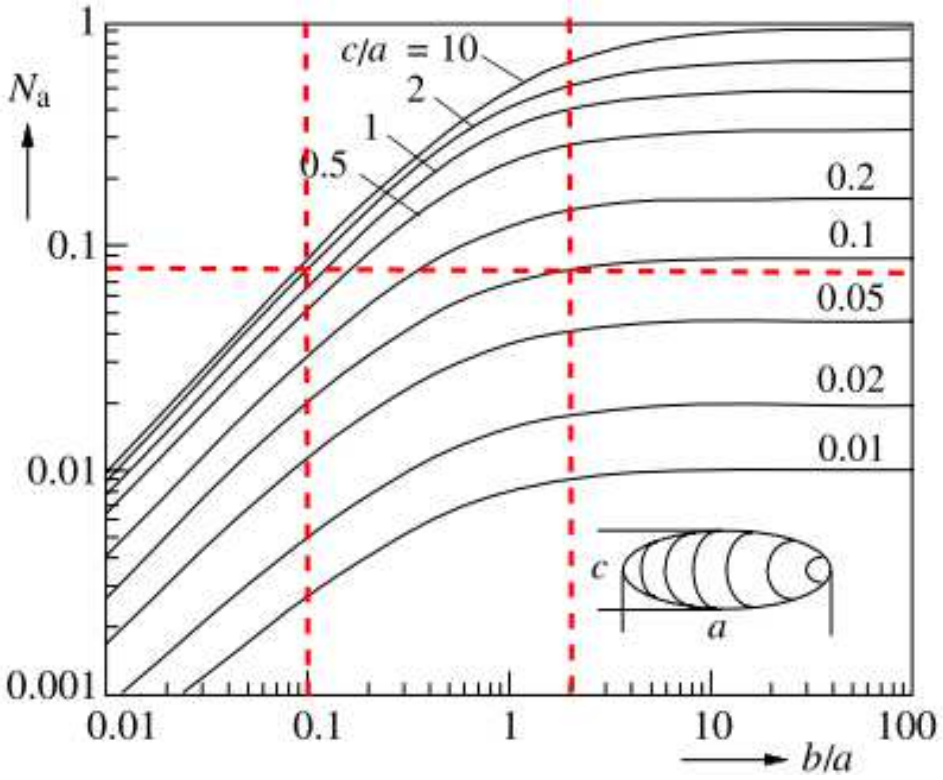
1
N_a
0.1
0.01
0.001
0.01
0.1
1
10
100
b/a
c/a = 10
2
1
0.5
0.2
0.1
0.05
0.02
0.01
c
a

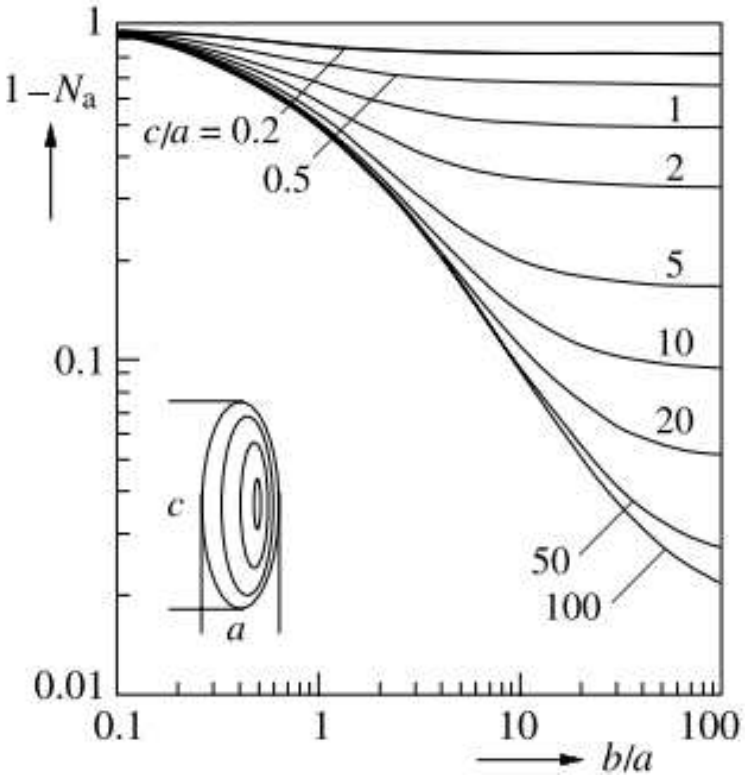
1
$1-N_a$
0.1
0.01
0.1
1
10
100
b/a
c/a = 0.2
0.5
1
2
5
10
20
50
100
c
a

Elipsoide de revolución a, c, c

prolado

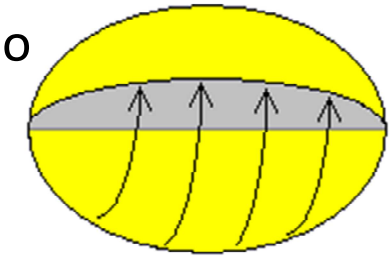

(a, c, c)

$$N_a = \frac{\alpha^2}{1-\alpha^2}\left[\frac{1}{\sqrt{1-\alpha^2}}\text{arcsinh}\left(\frac{\sqrt{1-\alpha^2}}{\alpha}\right) - 1\right]$$

$$N_c = \tfrac{1}{2}(1 - N_a) \qquad \alpha = c/a < 1$$

oblado

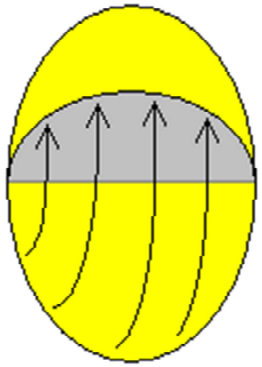

$$N_a = \frac{\alpha^2}{\alpha^2-1}\left[1 - \frac{1}{\sqrt{\alpha^2-1}}\arcsin\left(\frac{\sqrt{\alpha^2-1}}{\alpha}\right)\right]$$

$$N_c = \tfrac{1}{2}(1 - N_a) \qquad \alpha > 1$$

Energía magnetostática

a partir de

$$E_{\mathrm{d}} = -\tfrac{1}{2} \int_{\text{sample}} \boldsymbol{H}_{\mathrm{d}} \cdot \boldsymbol{J}\, \mathrm{d}V \qquad \boldsymbol{H}_{\mathrm{d}} = -\boldsymbol{N} \cdot \boldsymbol{J}/\mu_0$$

$$\boldsymbol{J} \cdot \boldsymbol{H}_d = -\frac{\boldsymbol{J}^T \cdot \boldsymbol{N} \cdot \boldsymbol{J}}{\mu_0} = \frac{J_S^2}{\mu_0} \boldsymbol{m}^T \cdot \boldsymbol{N} \cdot \boldsymbol{m} = -\frac{J_S^2}{\mu_0} \left(N_x m_x^2 + N_y m_y^2 + N_z\, m_z^2\right)$$

Para ***m*** uniforme:

$$E_d = \frac{J_S^2 V}{2\mu_0} \left(N_x m_x^2 + N_y m_y^2 + N_z\, m_z^2\right) = K_d V \left(N_x m_x^2 + N_y m_y^2 + N_z\, m_z^2\right)$$

Elementos finitos

(C) Three-Dimensional Finite Element Calculations. Except in favourable cases as discussed in (B), stray field calculations are complex and regularly call for numerical evaluation. The problem is that the direct computation of the sixfold integral (3.19b) would be forbiddingly time consuming. One should therefore try to perform as many steps as possible analytically. One

Elementos con forma de figuras o cuerpos rectangulares ⇨ Integrales múltiples de la función $F_{000} = 1/r$

En el procedimiento de cálculo aparecen, entre otras, las integrales y funciones analíticas

$$F_{000} = 1/r,$$

$$F_{100} = \int F_{000}\mathrm{d}x = L_x,$$

$$F_{200} = \int F_{100}\mathrm{d}x = xL_x - r,$$

$$F_{110} = \int F_{100}\mathrm{d}y = yL_x + xL_y - P_z,$$

$$F_{210} = xyL_x + \tfrac{1}{2}(u-w)L_y - xP_z - \tfrac{1}{2}yr,$$

$$F_{111} = xyL_z + xzL_y + yzL_x - \tfrac{1}{2}(xP_x + yP_y + zP_z),$$

$$F_{220} = \tfrac{1}{2}\left[x(v-w)L_x + y(u-w)L_y\right] - xyP_z + \tfrac{1}{6}r(3w - r^2)$$

donde

$$u = x^2, \quad v = y^2, \quad w = z^2, \quad r = \sqrt{u + c + w},$$

$$L_x = \operatorname{arctanh}(x/r) = \tfrac{1}{2} \ln [(r + x)/(r - x)] \quad \text{etc.},$$

$$P_x = x \arctan(yz/xr) \quad \text{etc.},$$

$$L_x = 0 \quad \text{and} \quad P_x = 0 \quad \text{for} \quad x = 0 \quad \text{etc.},$$

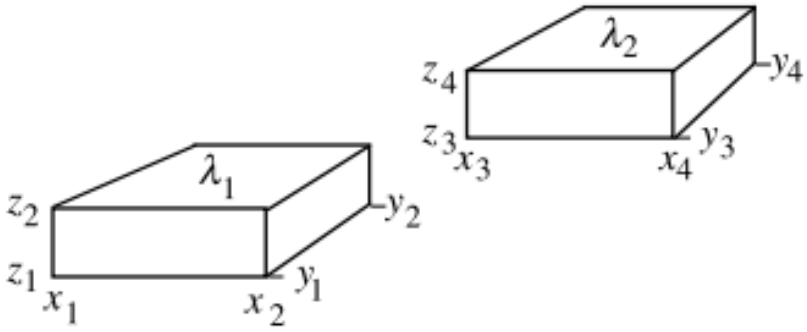

Por ejemplo la interacción entre dos celdas prismas Rectangulares con densidades de carga λ_1 y λ_2 resulta ser

$$E_{\text{inter}} = \tfrac{1}{2\pi} \lambda_1 \lambda_2 K_d [F_2(z_4 - z_1) - F_2(z_4 - z_2) - F_2(z_3 - z_1) + F_2(z_3 - z_2)]$$

con

$$F_2(z) = F_1(y_4 - y_1,\, z) - F_1(y_4 - y_2,\, z) - F_1(y_3 - y_1,\, z) + F_1(y_3 - y_2,\, z)$$

y

$$F_1(y,\, z) = F(x_4 - x_1,\, y,\, z) - F(x_4 - x_2,\, y,\, z) - F(x_3 - x_1,\, y,\, z) + F(x_3 - x_2,\, y,\, z)$$

siendo $F = F_{222}$

Mientras que la autoenergía resulta

Ver artículo de Aharoni

$$E_{\text{self}} = \frac{2}{\pi}\lambda_1^2 K_{\text{d}}\big[F(x_2-x_1,\, y_2-y_1,\, z_2-z_1) - F(x_2-x_1,\, y_2-y_1,\, 0) - F(x_2-x_1,\, 0,\, z_2-z_1) - F(0,\, y_2-y_1,\, z_2-z_1) + F(x_2-x_1,\, 0,\, 0) + F(0,\, y_2-y_1,\, 0) + F(0,\, 0,\, z_2-z_1)\big] \quad (3.29)$$

$$\boxed{F = F_{222}}$$

Entonces, para un conjunto de n celdas:

$$E_{\text{d}} = \frac{1}{2}\sum_{i=1}^{n}\sum_{j=1}^{n} E_{\text{inter}}(i,j)$$

El resultado se puede usar para obtener la componente del tensor desmagnetizante N^{en} en la dirección en la que ha sido saturado el cuerpo de volumen V,

$$E_{\text{d}} = N^{\text{en}} K_{\text{d}} V$$

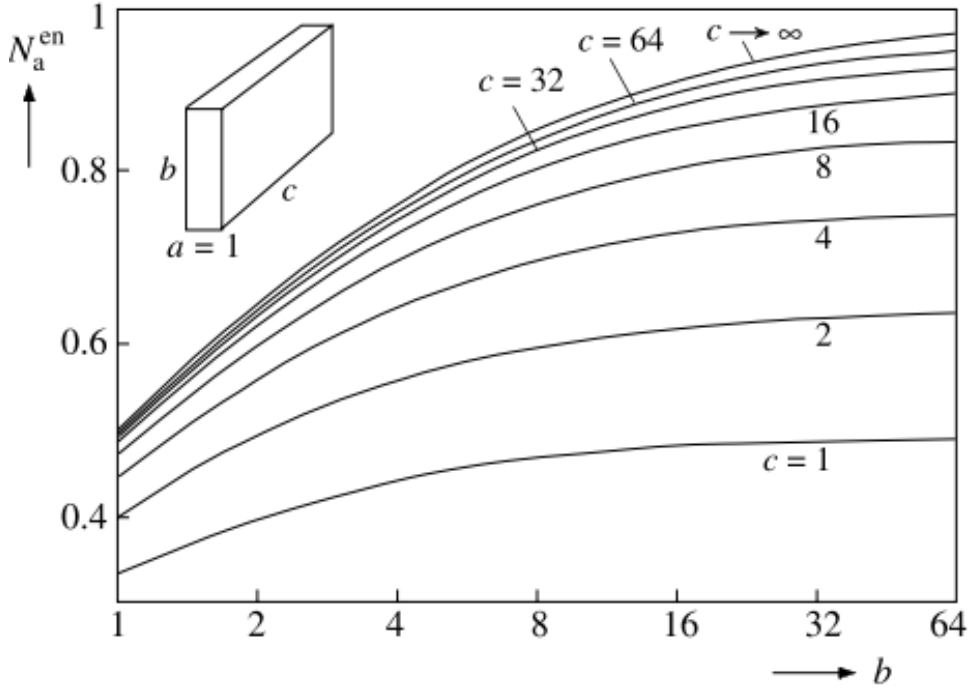

Ecuaciones micromagnéticas

Energía libre total

$$\underbrace{E_{\mathrm{tot}}}_{\text{Total}} = \int \Big[\underbrace{A(\mathbf{grad}\, \boldsymbol{m})^2}_{\text{exchange}} + \underbrace{F_{\mathrm{an}}(\boldsymbol{m})}_{\text{anisotropy}} - \underbrace{\boldsymbol{H}_{\mathrm{ex}} \cdot \boldsymbol{J}}_{\text{ext. field}} + \underbrace{\tfrac{1}{2}\boldsymbol{H}_{\mathrm{d}} \cdot \boldsymbol{J}}_{\text{stray field}}$$

$$- \underbrace{\boldsymbol{\sigma}_{\mathrm{ex}} \cdot \boldsymbol{\varepsilon}^0}_{\text{ext. stress}} + \underbrace{\tfrac{1}{2}(\boldsymbol{p}_{\mathrm{e}} - \boldsymbol{\varepsilon}^0) \cdot \boldsymbol{c} \cdot (\boldsymbol{p}_{\mathrm{e}} - \boldsymbol{\varepsilon}^0)}_{\text{magnetostrictive}} \Big] \mathrm{d}V \,.$$

- Simétrico, esfuerzos no-magnéticos
- Deformación magnetoelástica "libre"
- Distorsión real
- Tensor de constantes elásticas

to approach the free deformation $\boldsymbol{\varepsilon}^0$. The magnetization vector is $\boldsymbol{J} = J_{\mathrm{s}}\boldsymbol{m}$ with $\boldsymbol{m}^2 = 1$. The stray field $\boldsymbol{H}_{\mathrm{d}}$ and the distortion $\boldsymbol{p}_{\mathrm{e}}$ must fulfil the following conditions:

$$\mathrm{div}\,(\mu_0 \boldsymbol{H}_{\mathrm{d}} + \boldsymbol{J}) = 0\,, \qquad \mathbf{rot}\, \boldsymbol{H}_{\mathrm{d}} = 0\,, \tag{3.62a}$$

$$\mathrm{Div}\,[\boldsymbol{c} \cdot (\boldsymbol{p}_{\mathrm{e}} - \boldsymbol{\varepsilon}^0)] = 0\,, \qquad \mathbf{Rot}\, \boldsymbol{p}_{\mathrm{e}} = 0\,. \tag{3.62b}$$

Elastic effects introduce a new degree of freedom. A magnetic body will deform under the influence of a magnetic interaction, and this deformation is described by an (in general) asymmetric tensor of elastic *distortion* $\boldsymbol{p}(\boldsymbol{r})$. The distortion consists of a symmetric part, the tensor of elastic strain $\boldsymbol{\varepsilon}$, and an antisymmetric part, the tensor of lattice rotations $\boldsymbol{\omega}$. In a systematic approach, all parts of the free energy are expanded with respect to $\boldsymbol{p}$. Because magneto-elastic effects are small in ferromagnetism, these expansions only have to include the smallest non-vanishing order. The elements of zero

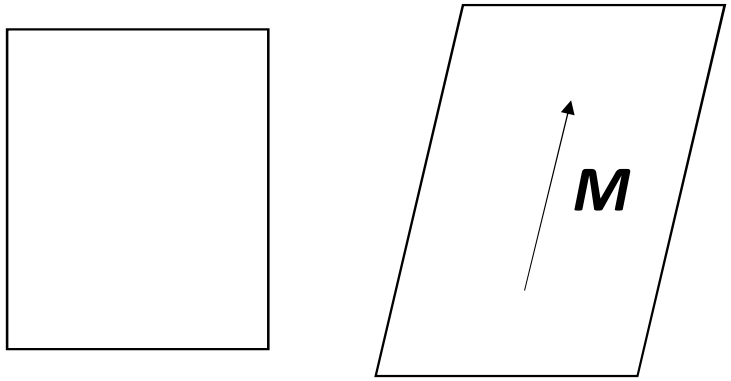

Tensor asimétrico de distorsión $\boldsymbol{p}(\boldsymbol{r})$

Tensor simétrico de deformación $\boldsymbol{\varepsilon}(\boldsymbol{r})$

Tensor de rotaciones de red $\boldsymbol{\omega}(\boldsymbol{r})$

La energía libre total y las condiciones (3.62) conducen a:

$$
\begin{aligned}
&-2A\Delta \boldsymbol{m} + \mathbf{grad}_{\boldsymbol{m}} F_{\mathrm{an}}(\boldsymbol{m}) - (\boldsymbol{H}_{\mathrm{ex}} + \boldsymbol{H}_{\mathrm{d}}) J_{\mathrm{s}} \\
&\quad -(\boldsymbol{\sigma}_{\mathrm{ex}} + \boldsymbol{\sigma}^{\mathrm{ms}})\, \mathbf{Grad}_{\boldsymbol{m}}\, \boldsymbol{\varepsilon}^{0} = f_{\mathrm{L}} \boldsymbol{m}\,, \\
&\mathrm{div}\,(\mu_0 \boldsymbol{H}_{\mathrm{d}} + \boldsymbol{J}) = 0\,, \qquad \mathbf{rot}\boldsymbol{H}_{\mathrm{d}} = 0\,, \\
&\mathrm{Div}\,[\boldsymbol{c} \cdot (\boldsymbol{p}_{\mathrm{e}} - \boldsymbol{\varepsilon}^{0})] = 0\,, \qquad \mathbf{Rot}\boldsymbol{p}_{\mathrm{e}} = 0\,,
\end{aligned}
\qquad (*)
$$

En estas expresiones ***m*** es la única variable independiente.

El miembro izquierdo de (*) se puede escribir como $-J_{\mathrm{s}} \boldsymbol{H}_{\mathrm{eff}}$ donde

$$
\begin{aligned}
\boldsymbol{H}_{\mathrm{eff}} = \boldsymbol{H}_{\mathrm{ex}} + \boldsymbol{H}_{\mathrm{d}} + [&2A\triangle \boldsymbol{m} - \mathbf{grad}_{\boldsymbol{m}} F_{\mathrm{an}}(\boldsymbol{m}) \\
&+ (\boldsymbol{\sigma}_{\mathrm{ex}} + \boldsymbol{\sigma}^{\mathrm{ms}}) \mathbf{Grad}_{\boldsymbol{m}} \boldsymbol{\varepsilon}^{0}(\boldsymbol{m})]/J_{\mathrm{s}}\,.
\end{aligned}
$$

contributions of domain walls. (iii) The magnetostrictive deformations, although small in scale, play an important technical role. The noise of common transformers has its origin in these effects. Because it is difficult to find a

Campo efectivo

El campo efectivo queda definido a menos de un vector en la dirección de ***J*** porque el torque $\boldsymbol{J} \times \boldsymbol{H}_{\text{eff}}$ no se vería afectado. Un ejemplo ocurre de hecho en el caso de la anisotropía uniaxial que puede escribirse en las dos formas alternativas:

$$F_{\text{an}}^{\text{a}}(\boldsymbol{m}) = K(m_1^2 + m_2^2) \qquad F_{\text{an}}^{\text{b}}(\boldsymbol{m}) = K(1 - m_3^2)$$

$$\boldsymbol{H}_{\text{eff}}^{\text{a}} = -\mathbf{Grad}_{\mathbf{m}} F_{\text{an}} = -2K(m_1, m_2, 0) \qquad \boldsymbol{H}_{\text{eff}}^{\text{b}} = -\mathbf{Grad}_{\mathbf{m}} F_{\text{an}} = 2K(0, 0, m_3)$$

$$\boldsymbol{H}_{\text{eff}}^{\text{b}} - \boldsymbol{H}_{\text{eff}}^{\text{a}} = 2K\boldsymbol{m} = 2K\boldsymbol{J}/J_S\mu_0$$

El estado de equilibrio corresponde a $\boldsymbol{J} \times \boldsymbol{H}_{\text{eff}} = 0$

Dinámica de la magnetización

(C) Magnetization Dynamics. Dynamically, the angular momentum connected with the magnetic moment will lead to a gyrotropic reaction if a torque $\boldsymbol{J} \times \boldsymbol{H}_{\text{eff}}$ exists, which is described by the following equation:

$$\dot{\boldsymbol{J}} = -\gamma \boldsymbol{J} \times \boldsymbol{H}_{\text{eff}}\,, \gamma = \mu_0 ge/2m_{\text{e}} = g \cdot 1.105 \cdot 10^5 \text{m/As} \qquad (3.66)$$

where γ is the gyromagnetic ratio. The Landé factor g has values close to 2 for many ferromagnetic materials.

Losses in magnetism in general can have many origins: eddy currents, macroscopic discontinuities (Barkhausen jumps), diffusion and the reorientation of lattice defects, or spin-scattering mechanisms can all introduce irreversibilities and losses.

the *Landau-Lifshitz-Gilbert* equation [22, 575]. In this equation a dimensionless empirical damping factor α_{G} is introduced to describe unspecified local or quasi-local dissipative phenomena, like the relaxation of magnetic impurities or the scattering of spin waves on lattice defects. We thus obtain: $\dot{\boldsymbol{m}} = -\gamma_{\text{G}} \boldsymbol{m} \times \boldsymbol{H}_{\text{eff}} - \alpha_{\text{G}} \boldsymbol{m} \times \dot{\boldsymbol{m}}$

Gilbert vs. L&L

The *Gilbert* equation (3.66a) is a variant of the original Landau-Lifshitz equation:

$$\dot{\boldsymbol{m}} = -\gamma_{\mathrm{LL}} \boldsymbol{m} \times \boldsymbol{H}_{\mathrm{eff}} + \alpha_{\mathrm{LL}} \boldsymbol{m} \times (\boldsymbol{m} \times \boldsymbol{H}_{\mathrm{eff}}). \qquad (3.66\mathrm{b})$$

The two equations can be converted into each other [34] by inserting (3.66b) into (3.66a) and comparing the coefficients of the vector expressions, which leads to: $\gamma_{\mathrm{LL}} = \gamma_G/(1+\alpha_{\mathrm{G}}^2)$ and $\alpha_{\mathrm{LL}} = \alpha_{\mathrm{G}}\gamma_{\mathrm{G}}/(1+\alpha_{\mathrm{G}}^2)$. For zero damping $\alpha_{\mathrm{LL}} = \alpha_{\mathrm{G}} = 0$ we have $\gamma_{\mathrm{LL}} = \gamma_{\mathrm{G}} = \gamma$ of (3.66). The choice between the two versions of the dynamic equations is often based on mathematical convenience.

At low frequencies the loss term in the dynamic equation is predominant. The gyromagnetic term has to be taken into account only in the GHz range.

In not too complicated cases—such as in small particles and thin film elements—it is possible to numerically calculate the equilibrium structure of a given configuration. One approach consists in using the dynamical versions (3.66a) or (3.66b) of the micromagnetic equations. A selected starting con-

Longitudes características

(E) Length Scales and Computability of Magnetic Microstructures. The micromagnetic equations are non-linear and non-local coupled partial differential equations of second order. They are non-linear in the magnetization components because of the condition $\boldsymbol{m}^2 = 1$. Nonlinearities arise, in addition, in cubic crystals, where higher powers of the magnetization components appear in the anisotropy energy (3.9). The non-locality of the equations results from the stray field term $\boldsymbol{H}_\mathrm{d}$ and from the magneto-elastic displacement vector $\boldsymbol{u}$

Only in few cases can the micromagnetic equations be linearized and solved analytically.

Numerical techniques suffer from the wide range of *scales* appearing in magnetic problems

Cúbico, anisotropía baja-media

hexagonal, anisotropía alta

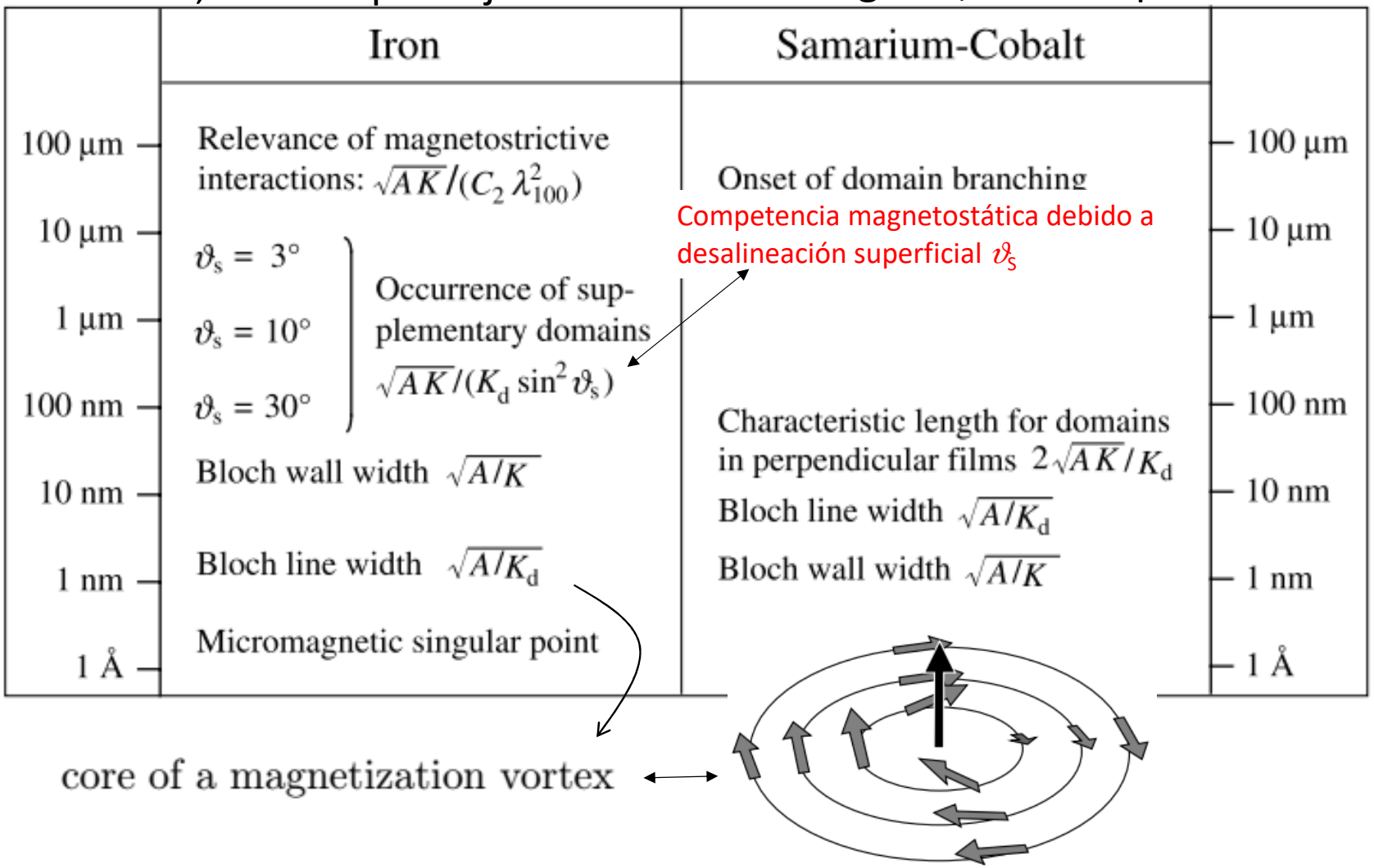

Competencia magnetostática debido a desalineación superficial ϑ_s

core of a magnetization vortex

Contribuciones a la energía de un ferromagneto

Energy term	Coefficient	Definition	Range
Exchange energy	A [J/m]	Material constant	$10^{-12} - 2 \cdot 10^{-11}$ J/m
Anisotropy energies	$K_u, K_c \ldots$ [J/m^3]	Material constants	$\pm(10^2 - 2 \cdot 10^7)$ J/m^3
External field energy	$H_{ex} J_s$ [J/m^3]	H_{ex} = external field J_s = saturation magnetization	Open, depending on field magnitude
Stray field energy	K_d [J/m^3]	$K_d = J_s^2 / 2\,\mu_0$	$0 - 3 \cdot 10^6$ J/m^3
External stress energy	$\sigma_{ex}\lambda$ [J/m^3]	σ_{ex} = external stress λ = magnetostriction constant	Open, depending on stress magnitude
Magnetostrictive self energy	$C\,\lambda^2$ [J/m^3]	C = shear modulus	$0 - 10^3$ J/m^3
Anisotropía superficial	**K_S**	**Constante del material**	**$10^{-4} - 10^{-3}$ J/m^2**

Película delgada

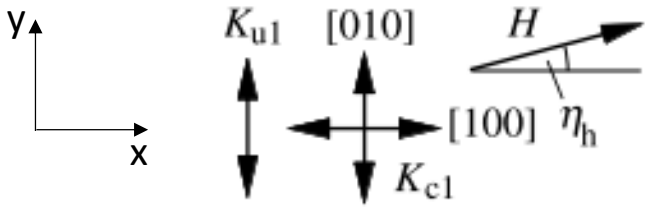

Densidad de energía

$$e_K = K_c sen^2\varphi cos^2\varphi + K_u cos^2\varphi$$

$$e_{tot} = K_c sen^2\varphi cos^2\varphi + K_u cos^2\varphi - HJ_S cos(\varphi - \eta)$$

Energía reducida

$$\left.\begin{array}{r} g_K = Q_c sen^2\varphi cos^2\varphi + Q_u cos^2\varphi \\ h = \mu_0 H/J_S \\ m = cos(\varphi - \eta) \end{array}\right\} \quad g_{tot} = g_K - 2hm \quad \left\{\begin{array}{l} \dfrac{dg_{tot}}{dm} = \dfrac{dg_K}{dm} - 2h = 0 \\ \boxed{h = \dfrac{1}{2}\dfrac{dg_K}{dm}} \end{array}\right.$$

$$Q = \frac{K}{K_d} \qquad K_d = \frac{J_S^2}{2\mu_0}$$

Película delgada

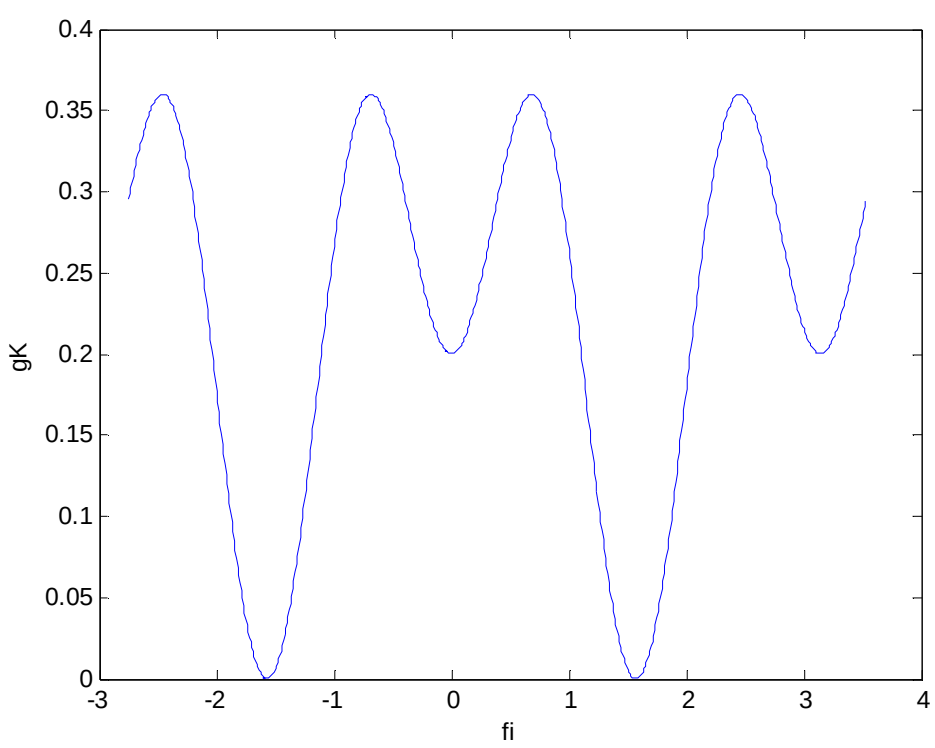

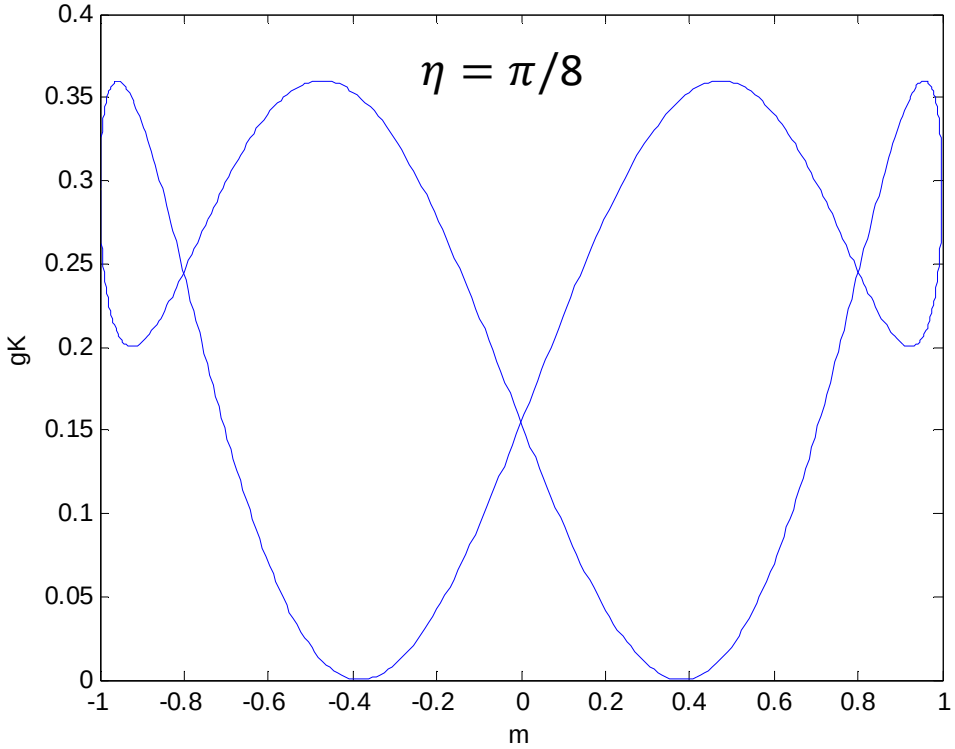

Película delgada

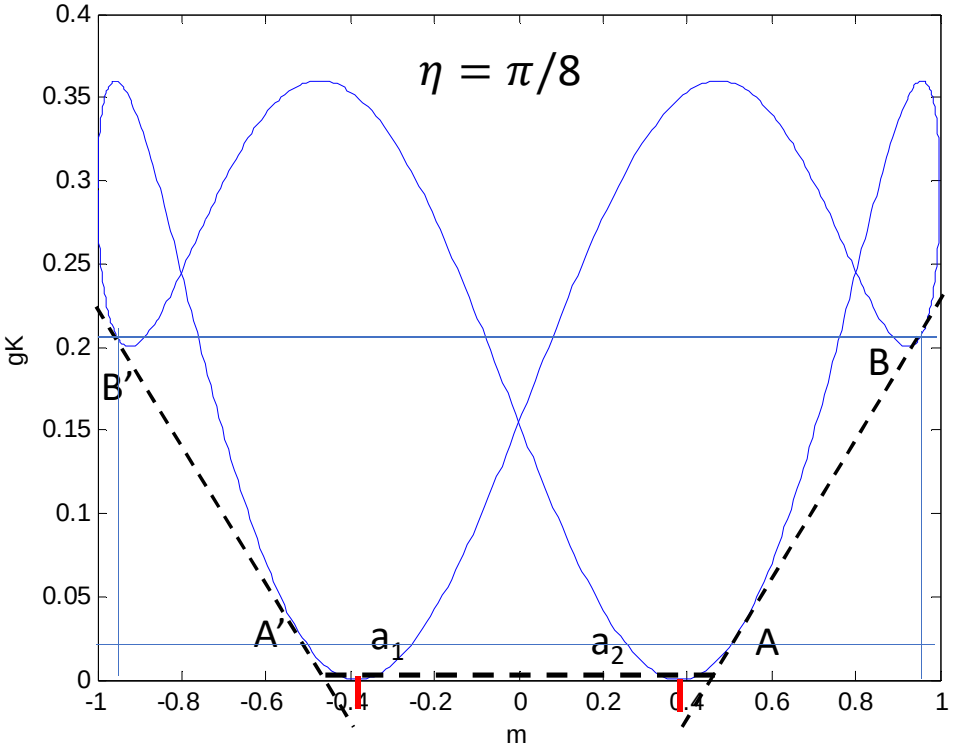

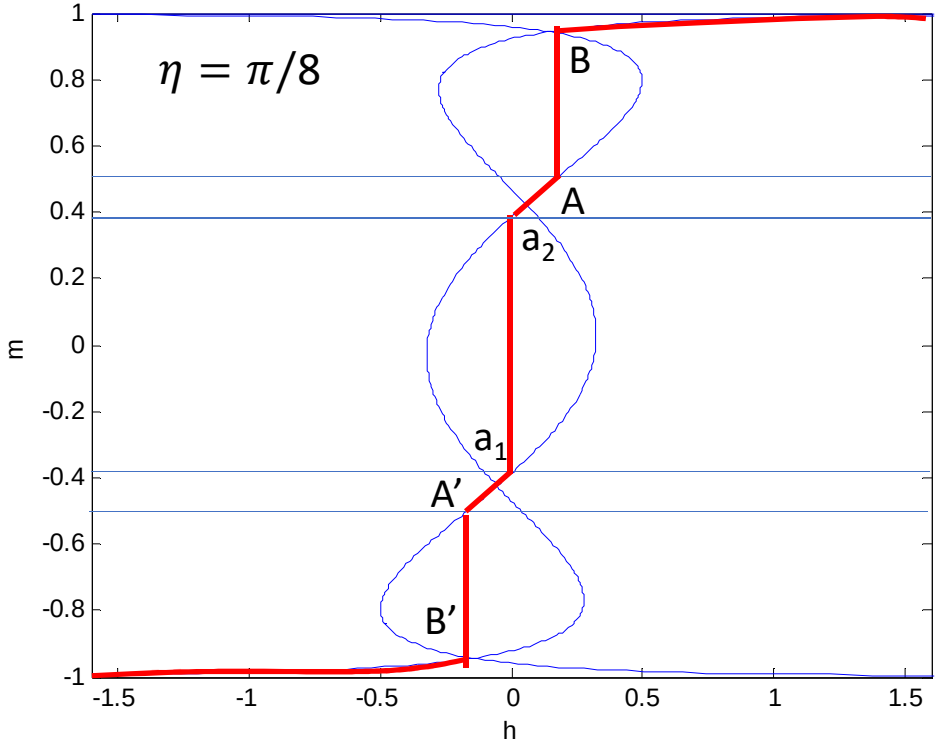

Película delgada

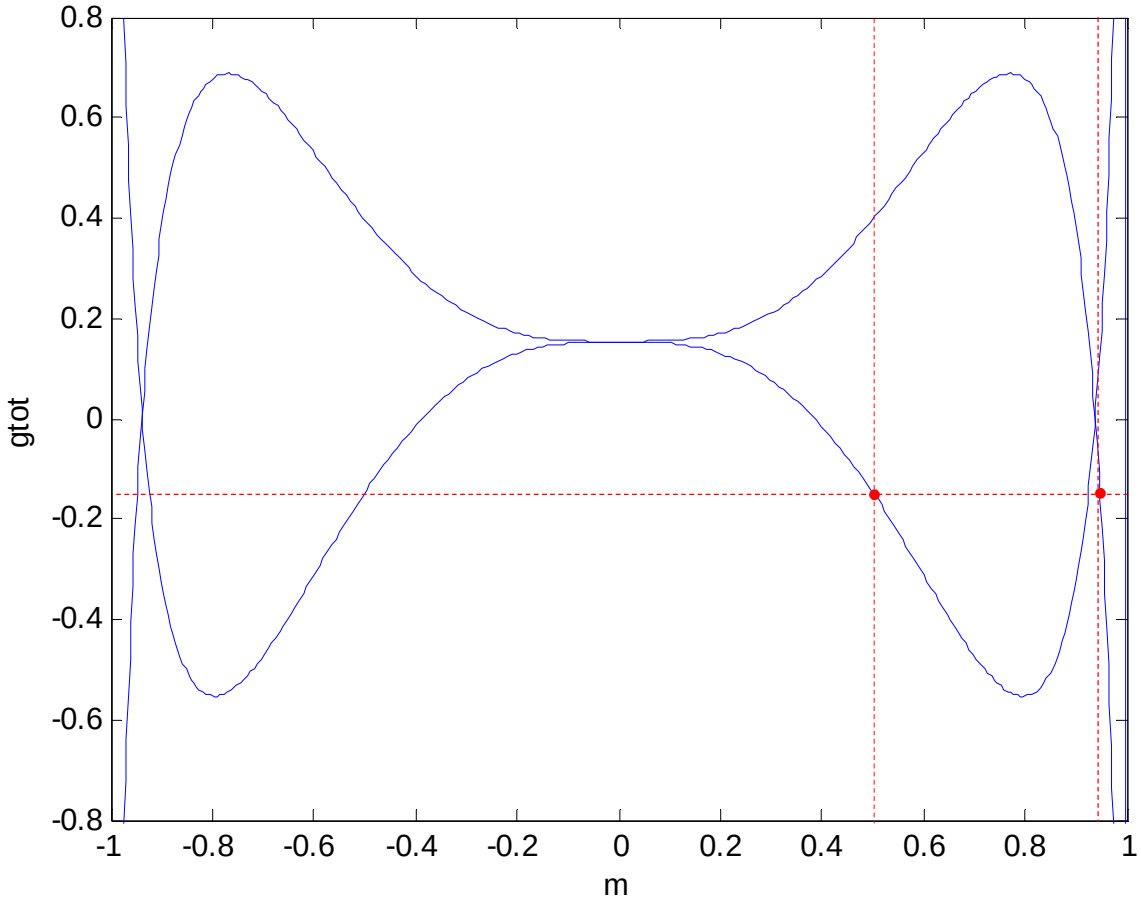

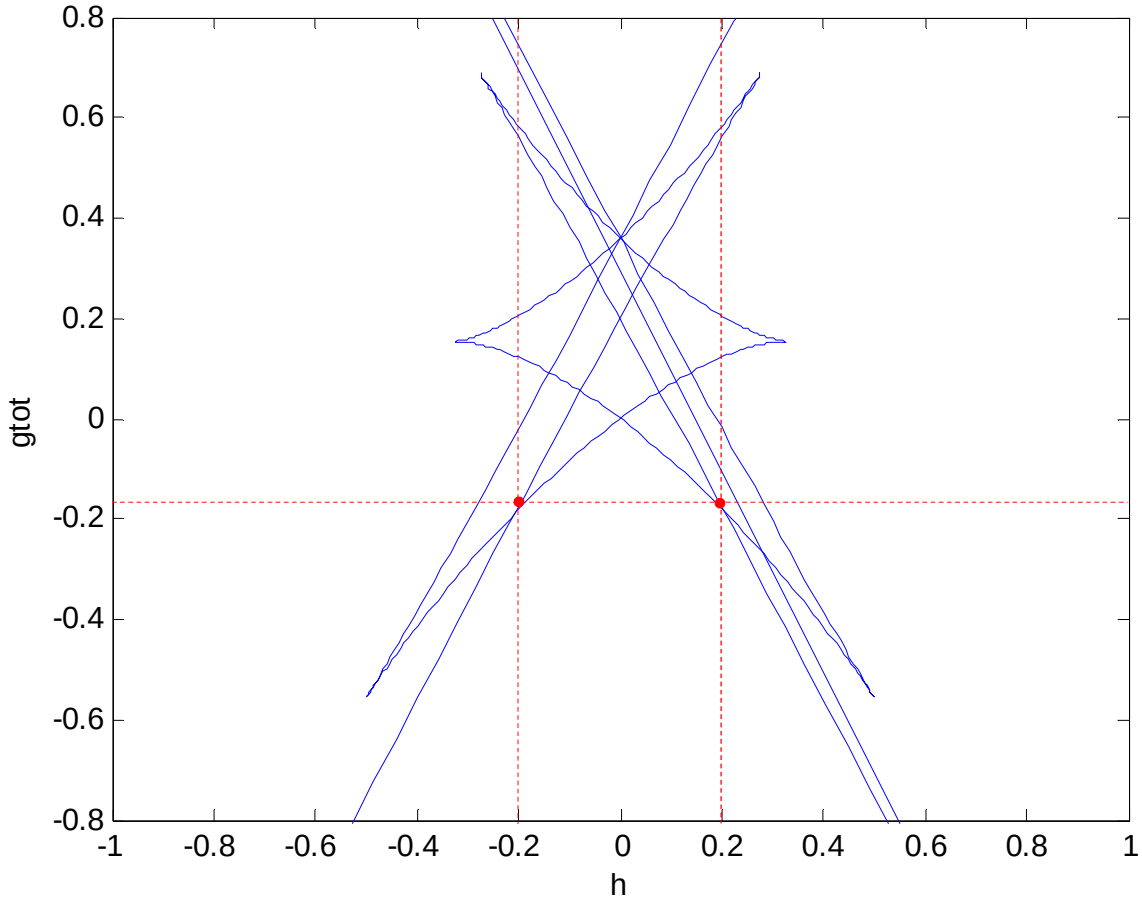
0.8
0.6
0.4
0.2
0
-0.2
-0.4
-0.6
-0.8
gtot
-1
-0.8
-0.6
-0.4
-0.2
0
0.2
0.4
0.6
0.8
1
h

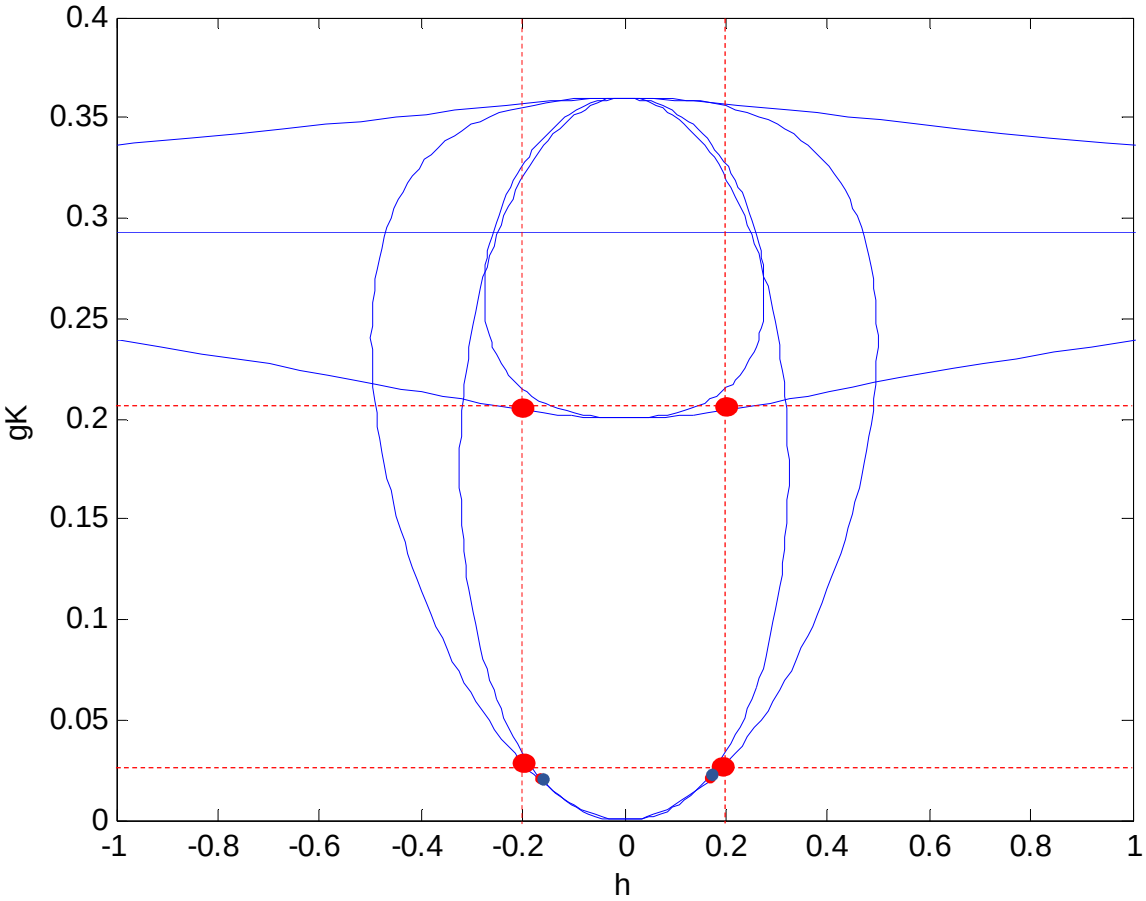
0.4
0.35
0.3
0.25
0.2
0.15
0.1
0.05
0
gK
-1
-0.8
-0.6
-0.4
-0.2
0
0.2
0.4
0.6
0.8
1
h

Película delgada

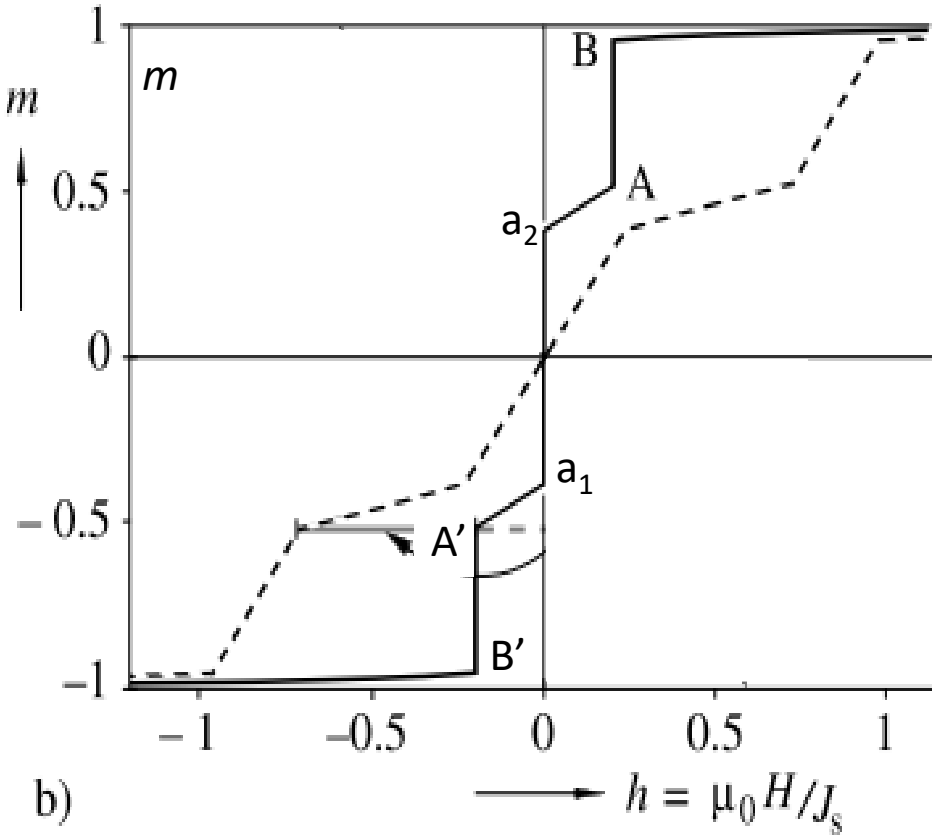

NP uniaxial

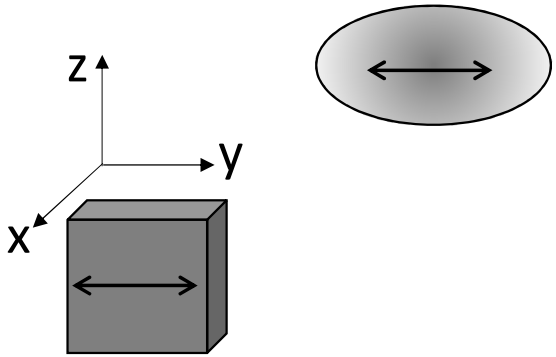

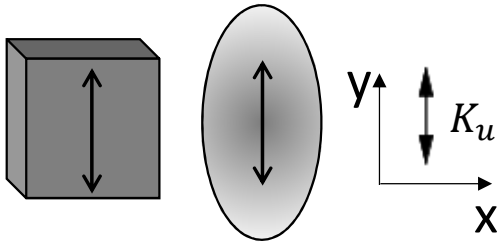

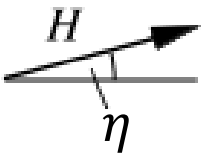

Densidad de energía

$$e_K = K_u cos^2\varphi$$

$$e_{tot} = K_u cos^2\varphi - HJ_S cos(\varphi - \eta)$$

Energía reducida

$$\left.\begin{aligned} g_K &= Q_u cos^2\varphi \\ h &= \mu_0 H/J_S \\ m &= cos(\varphi - \eta) \end{aligned}\right\} \quad g_{tot} = g_K - 2hm \quad \left\{\begin{aligned} &\frac{dg_{tot}}{dm} = \frac{dg_K}{dm} - 2h = 0 \\ &\boxed{h = \frac{1}{2}\frac{dg_K}{dm}} \end{aligned}\right.$$

NP uniaxial

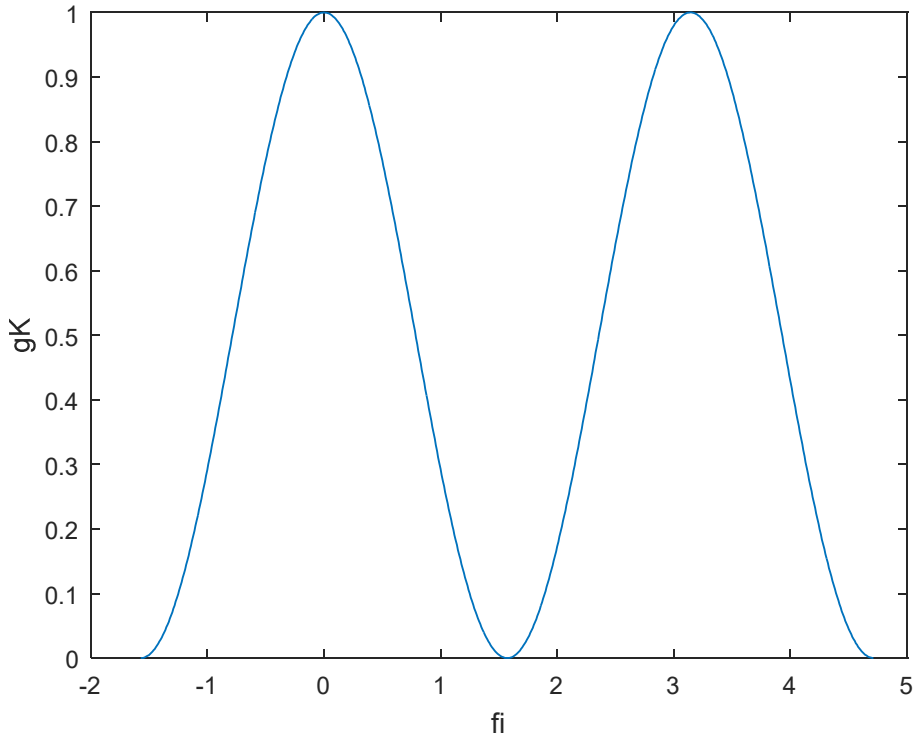
gK
fi
1
0.9
0.8
0.7
0.6
0.5
0.4
0.3
0.2
0.1
0
-2
-1
0
1
2
3
4
5

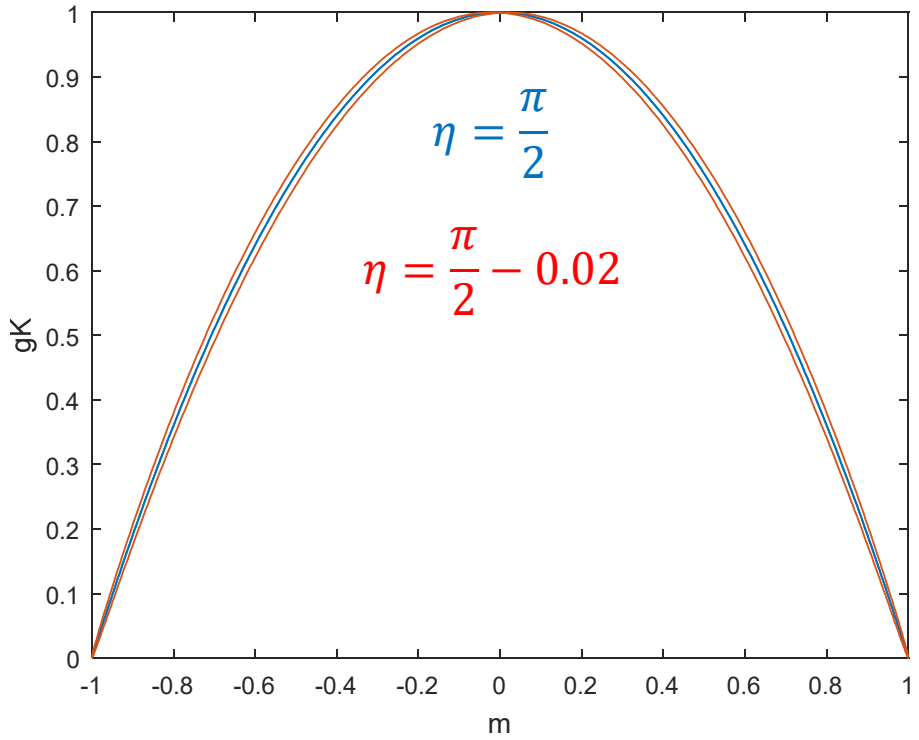
$\eta = \frac{\pi}{2}$
$\eta = \frac{\pi}{2} - 0.02$
gK
m
1
0.9
0.8
0.7
0.6
0.5
0.4
0.3
0.2
0.1
0
-1
-0.8
-0.6
-0.4
-0.2
0
0.2
0.4
0.6
0.8
1

NP uniaxial

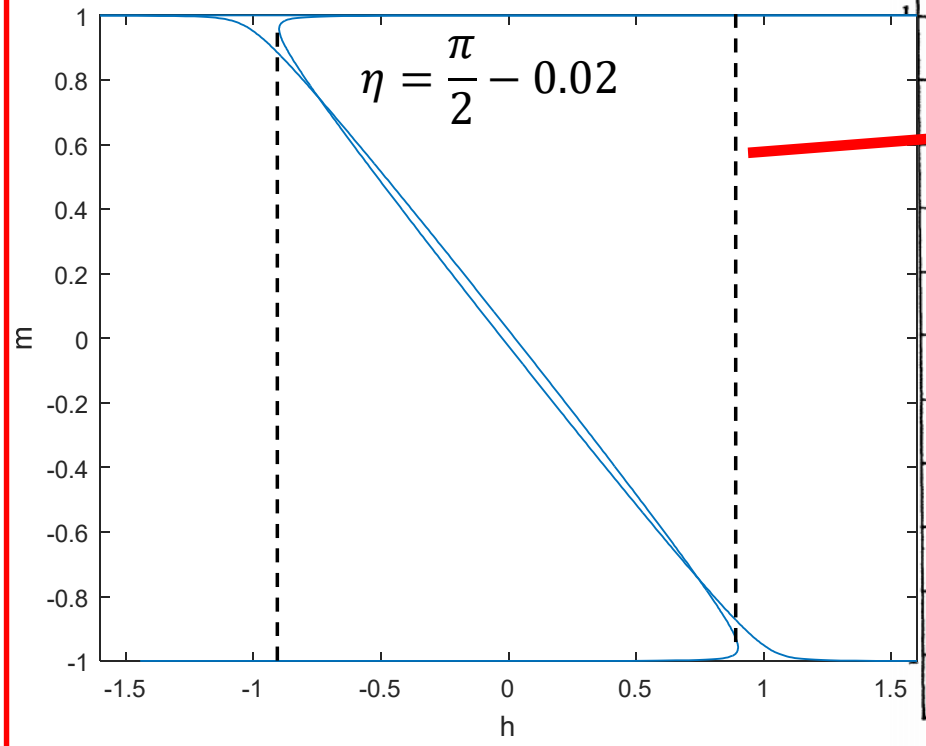
$\eta = \frac{\pi}{2} - 0.02$
m
h
1
0.8
0.6
0.4
0.2
0
-0.2
-0.4
-0.6
-0.8
-1
-1.5
-1
-0.5
0
0.5
1
1.5

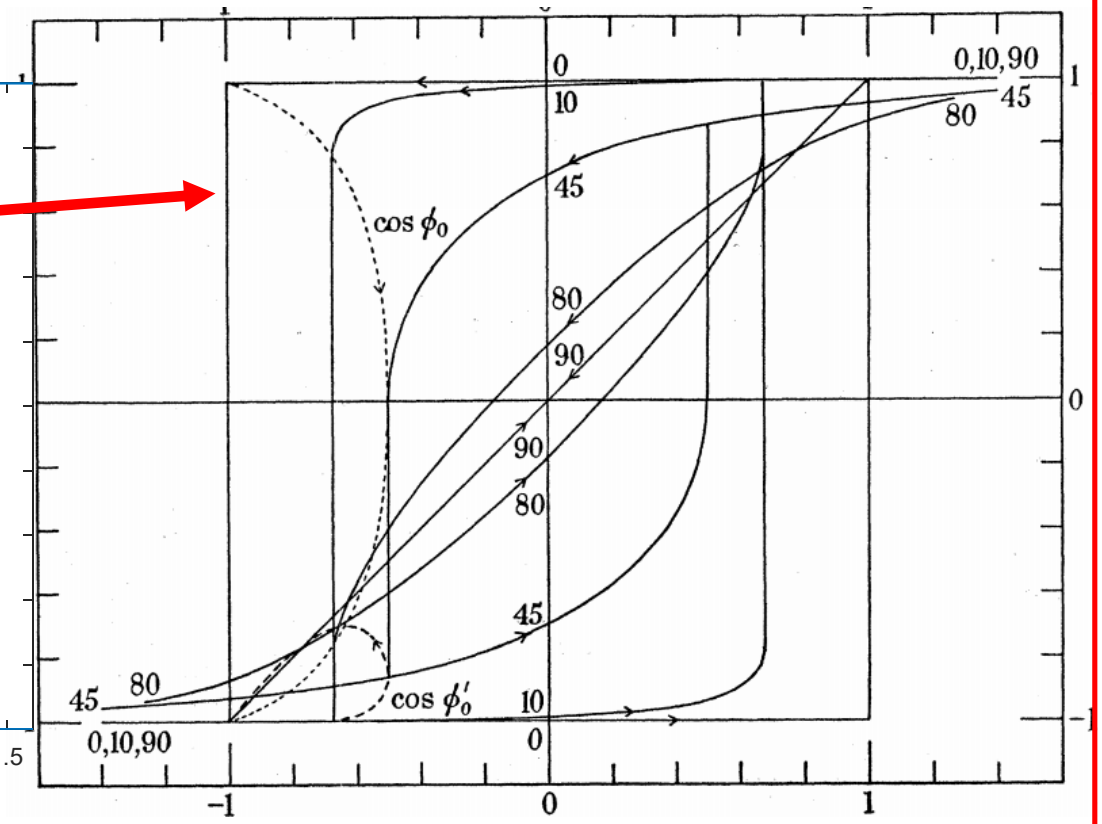
0
10
45
80
90
0,10,90
cos ϕ_0
cos ϕ_0'
−1
0
1

NP uniaxial

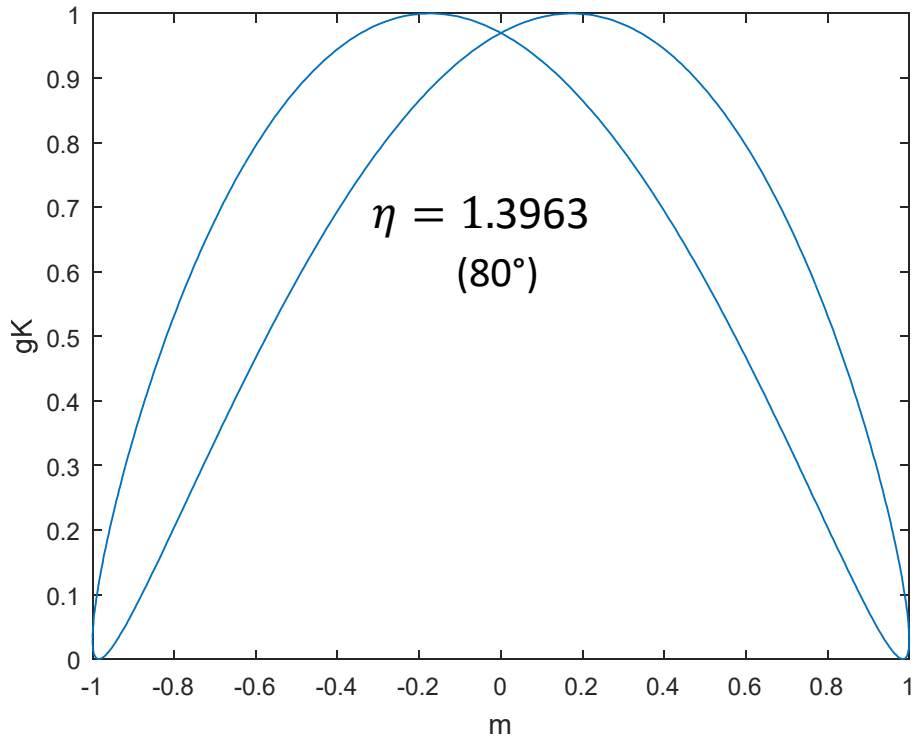
$\eta = 1.3963$
(80°)
gK
m
1
0.9
0.8
0.7
0.6
0.5
0.4
0.3
0.2
0.1
0
-1
-0.8
-0.6
-0.4
-0.2
0
0.2
0.4
0.6
0.8
1

NP uniaxial

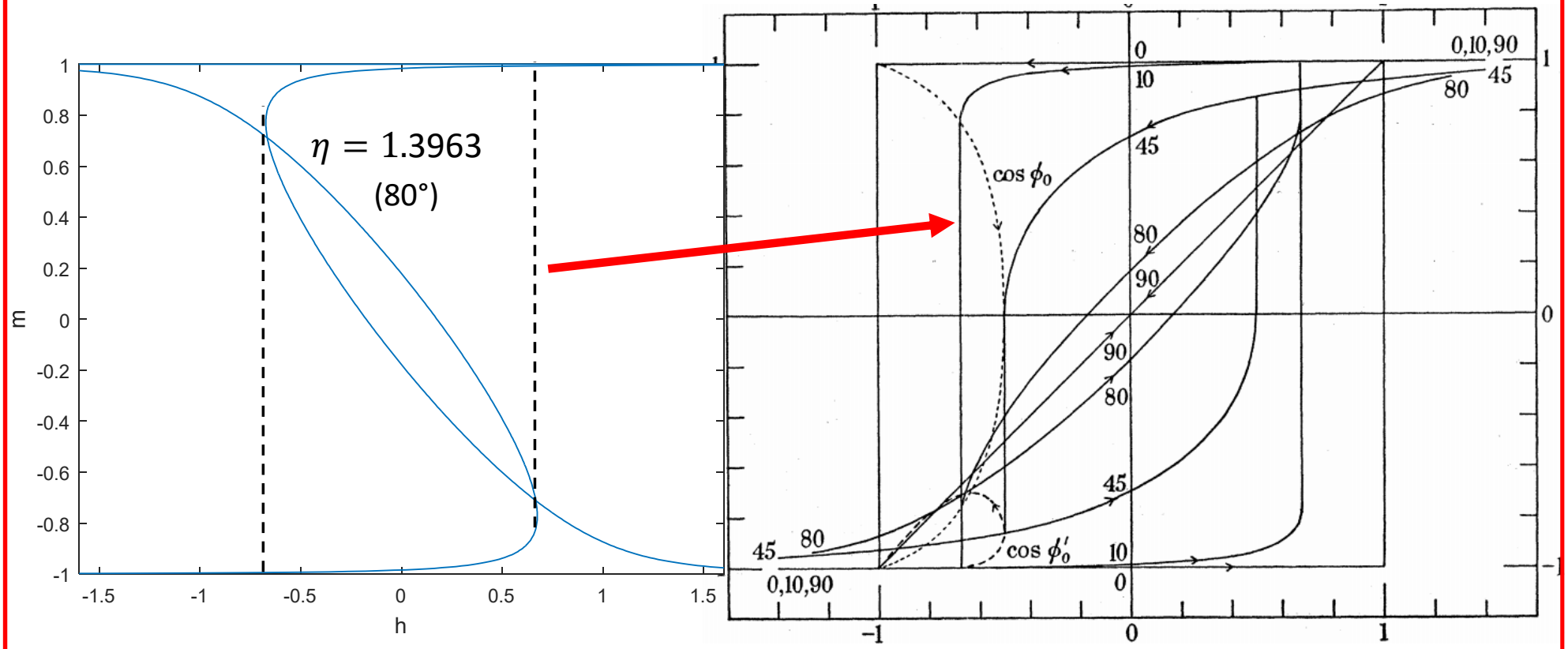
$\eta = 1.3963$
(80°)
m
h
1
0.8
0.6
0.4
0.2
0
-0.2
-0.4
-0.6
-0.8
-1
-1.5
-1
-0.5
0
0.5
1
1.5
$\cos\phi_0$
$\cos\phi_0'$
0,10,90
10
45
80
90
0
1
-1

NP uniaxial

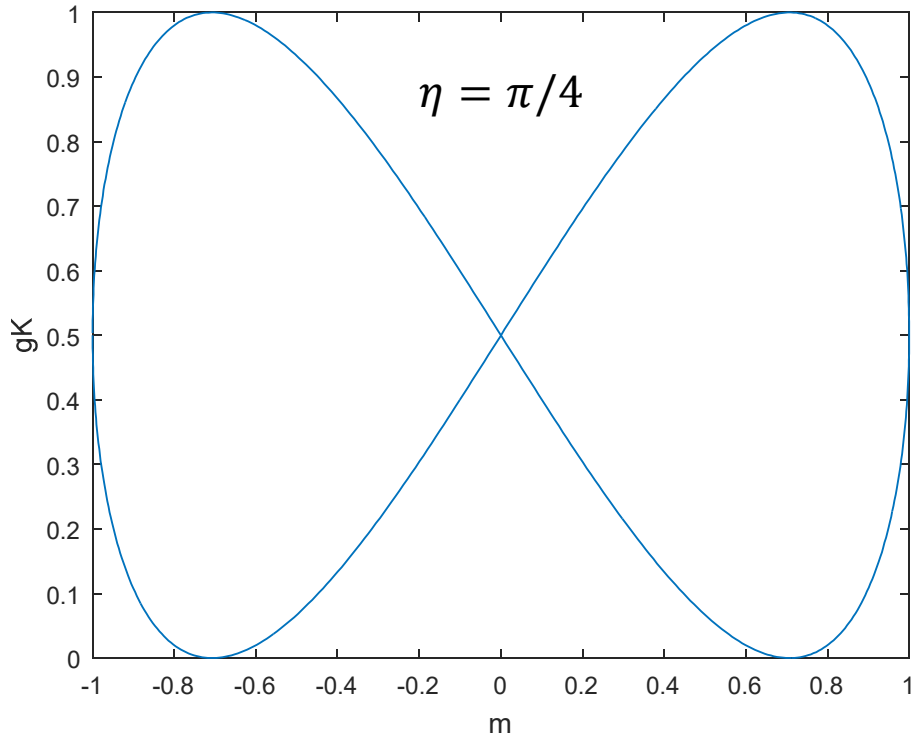

NP uniaxial

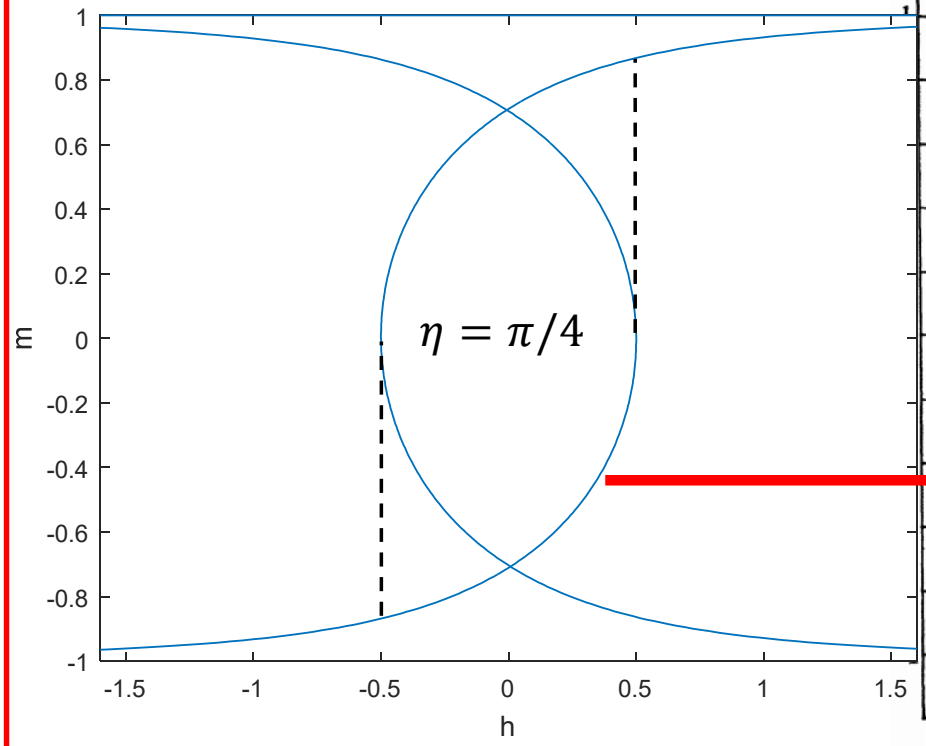

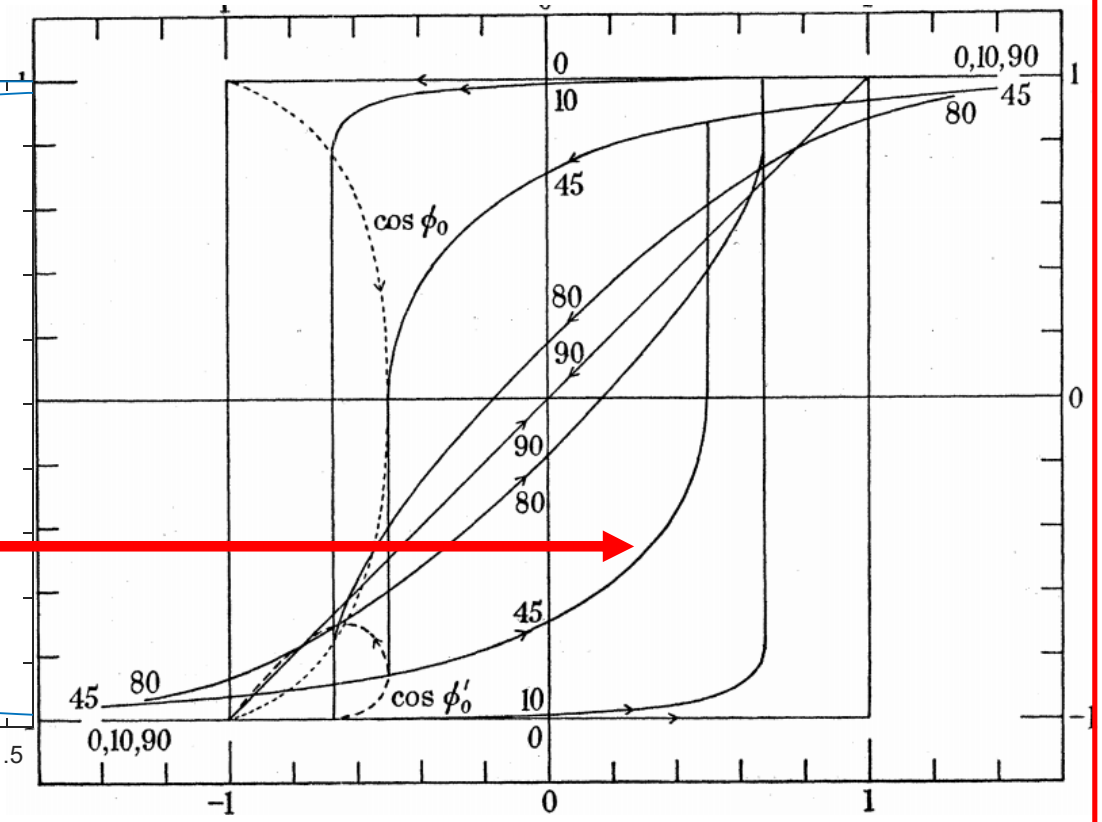

NP uniaxial

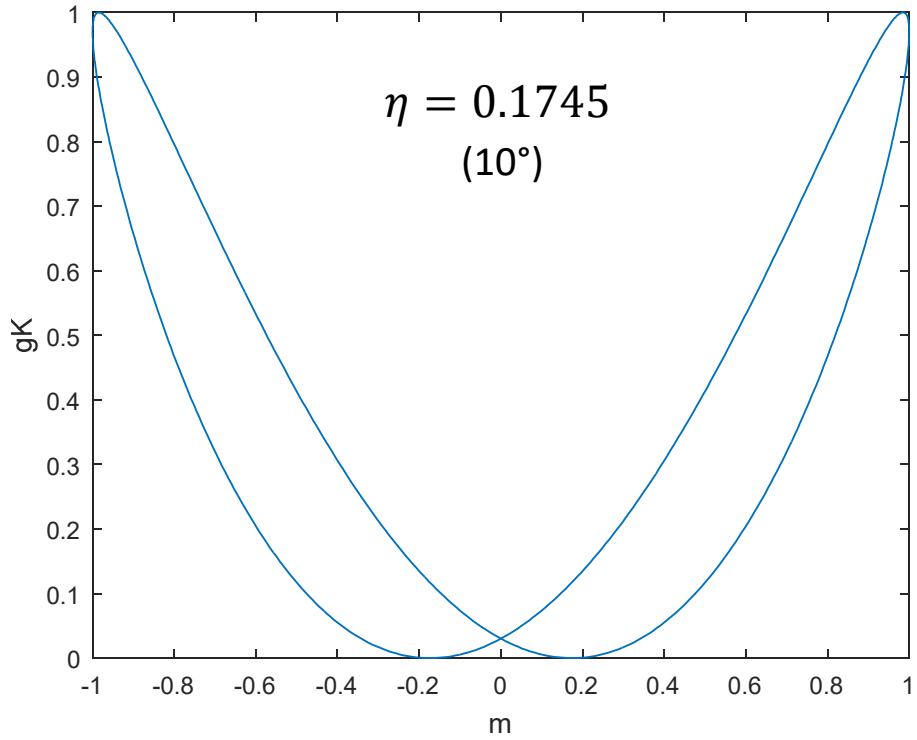
$\eta = 0.1745$
(10°)
gK
m
1
0.9
0.8
0.7
0.6
0.5
0.4
0.3
0.2
0.1
0
-1
-0.8
-0.6
-0.4
-0.2
0
0.2
0.4
0.6
0.8
1

NP uniaxial

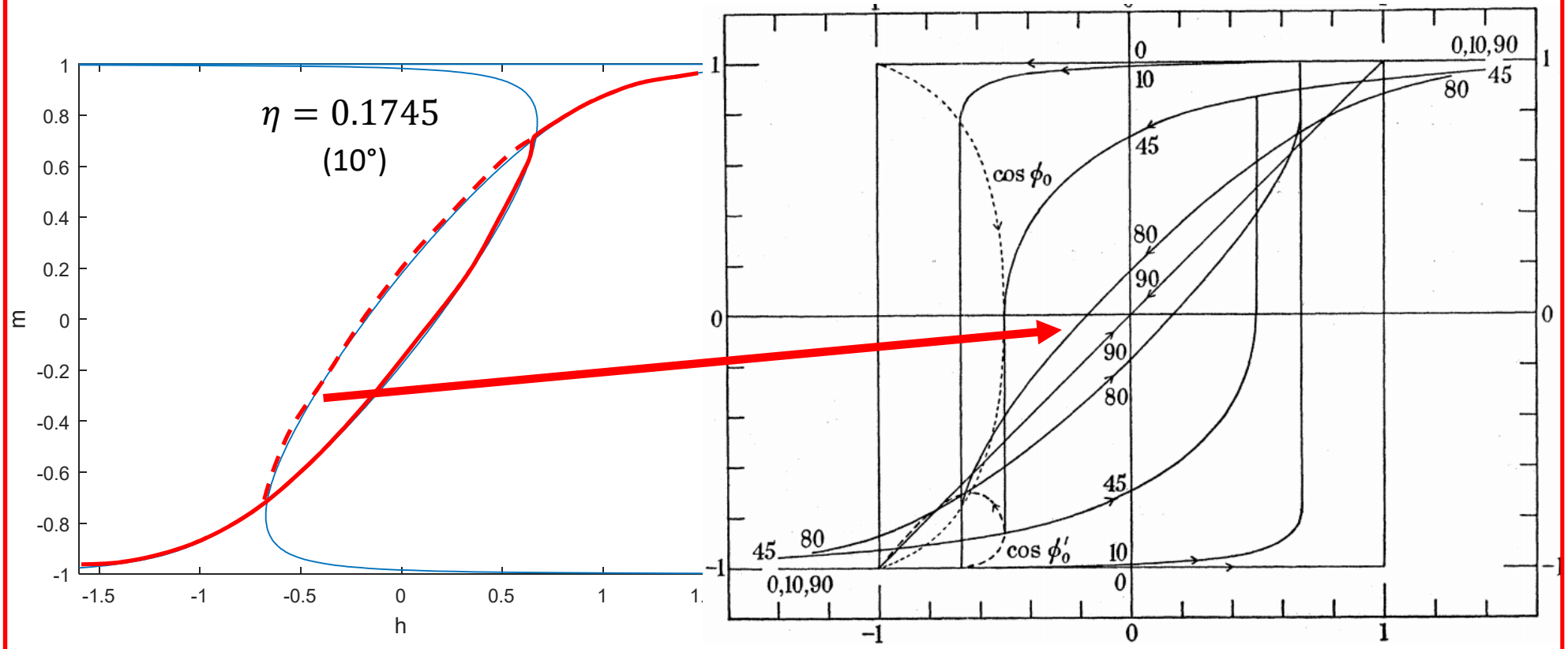
$\eta = 0.1745$
(10°)
m
h
1
0.8
0.6
0.4
0.2
0
-0.2
-0.4
-0.6
-0.8
-1
-1.5
-1
-0.5
0
0.5
1
cos ϕ_0
cos ϕ_0'
0
10
45
80
90
0,10,90

NP uniaxial

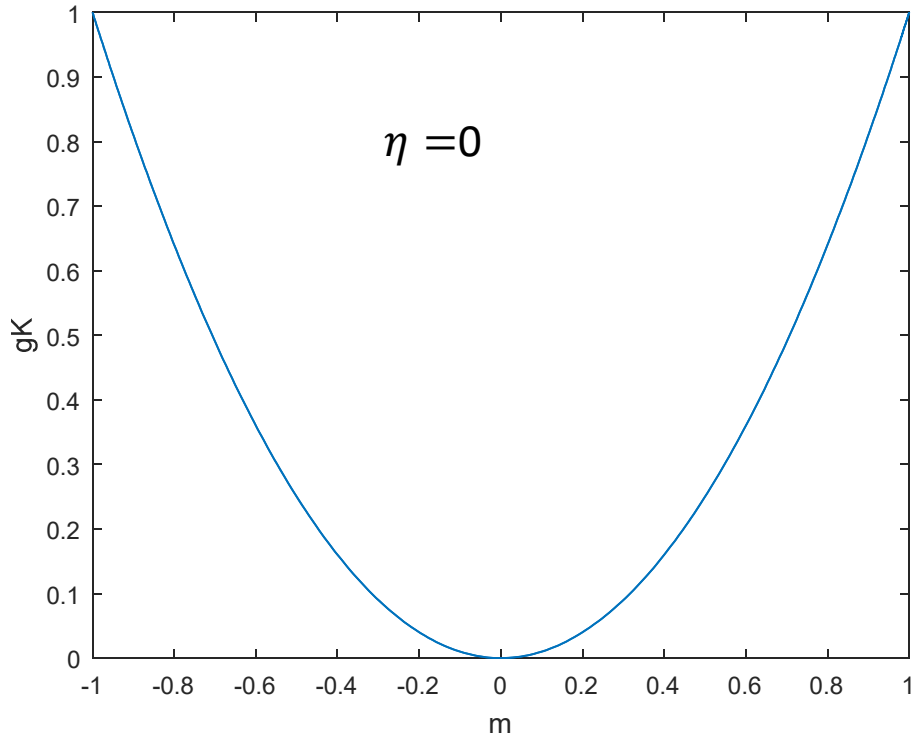

NP uniaxial

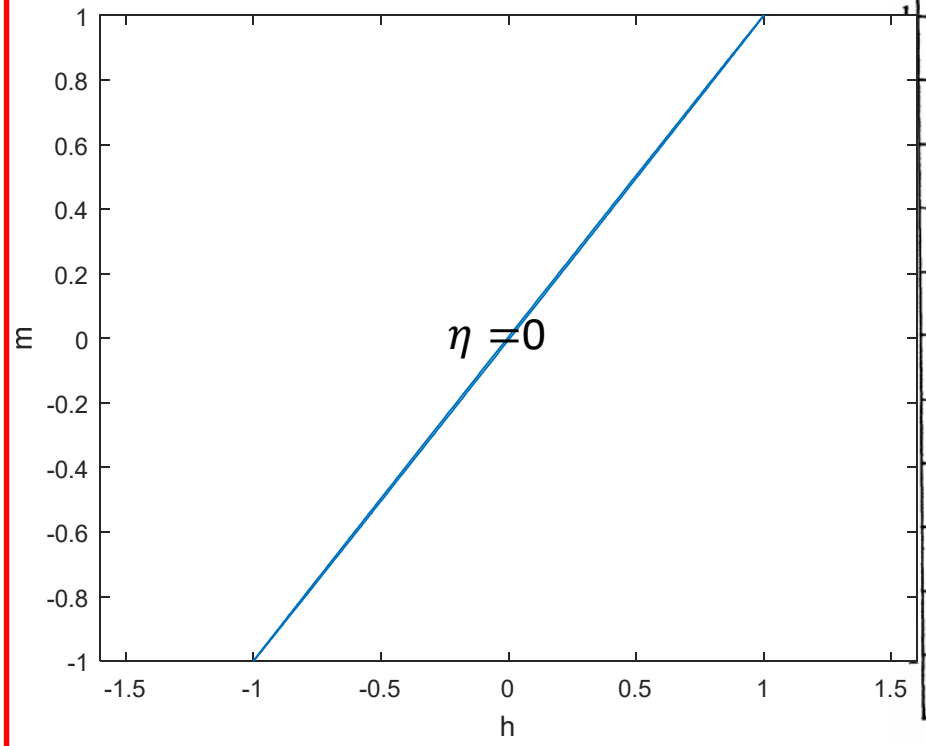
$\eta = 0$
m
h
1
0.8
0.6
0.4
0.2
0
-0.2
-0.4
-0.6
-0.8
-1
-1.5
-1
-0.5
0
0.5
1
1.5

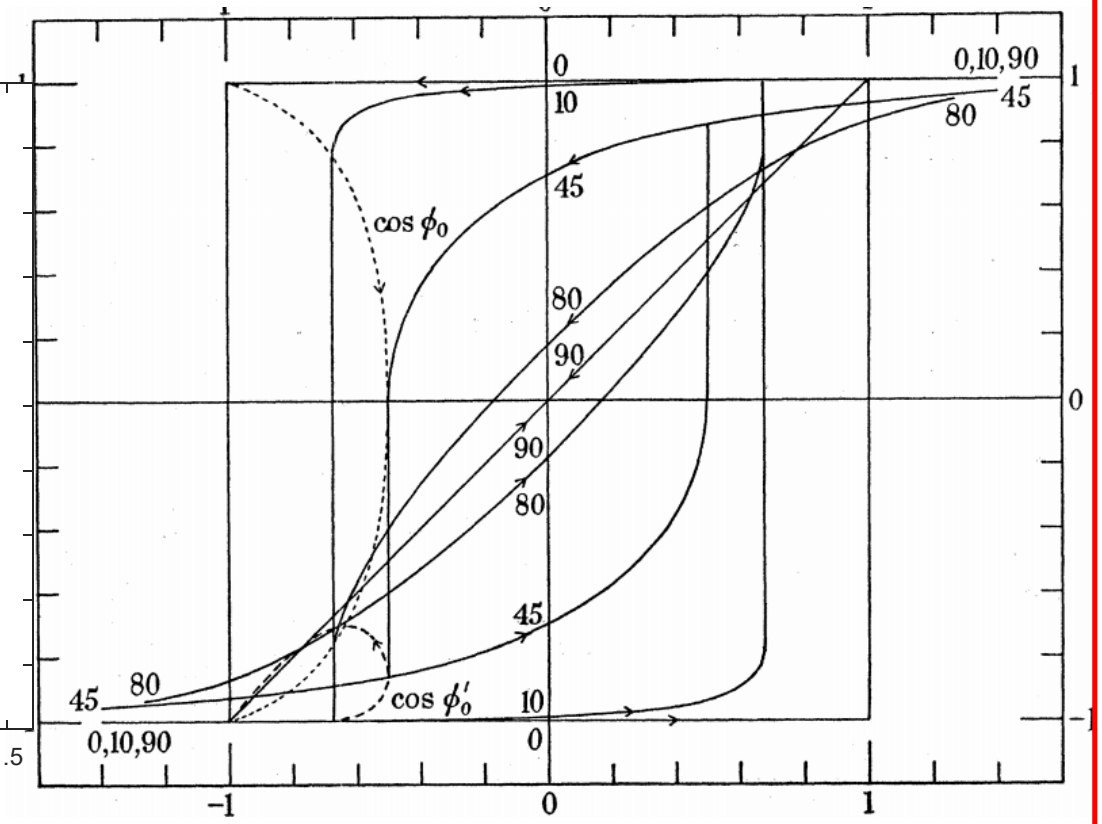
0
0,10,90
10
45
80
cos ϕ_0
80
90
90
80
45
45
80
cos ϕ_0'
10
0,10,90
0
1
0
−1
−1
0
1

Partículas con anisotropía alta $Q = K_u/K_d \gg 1$

$$E_d = \frac{\mu_0}{2}\left(N_x M_x^2 + N_y M_y^2 + N_z M_z^2\right)V$$

$$M_x^2 + M_y^2 + M_z^2 = M^2$$

Si está magnetizada a lo largo de un eje principal *u*

$$E_d = \frac{\mu_0}{2} N_u M_u^2 V$$

Si es monodominio

$$E_d = \frac{\mu_0}{2} N_u M_S^2 V = N_u J_S^2 V/2\mu_0$$

Se puede dar una valor de esta energía relativo a la referencia magnetostática $K_d = J_S^2/2\mu_0$ que en el caso monodominio es simplemente la componente *u* del tensor desmagnetizante

Energía reducida monodominio

$$\varepsilon_d = E_d/(VK_d) = N_u$$

thin wall having a size-independent specific energy γ_w

Partículas multidominio

Llamando γ_w a la energía de pared de dominio por unidad de área y F_w al área total de pared,

$$E_{tot} = E_d + F_w\gamma_w - HJ_S m$$

Densidad de energía

$$e_{tot} = E_{tot}/V$$

Energía reducida

$$\varepsilon_{tot} = \frac{e_{tot}}{K_d} = \varepsilon_d + \frac{f_w}{l_p}\frac{\gamma_w}{K_d} - 2hm$$

Decrece al aumentar el tamaño de NP

siendo

$$f_w = \frac{F_w}{V^{2/3}} \qquad l_p = V^{1/3}$$

Las energías de anisotropía e intercambio sólo aparecen indirectamente a través de γ_w

Tamaño crítico monodominio

Energía reducida monodominio = Energía reducida monodominio

$$N_u = \varepsilon_d + \frac{f_w}{l_{SD}}\frac{\gamma_w}{K_d} \quad \Rightarrow \quad l_{SD} = \left[\frac{f_w}{N_u - \varepsilon_d}\right]\frac{\gamma_w}{K_d}$$

Tamaño crítico monodominio

NPs esféricas

El tamaño monodominio crítico para una esfera fue calculado por Kittel:

$$D_{\mathrm{SD}} \approx 9\gamma_{\mathrm{w}}/K_{\mathrm{d}}$$

Un valor más preciso fue obtenido por Néel

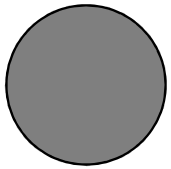

$\varepsilon_d = N_u = 1/3$ (1 dom) $\qquad \varepsilon_d = 0.1618$ (2 dom)

$$f_{\mathrm{w}} = \pi(4\pi/3)^{-2/3}$$

$$l_{\mathrm{SD}} = 7.048\gamma_{\mathrm{w}}/K_{\mathrm{d}}$$

Cómo éste es equivalente a un volumen l_{SD}^3, el diámetro de la esfera equivalente es

$$D_{\mathrm{SD}} = 8.745\gamma_{\mathrm{w}}/K_{\mathrm{d}}$$

NPs cúbicas

$\varepsilon_d = N_u = 1/3$ (1 dom) $\quad \varepsilon_{\mathrm{d}} = 0.1707$ (2 dom)

$f_{\mathrm{w}} = 1$

$$l_{\mathrm{SD}} = 6.15\gamma_{\mathrm{w}}/K_{\mathrm{d}}$$

$$l_p \leq 6.15\frac{\gamma_w}{K_d}$$ 

$$6.15\frac{\gamma_w}{K_d} \leq l_p \leq 15.2\frac{\gamma_w}{K_d}$$ 

$$15.2\frac{\gamma_w}{K_d} \leq l_p \leq 19\frac{\gamma_w}{K_d}$$ 

$$19\frac{\gamma_w}{K_d} \leq l_p \leq 40\frac{\gamma_w}{K_d}$$ 

Energía de pared $\gamma_w = 4\sqrt{AK_u}$ $W_L = \pi\sqrt{A/K_u}$ Espesor de pared

$$l_{SD} = 6.15\frac{\gamma_w}{K_d} = 6.15\frac{4\sqrt{AK_u}}{K_d} = \frac{4\times 6.15}{\pi}\pi\sqrt{A/K_u}\frac{K_u}{K_d} = 7.83QW_L \gg W_L$$

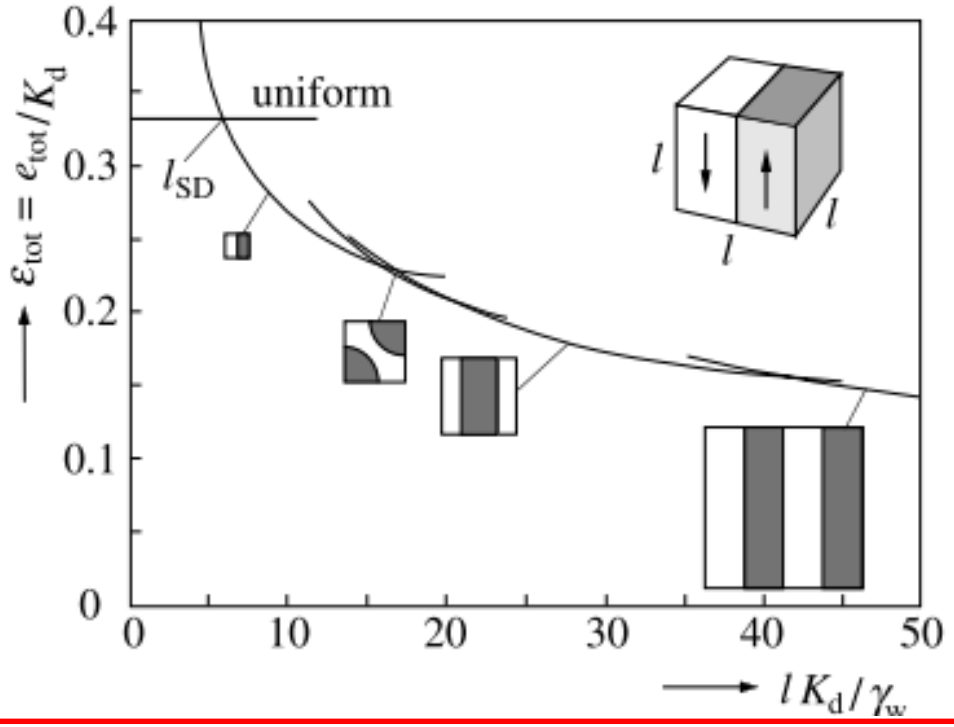

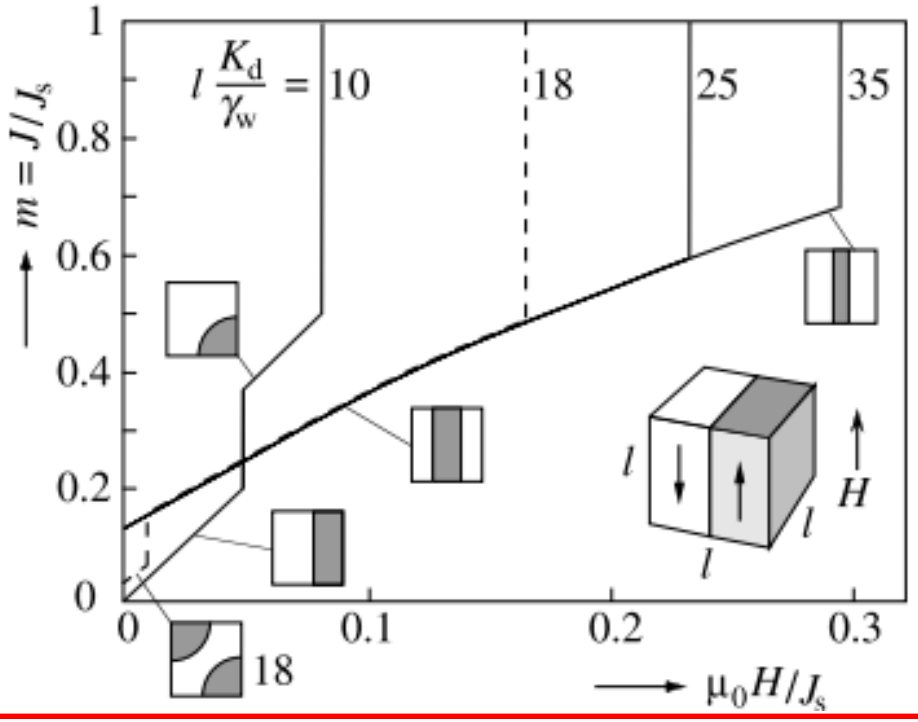

NPs oblongas

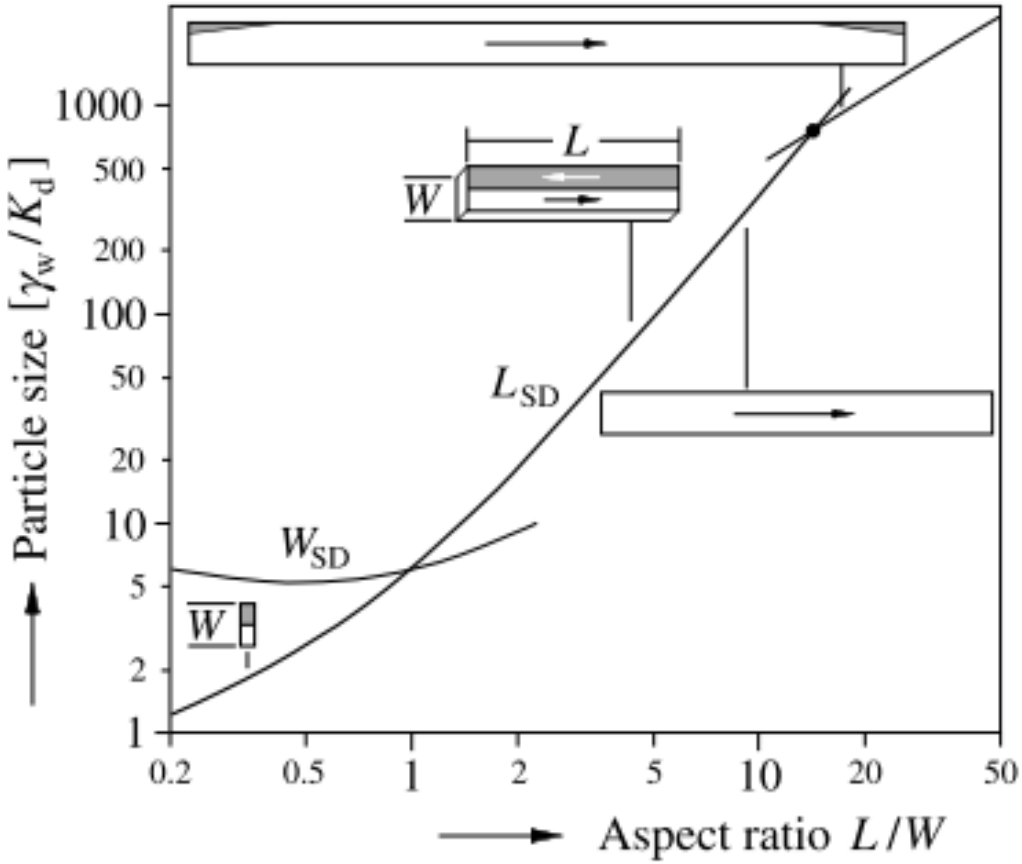

Partículas con anisotropía baja $Q \ll 1$

$$W_L = \pi\sqrt{A/K_u} \rightarrow \infty \quad \text{cuando } K_u \rightarrow 0$$

No es esperable la formación de una pared de dominio en partículas suficientemente pequeñas.
Para calcular el tamaño monodominio es necesario realizar un cálculo micromagnético.

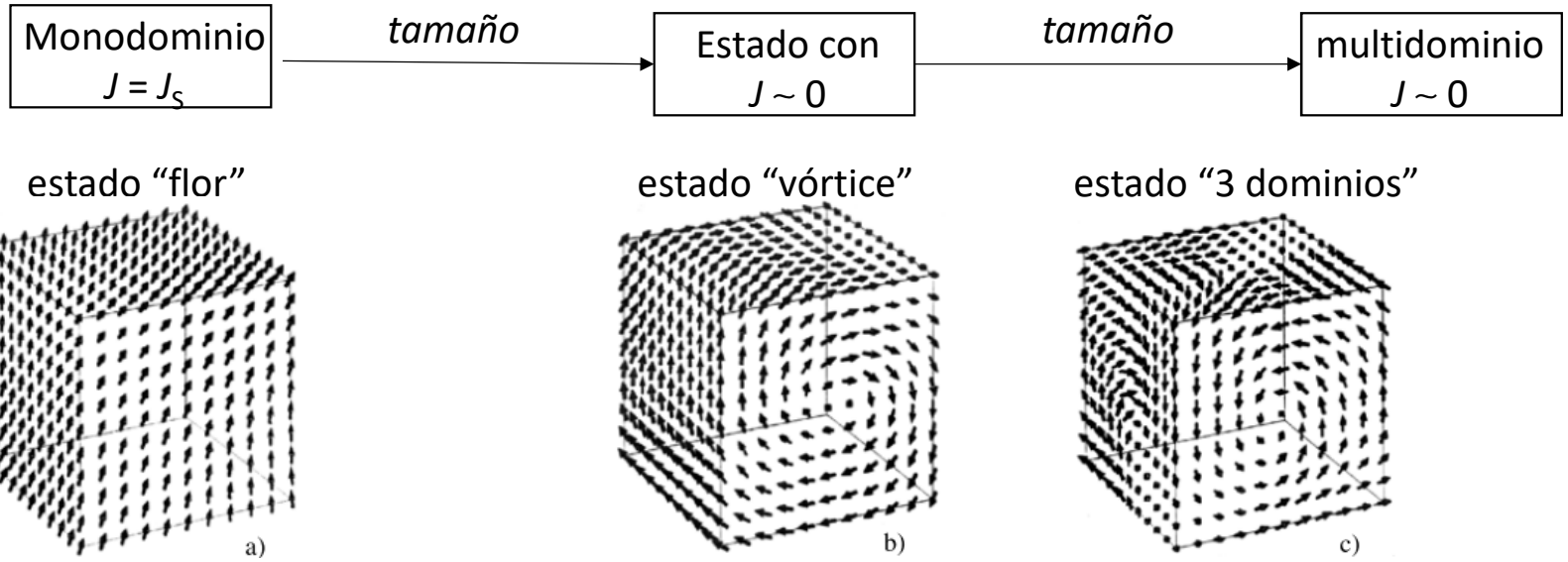

Tamaño monodominio

$$l_{SD} \propto \Delta_d, \qquad \Delta_d = \sqrt{A/K_d}$$

NPs cúbicas

$$l_{\mathrm{SD}} = 6.8\Delta_{\mathrm{d}} \qquad Q = 0.02$$
$$l_{\mathrm{SD}} = 7.27\Delta_{\mathrm{d}} \qquad Q = 0.0053$$

NPs esféricas

$$l_{\mathrm{SD}} = 4\Delta_{\mathrm{d}} \qquad Q \ll 1$$
$$l_{\mathrm{SD}} = 10.8\Delta_{\mathrm{d}} \qquad Q \approx 0.4$$

El tamaño monodominio aumenta cuanto mayor es la relación de aspecto

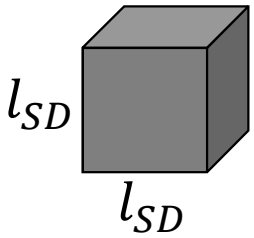

$\boxed{l_{SD} = 7\Delta_d}$

magnetita

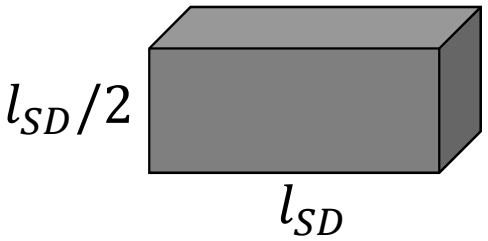

$\boxed{l_{SD} = 19\Delta_d}$

Critical single-domain grain sizes in elongated iron particles: implications for meteoritic and lunar magnetism

Adrian R. Muxworthy[1] and Wyn Williams[2]

Geophys. J. Int. (2015) **202,** 578–583

In this study, the following room-temperature values for metallic iron were used: $A = 2 \times 10^{-11}$ Jm^{-1} (Kittel 1949), $M_S = 1715 \times 10^3$ Am^{-1} (Dunlop & Özdemir 1997) and K_1 (cubic) $= 4.8 \times 10^4$ Jm^{-3} (Graham 1958). Butler & Banerjee (1975a) used values of: $A = 1 \times 10^{-11}$ Jm^{-1}, $M_S = 1720 \times 10^3$ Am^{-1} and $K_1 = 4.5 \times 10^4$ Jm^{-3}. The values used in this study are the ones now generally used in other micromagnetic studies of iron.

```
A=2e-11;
Ms=1715e3;
mu0=pi*4e-7;
K=4.8e4;
K/Kd=0.026;
Kd=mu0*Ms^2/2=1.848e6;%J/m^3
Dd=(A/Kd)^0.5=3.29e-9;%m
```

Cubos y prismas

Cubos y prismas

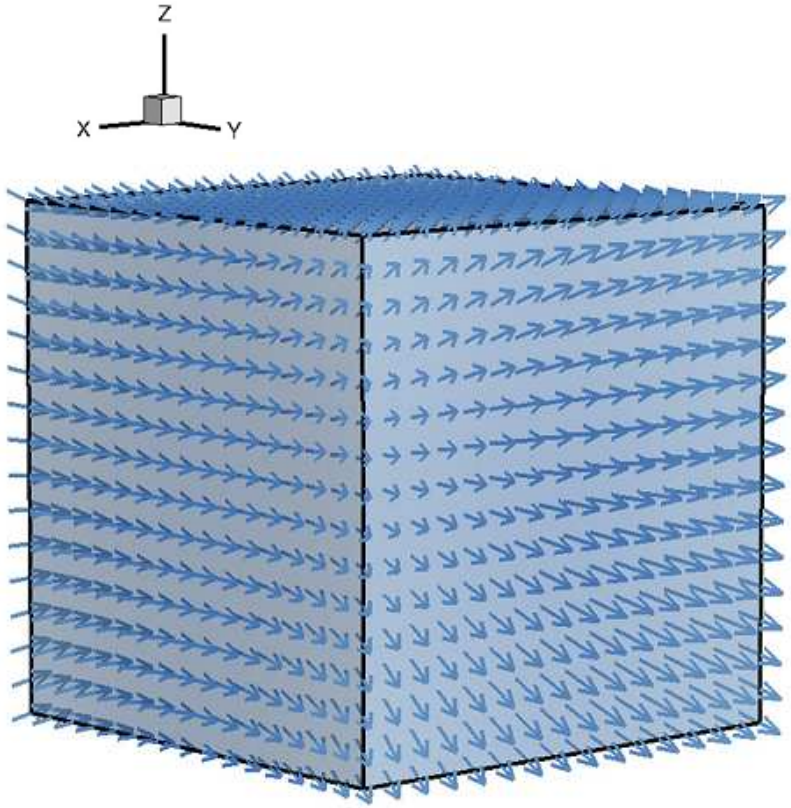

Flower

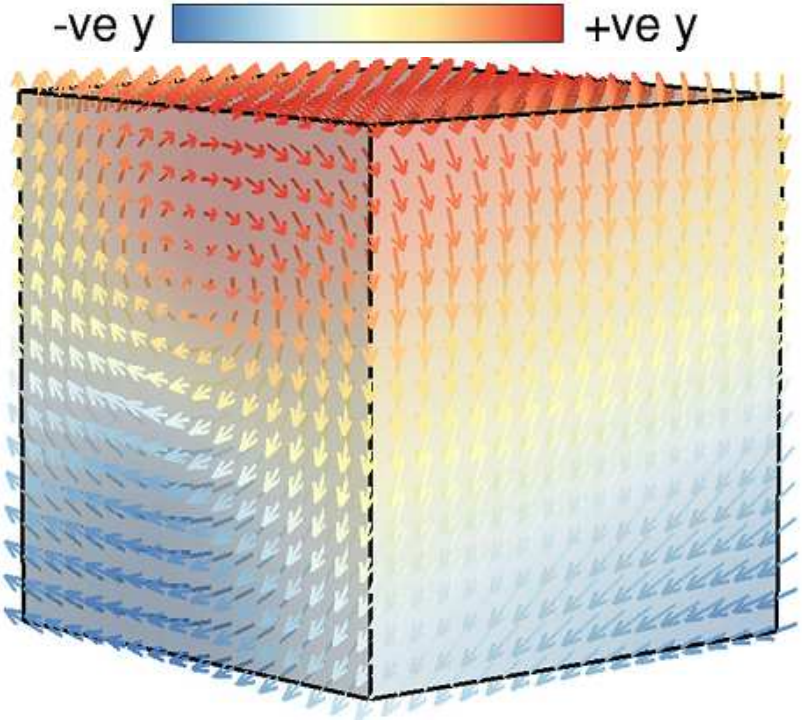

Vortex

Adrian R. Muxworthy[1] and Wyn Williams[2]

Geophys. J. Int. (2015) **202,** 578–583

Cubos y prismas

(Intercambio + Magnetostática + Anisotropía) / (Vol*K_d)

$\longleftrightarrow$

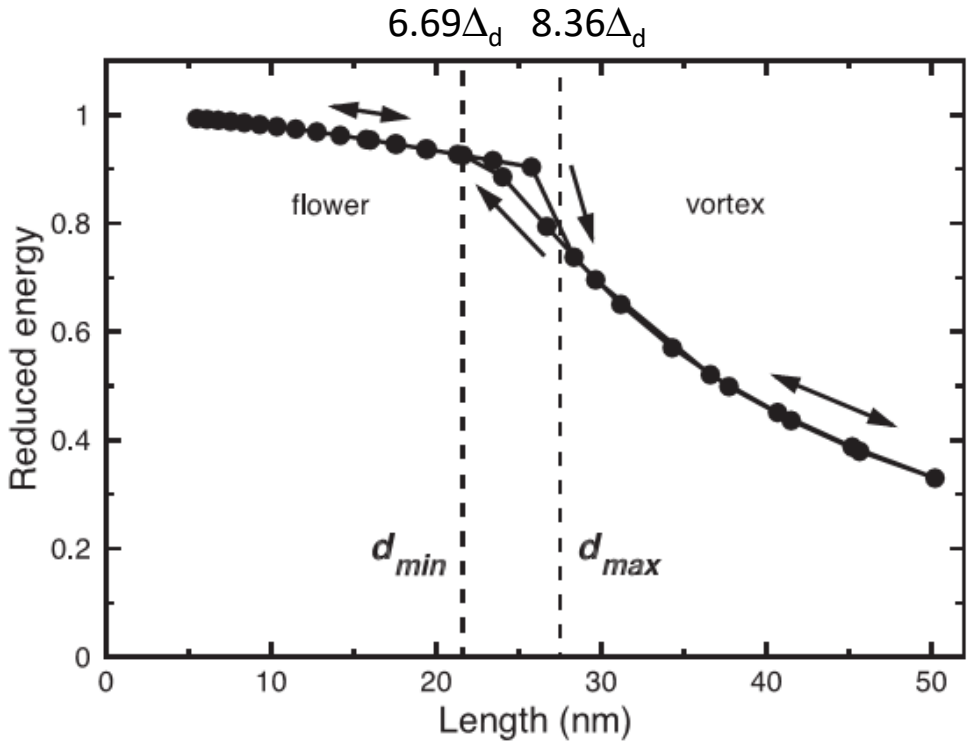

Adrian R. Muxworthy[1] and Wyn Williams[2]

Cubos y prismas

Tamaños críticos monodominio

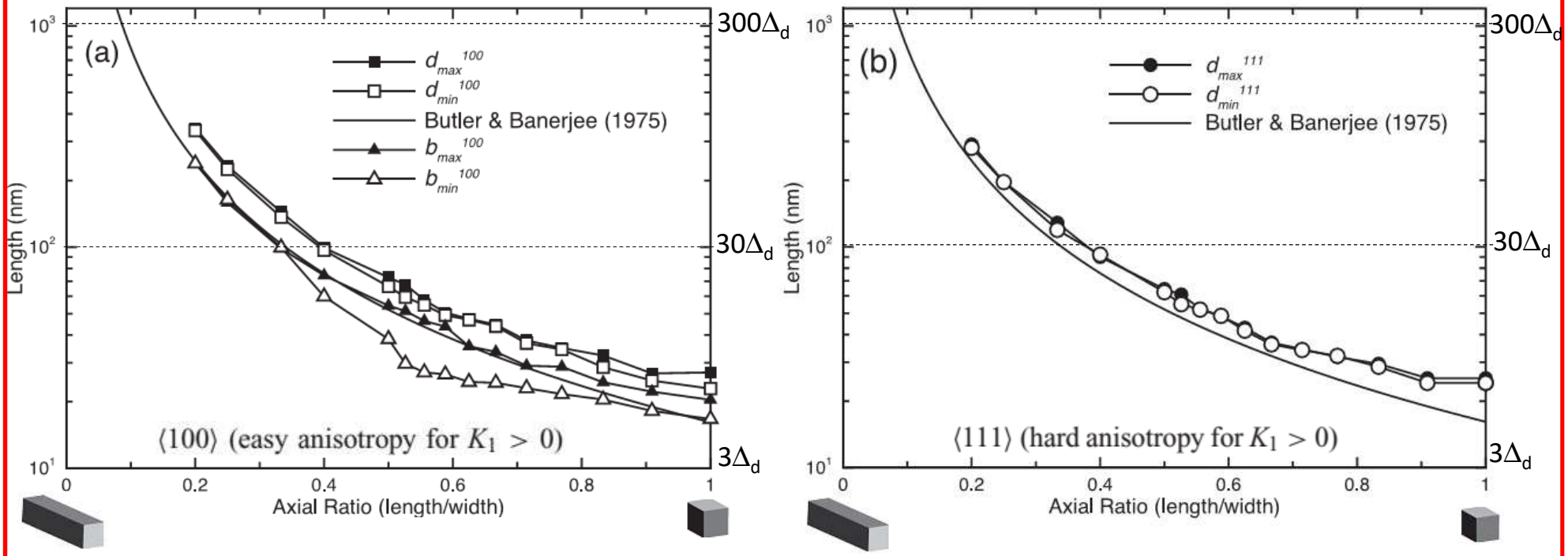

Adrian R. Muxworthy[1] and Wyn Williams[2]

Cubos y prismas

$t_m = \tau_0 \exp(E_A / kT)$ $E_A = K_{ef} V$ $K_{ef} = K_{mc} + K_{me}$

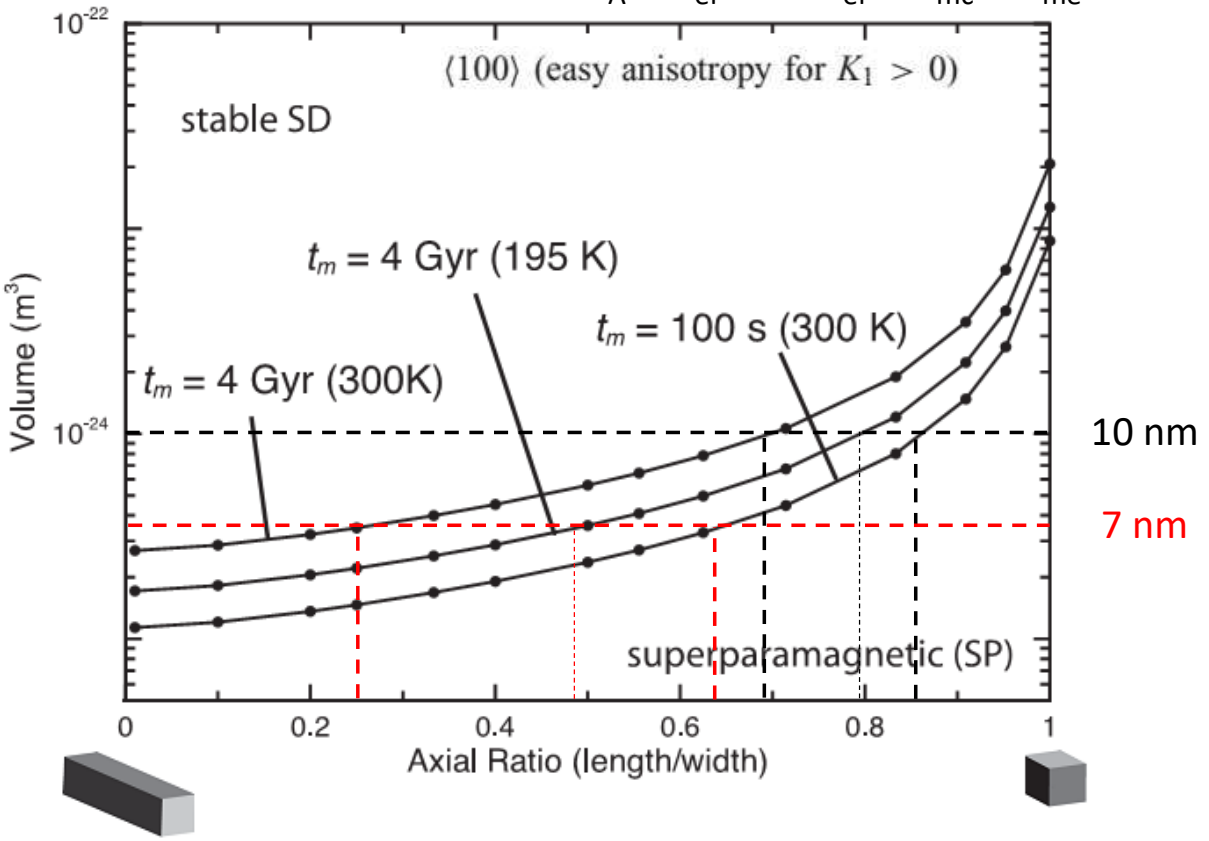

Adrian R. Muxworthy[1] and Wyn Williams[2]

Cubos y prismas

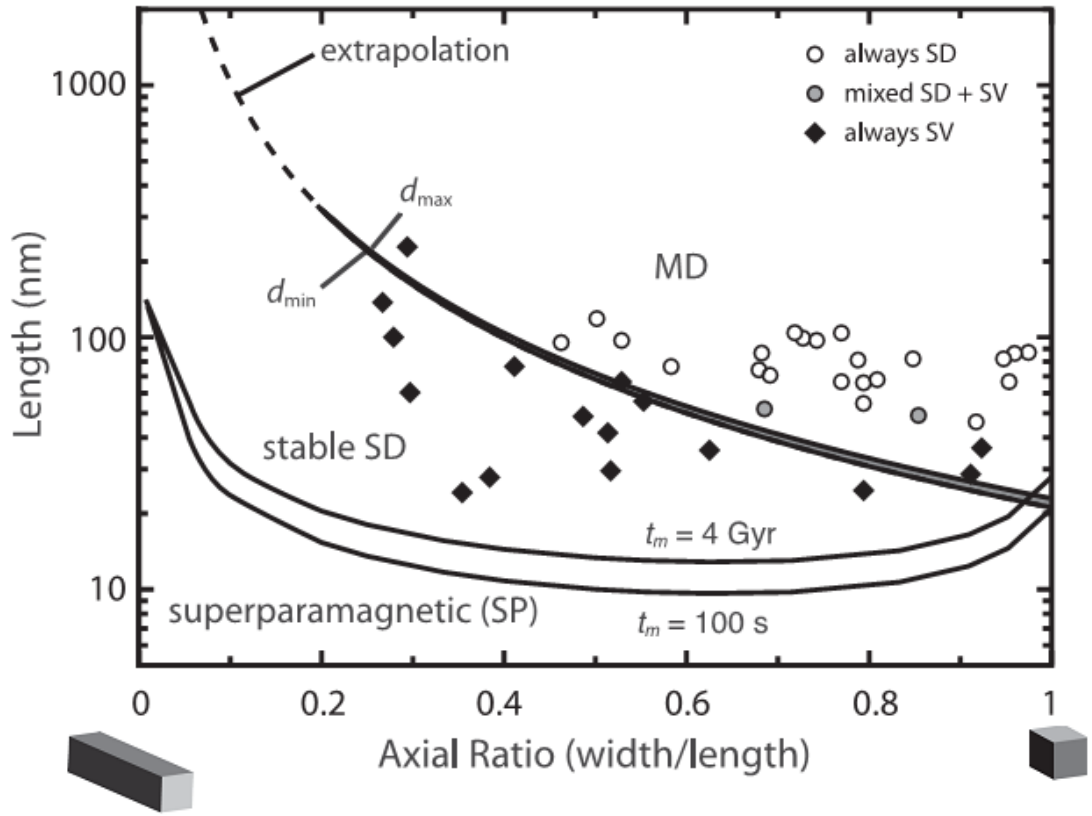

Adrian R. Muxworthy[1] and Wyn Williams[2]

Mineral magnetism of dusty olivine: A credible recorder of pre-accretionary remanence

Sophie-Charlotte L. L. Lappe et. al

17 December 2011
doi:10.1029/2011GC003811

Geochemistry Geophysics Geosystems G3

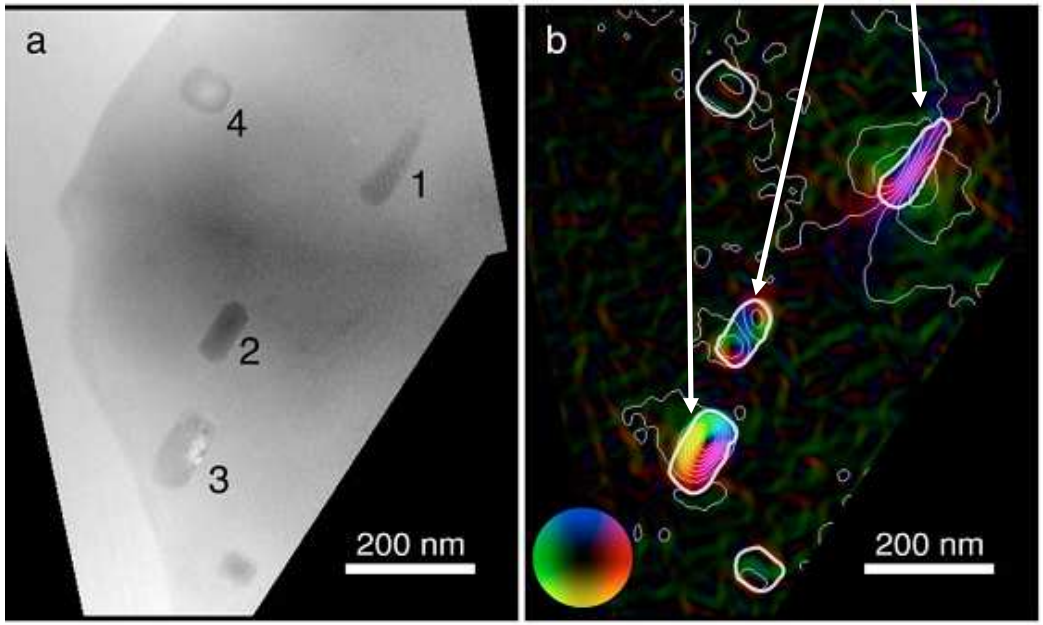

Electron holography results

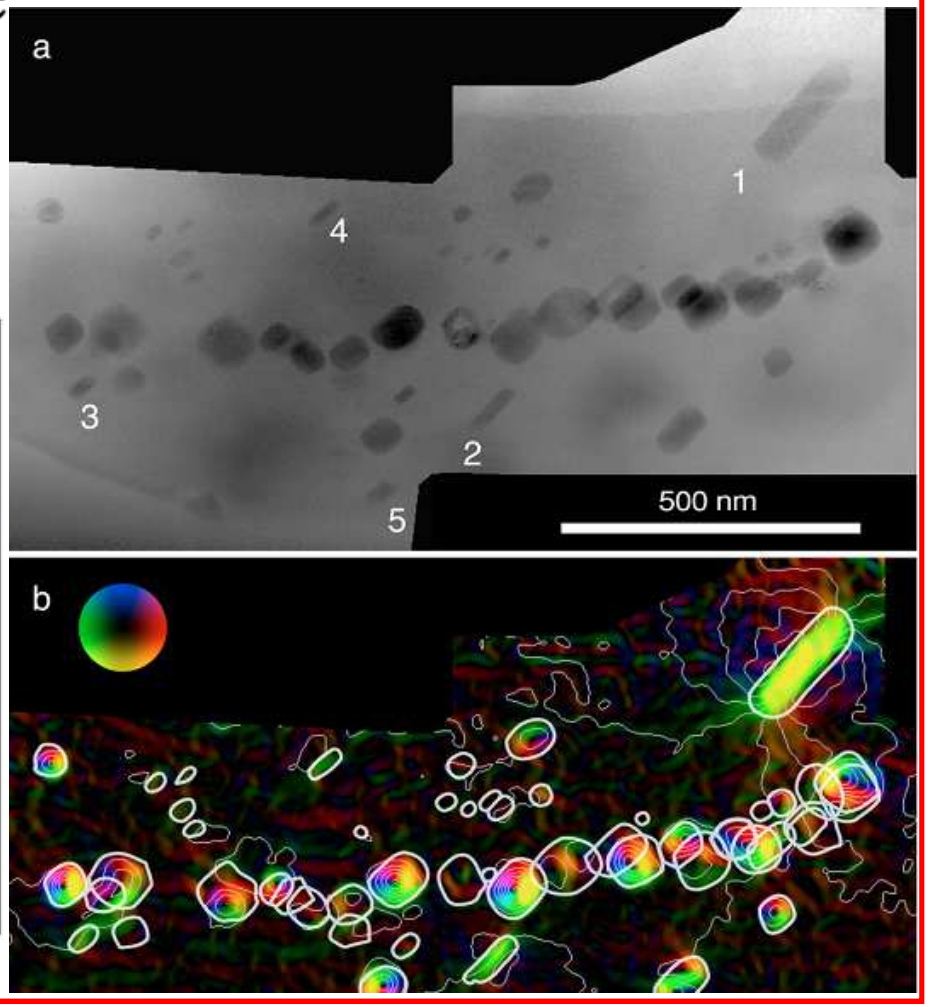

Lappe et. al 2011

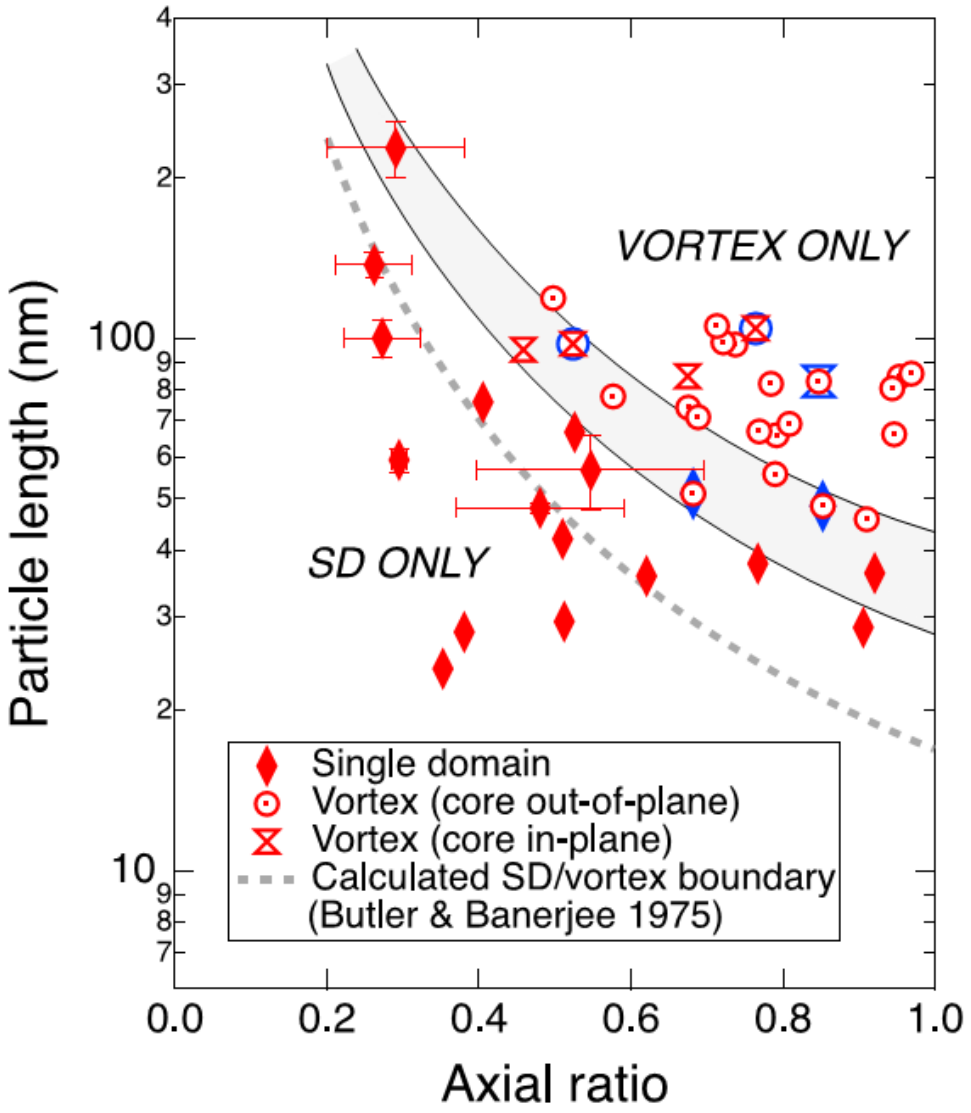

Películas delgadas bidimensionales

¿Real estructura de dominio o flujo continuo de ***J*** con $\nabla . \boldsymbol{J} = 0$?

$$L \gg \Delta_d = \sqrt{A/K_d}$$

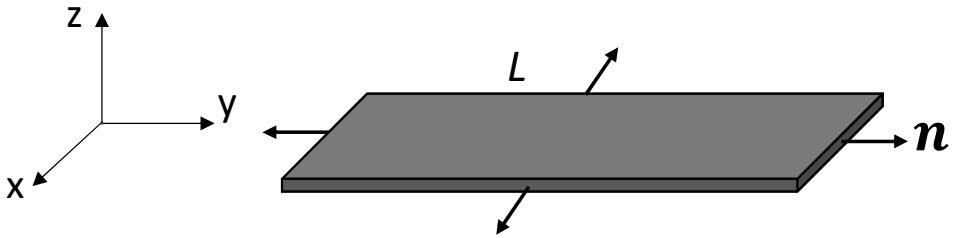

Condiciones ideales

$$m_z = 0$$

$$\boldsymbol{\nabla} \cdot \boldsymbol{m} = 0$$

$$\boldsymbol{m} \cdot \boldsymbol{n} = 0$$

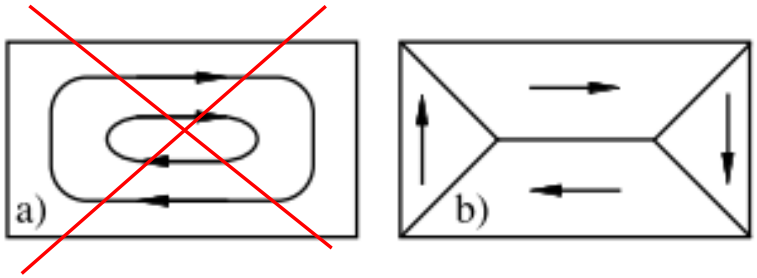

Self-consistent domain theory in soft-ferromagnetic media. II. Basic domain structures in thin-film objects

H. A. M. van den Berg (Received 17 January 1986; accepted for publication 31 March 1986)

Journal of Applied Physics **60**, 1104 (1986); doi: 10.1063/1.337352

Self-consistent domain theory in soft-ferromagnetic media. III. Composite domain structures in thin-film objects

H. A. M. van den Berg and A. H. J. van den Brandt (Received 10 September 1986; accepted for publication 10 April 1987)

Journal of Applied Physics **62**, 1952 (1987); doi: 10.1063/1.339533

Order in the domain structure in soft-magnetic thin-film elements: A review

by Hugo A. M. van den Berg

IBM J. RES. DEVELOP. VOL. 33 NO. 5 SEPTEMBER 1989

pp. 540 - 582

Película delgada blanda extendida $l_x \sim l_y >> l_z$

m(*x*,*y*) debe satisfacer

(i) Ser paralela a la superficie del film ($m_z = 0$)
(ii) Tener divergencia nula en el interior, $\nabla.\boldsymbol{m} = \partial m_x/\partial x + \partial m_y/\partial y = 0$ y satisfacer $\boldsymbol{m}.\boldsymbol{n} = 0$ en los bordes
(iii) Tener módulo constante $m = 1$

van den Berg mostró que la magnetización debe permanecer paralela a los bordes a menos que otro borde interfiera. Como consecuencia, si un borde es recto, entonces debe existir un dominio con magnetización uniforme en la vecindad del mismo.

"Receta" propuesta por van den Berg

- Tomar círculos que tocan los bordes en dos o más puntos y yacen completamente dentro de la película. Los centros de los círculos forman parte de las paredes de dominio.
- En cada círculo la magnetización es perpendicular a los radios que terminen en los bordes.
- Si un círculo toca bordes en más de dos puntos, su centro es una juntura.
- Si la circunferencia de contacto es osculatriz, la pared respectiva termina en el centro del círculo. Ese punto es el centro de una zona con rotación concéntrica de la magnetización.
- Si la película contiene una esquina aguda, una pared termina en dicha esquina.

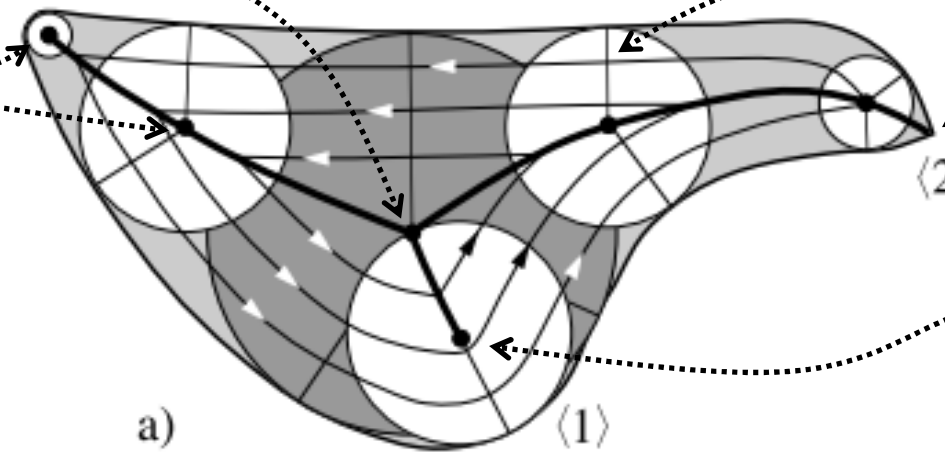

El patrón obtenido no es único. Por ejemplo, la magnetización puede invertirse en cada punto del film. Además pueden hacerse cortes virtuales de la figura y aplicar la receta a cada una de las partes resultantes.

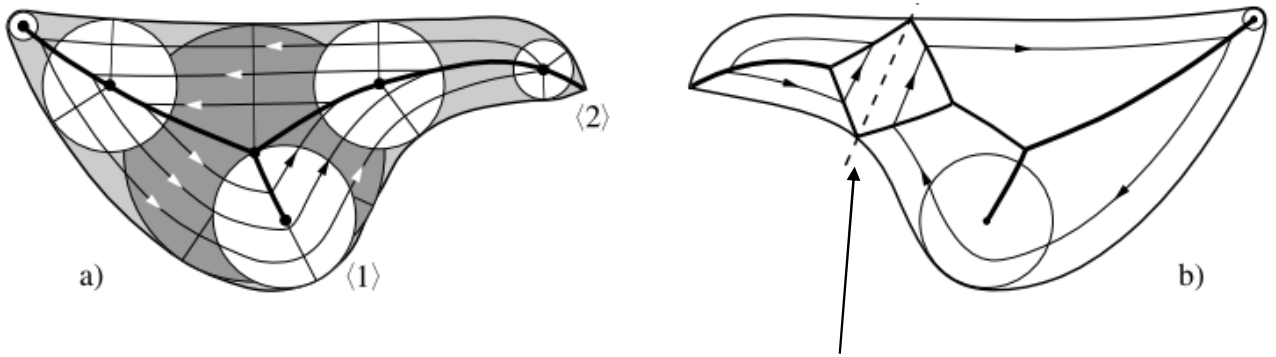

Al hacer cortes virtuales aparecen “edge clusters”, es decir, dos o más paredes confluyen en un punto del borde. van den Berg hizo una exploración de las reglas que deben satisfacer los Edge clusters:

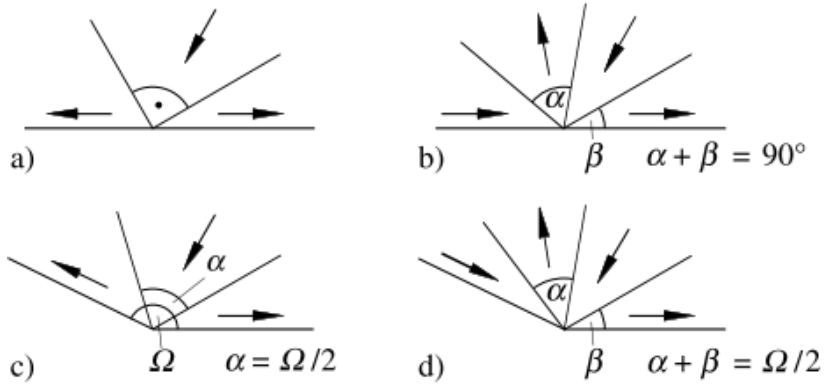

Películas de permaloy ($Fe_{19}Ni_{81}$), espesor = 240 nm
Estados desmagnetizados

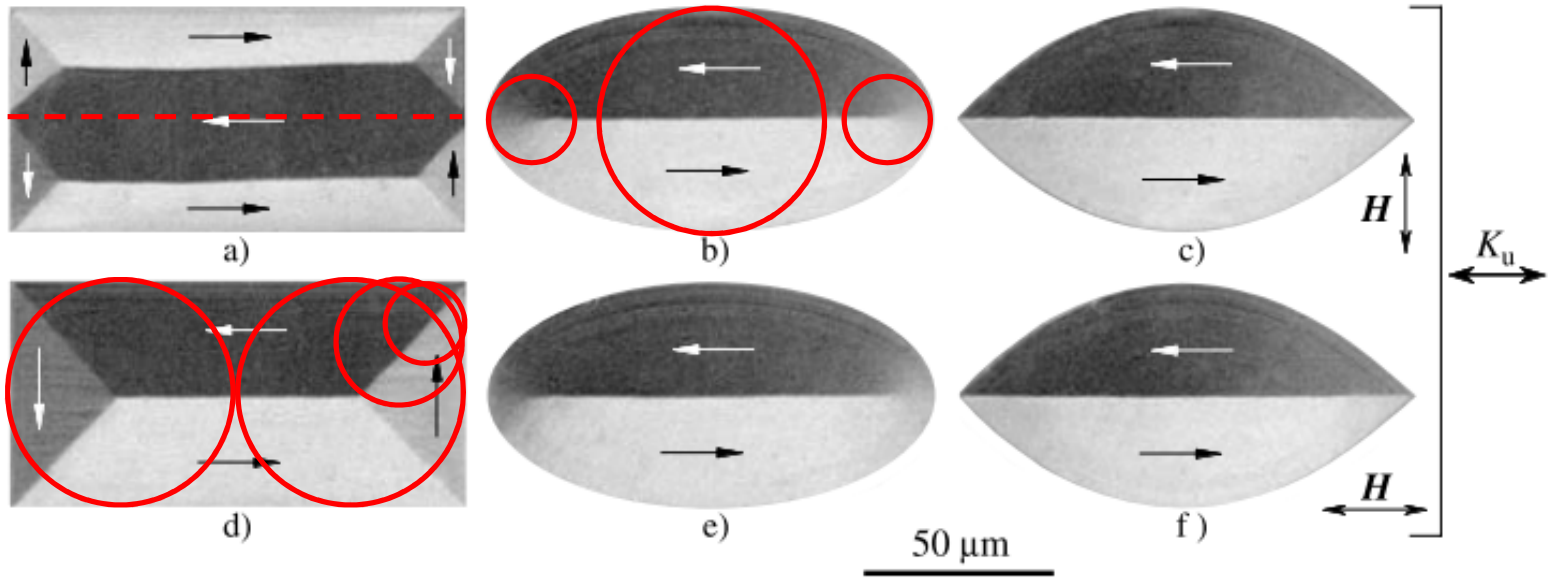

Películas de permaloy ($Fe_{19}Ni_{81}$), espesor = 240 nm
Estados desmagnetizados

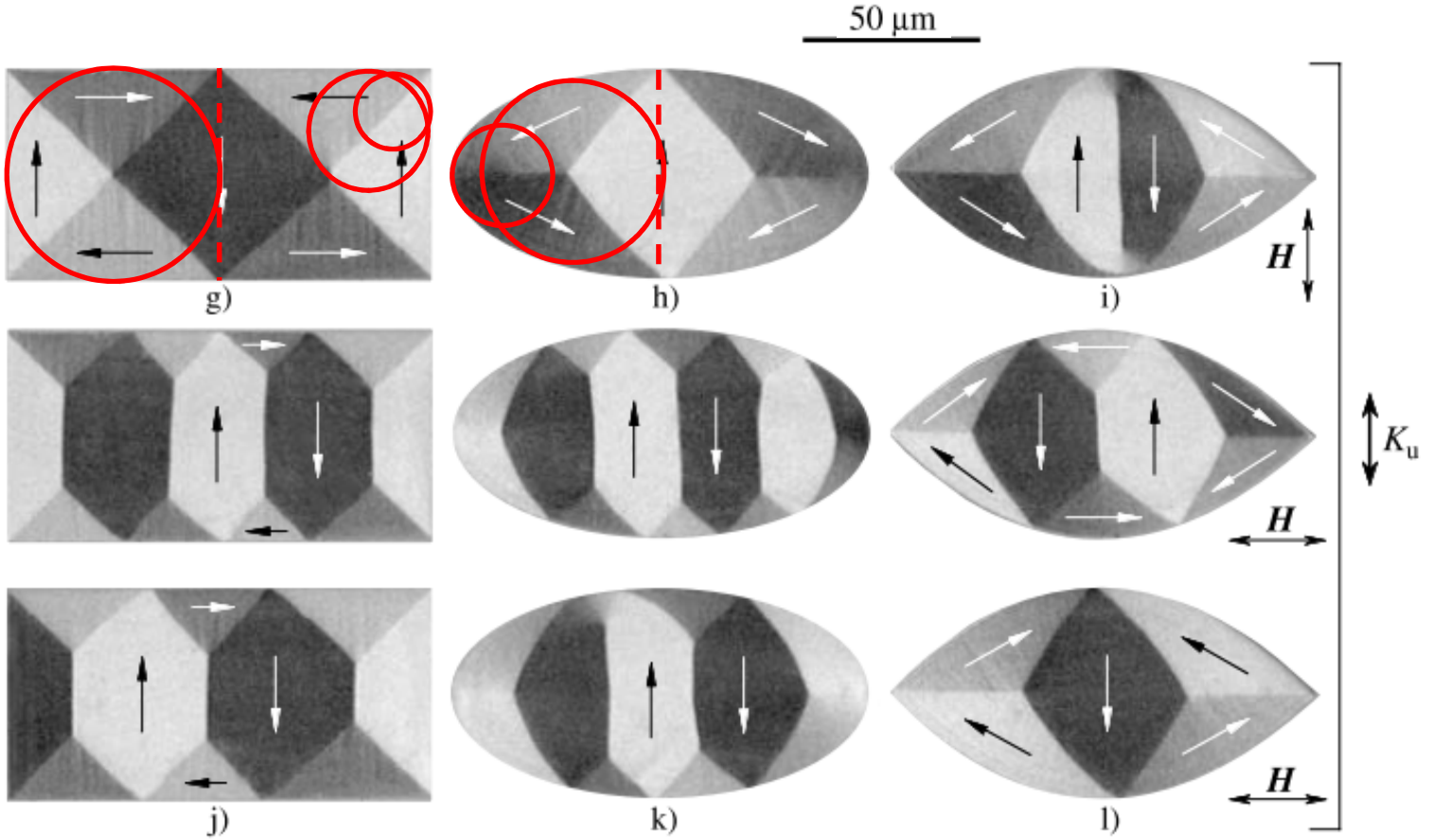

Películas de permaloy ($Fe_{19}Ni_{81}$), espesor = 240 nm
Estados desmagnetizados

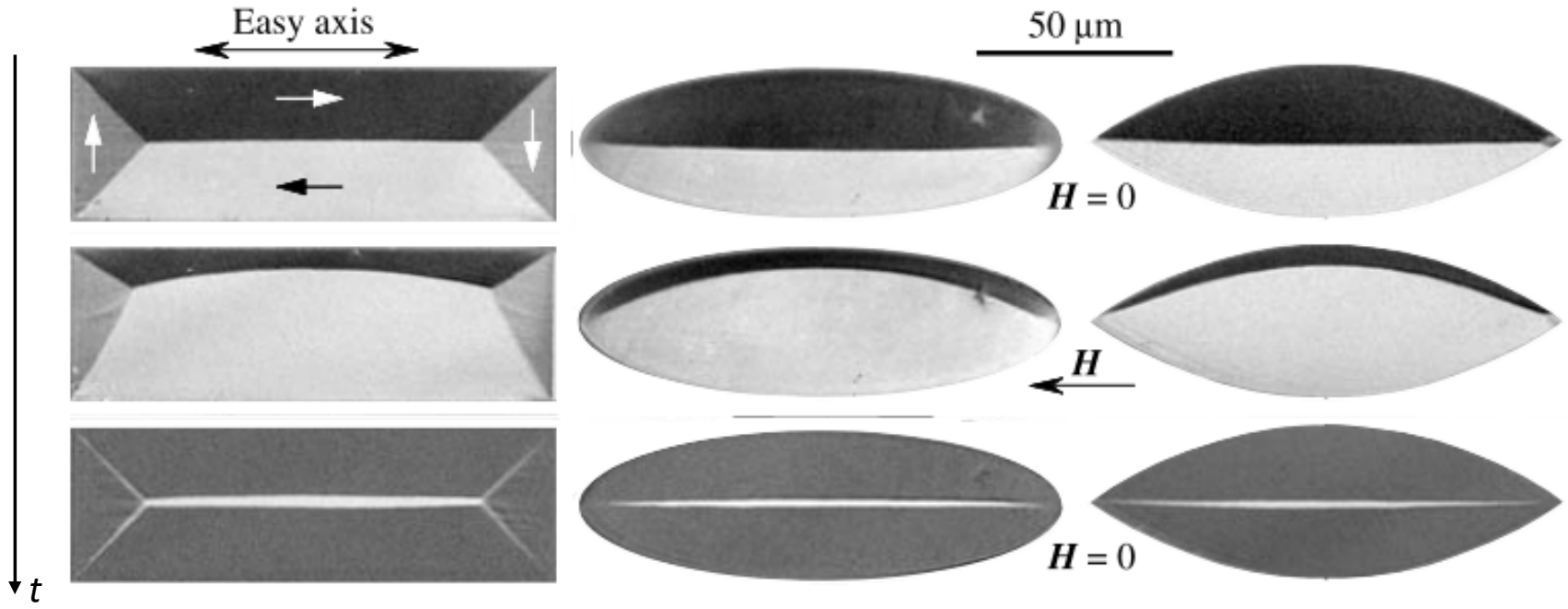

Películas circulares

vórtice

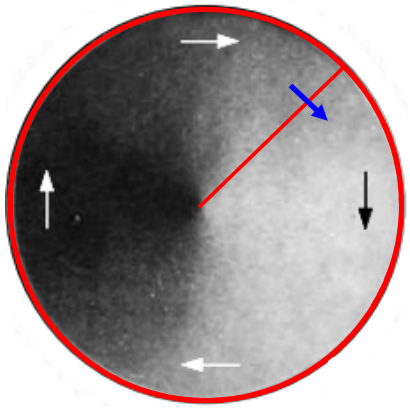

van den Berg

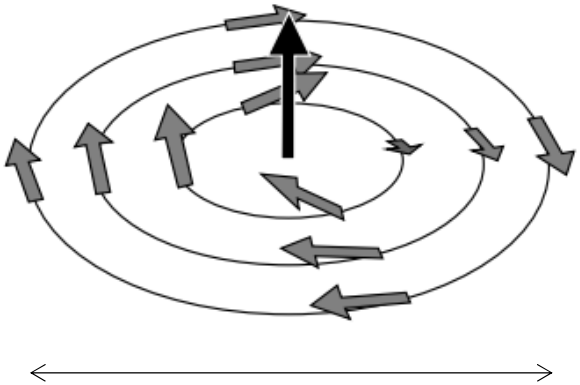

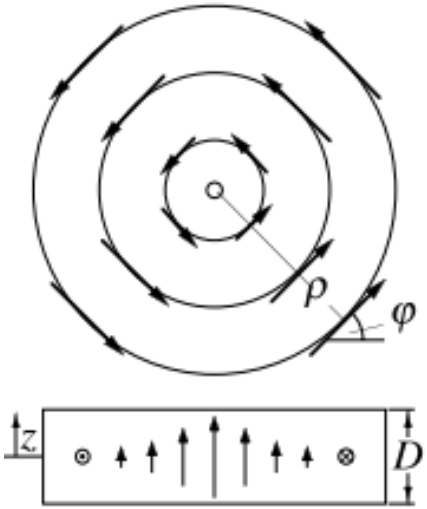

Películas circulares

Thin-film magnetic patterns in an external field

Paul Bryant and Harry Suhl

(Received 23 January 1989; accepted for publication 23 March 1989)

Appl. Phys. Lett. **54**, 2224 (1989); doi: 10.1063/1.101131

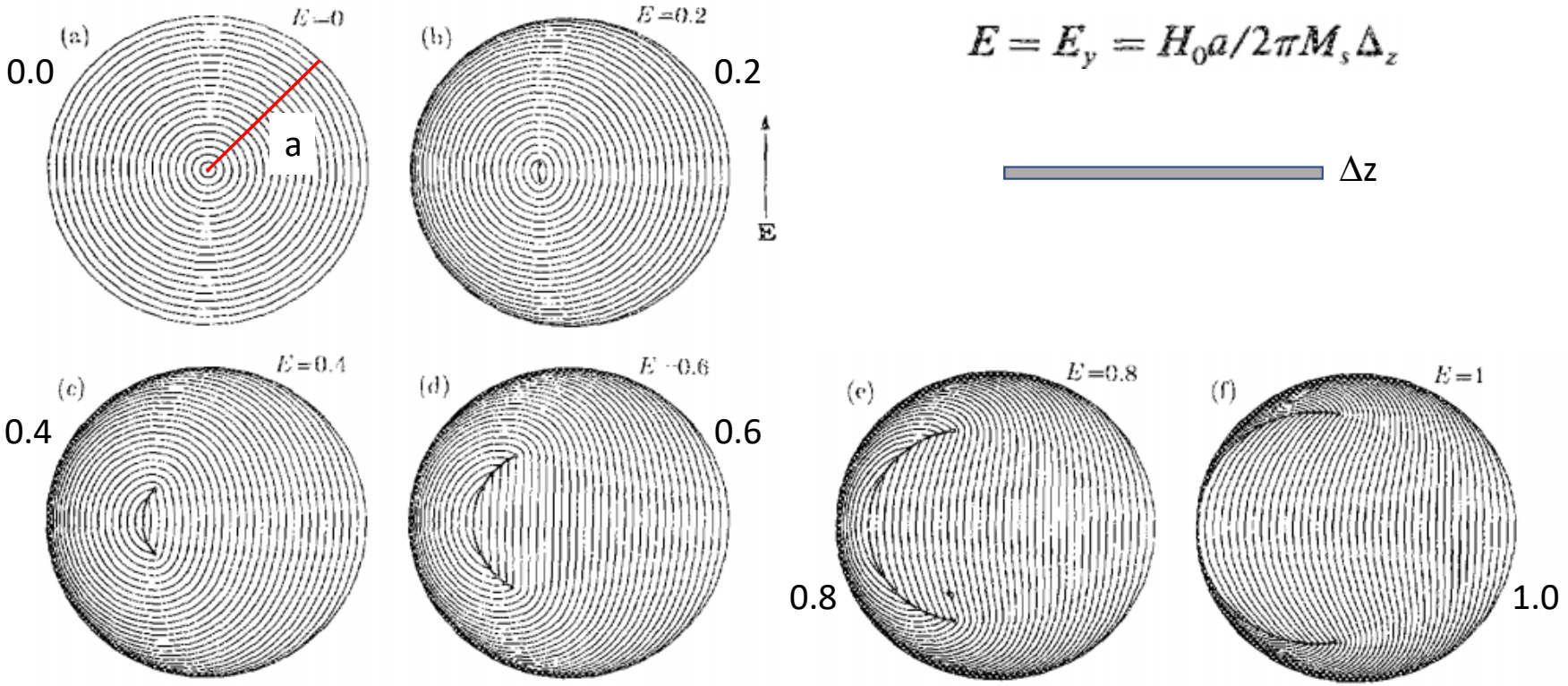

$$E = E_y = H_0 a / 2\pi M_s \Delta_z$$

Películas circulares

Imágenes Kerr

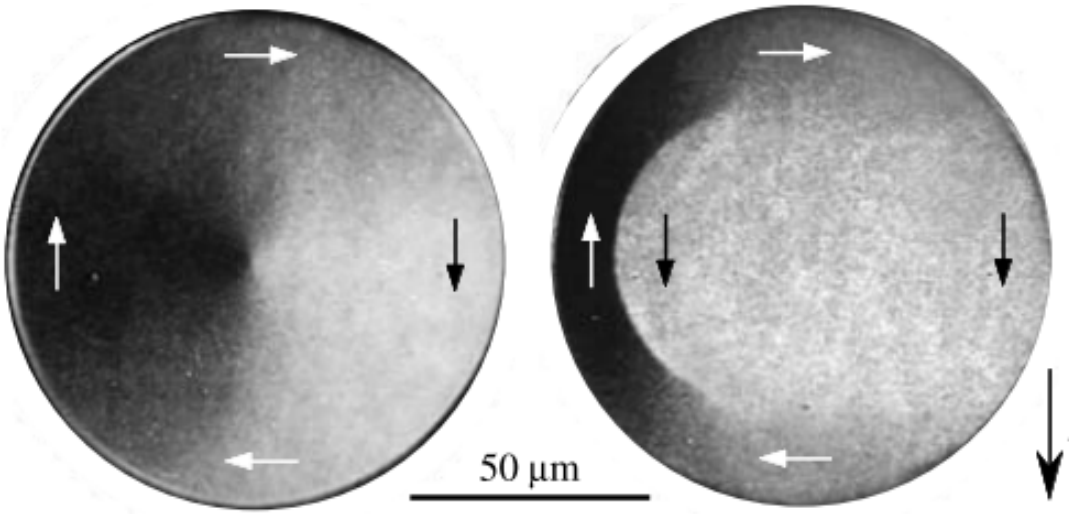

Bryant and Suhl

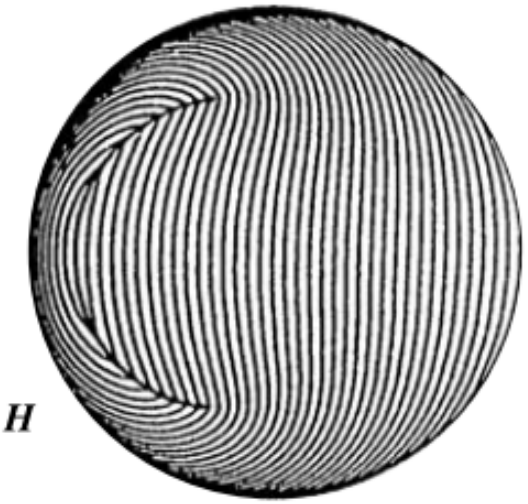

simulación

cilindros

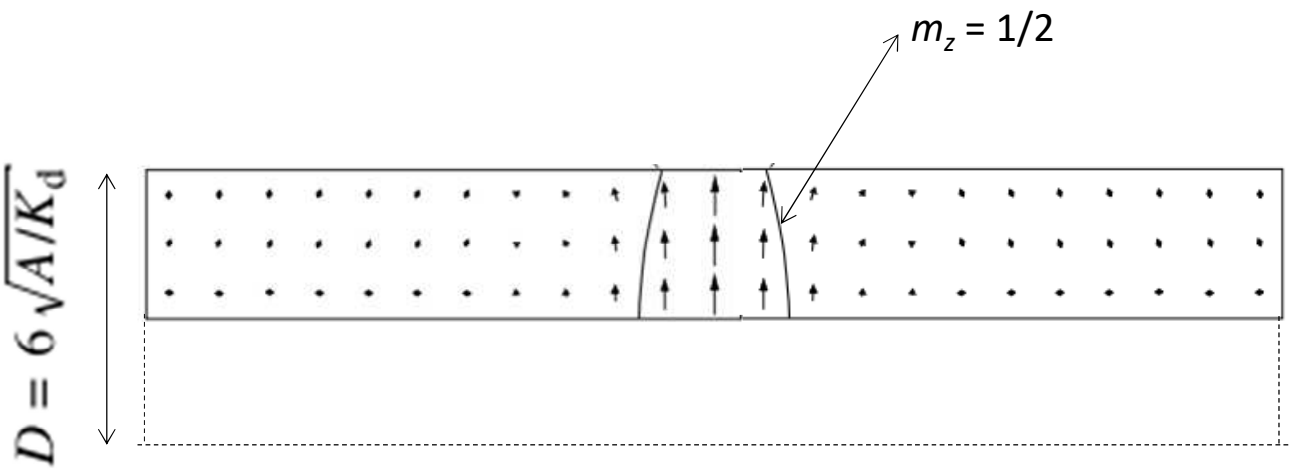

Bryant and Suhl

Cilindros (se muestra ¼ de cada uno)

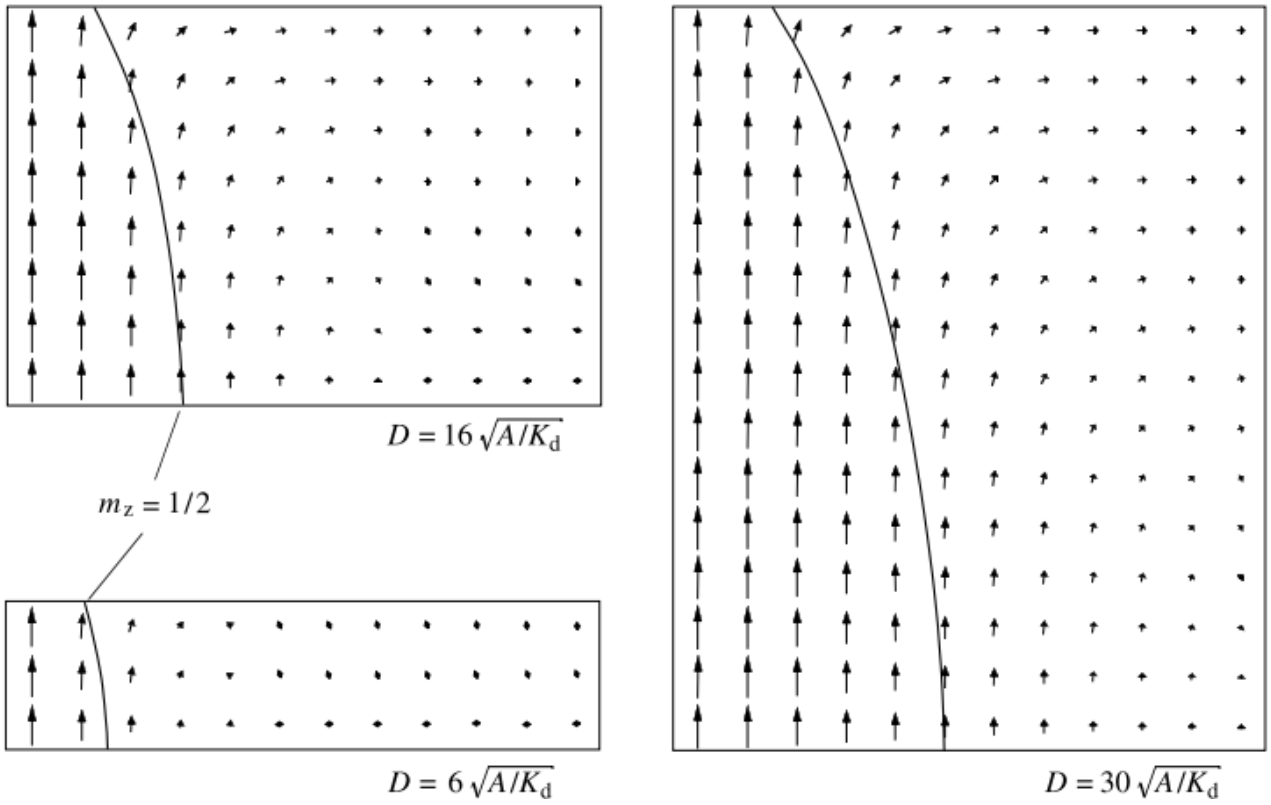

Bryant and Suhl

cilindros

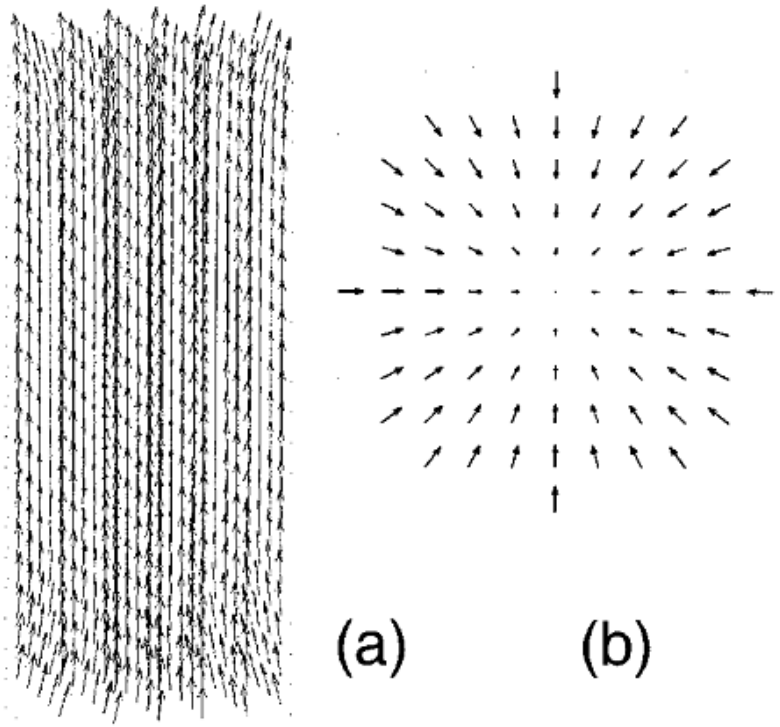

Estado Flower

C. A. Ross et al. PHYSICAL REVIEW B **65** 144417
(Received 27 July 2001; published 28 March 2002)

cilindros

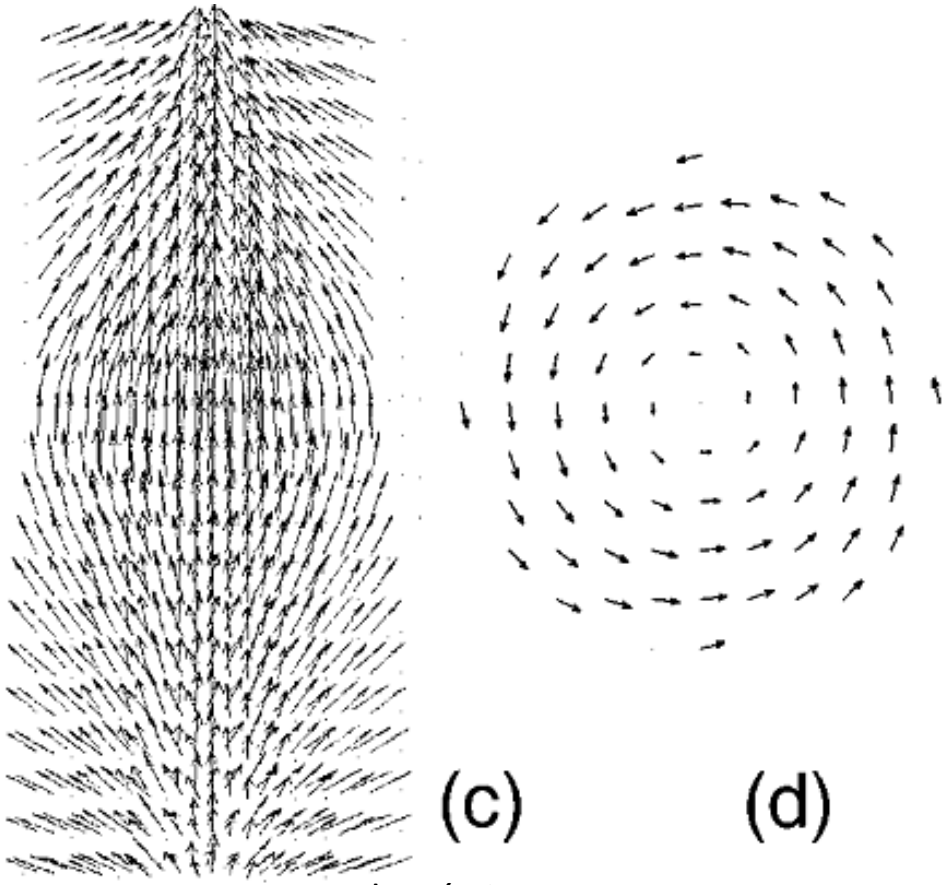

Estado Vórtice

C. A. Ross et al. PHYSICAL REVIEW B **65** 144417
(Received 27 July 2001; published 28 March 2002)

cilindros

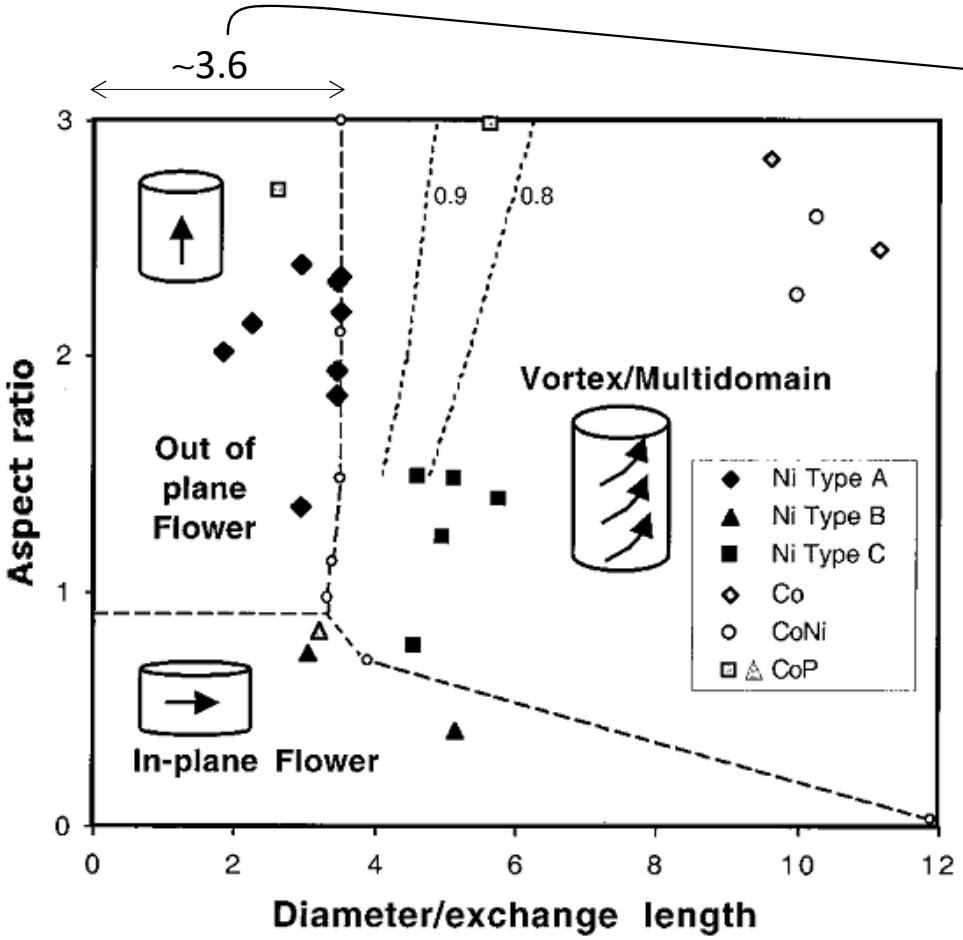

$D_{SD} \sim 3.6\,\xi_e$

$0.9 \leq \lambda$

$\lambda = D/L$

$(\xi_{ex} = \sqrt{A}/M_S)_{cgs}$

$(\xi_{ex} = \sqrt{2\pi}\sqrt{\frac{2A}{\mu_0 M_S^2}} = \sqrt{2\pi}\sqrt{\frac{A}{K_d}})_{SI}$

The important point of this discussion is that domains and walls can develop even without anisotropy. They can be induced simply by the boundary conditions and the principle of pole avoidance. Regions with a non-constant magnetization induced by a curved edge are a natural extension of the domain concept.

películas múltiplemente conexas

El procedimiento de vdB está diseñado para películas simplemente conectadas. En películas conectadas múltiplemente (con huecos por ejemplo) puede haber estados con menor energía que los obtenidos con ese procedimiento.

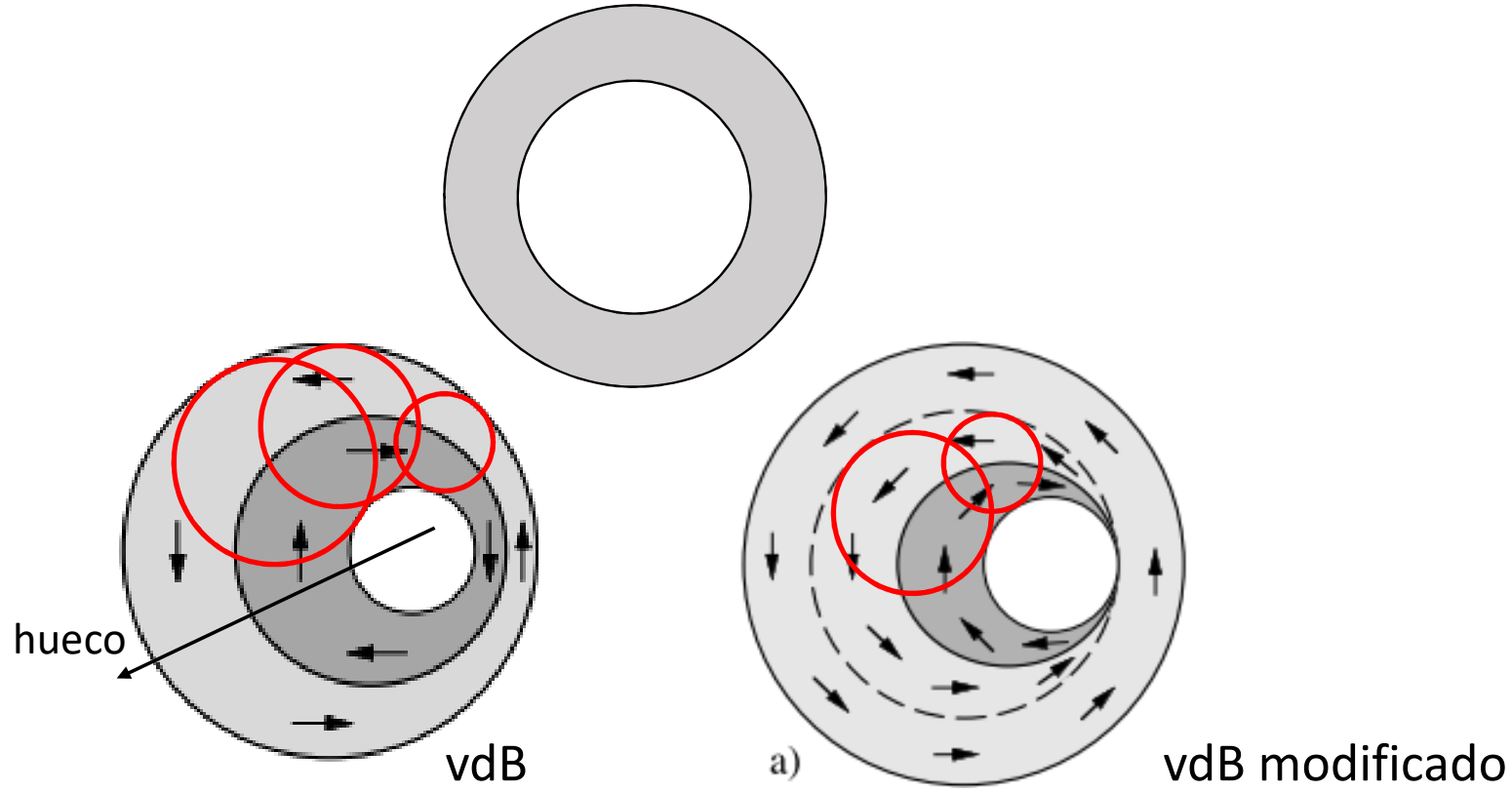

Efectos dipolares

Anisotropy-axis orientation effect on the magnetization of γ-Fe_2O_3 frozen ferrofluid

S Nakamae *et al* 2010 *J. Phys. D: Appl. Phys.* **43** 474001

<D> = 8.8 nm

σ = 0.23

H_{bias} = 15 kOe

Glicerina

T_M = 190 K

$\chi_A / \chi_R > 3$ → efectos de interacción

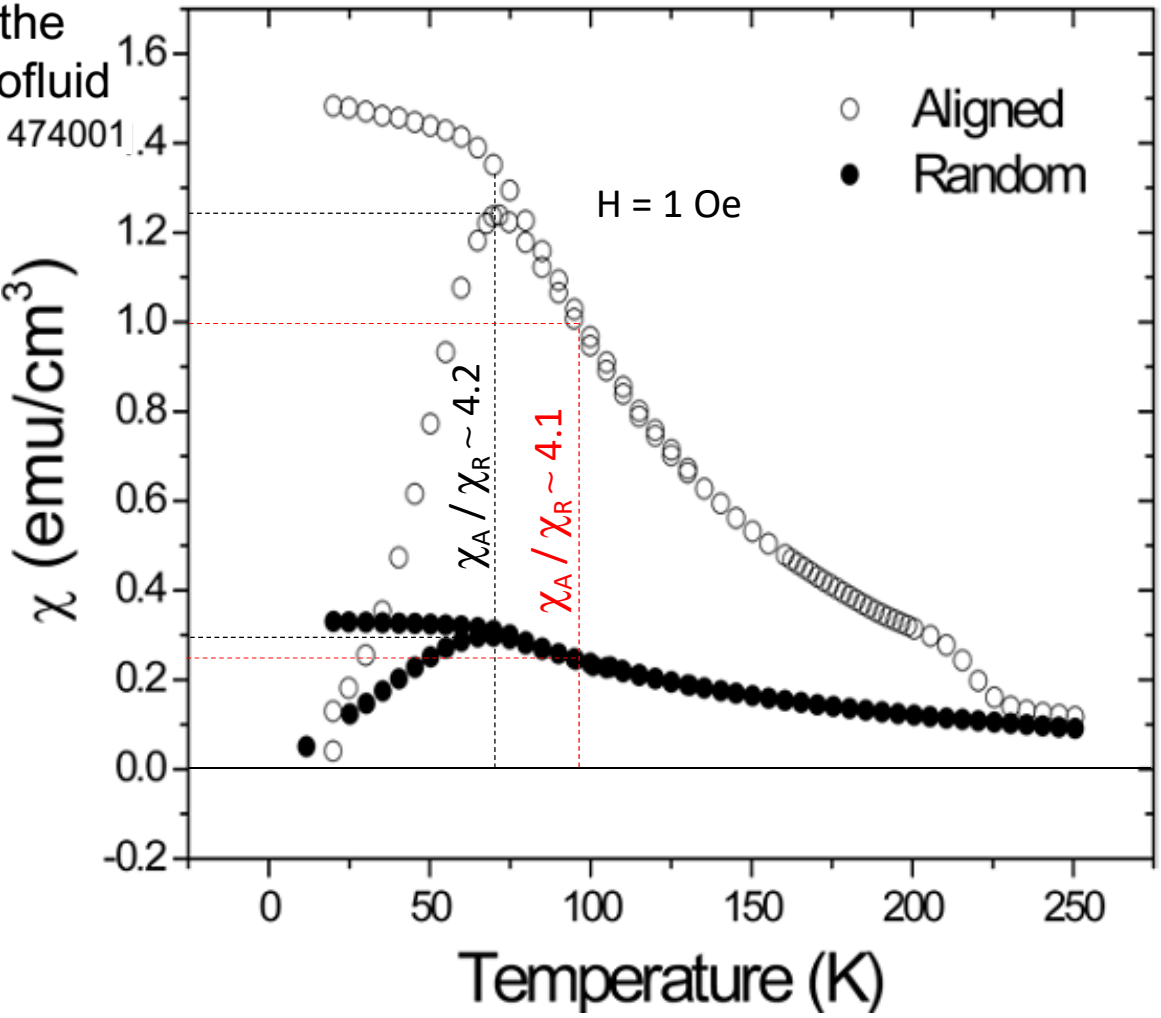

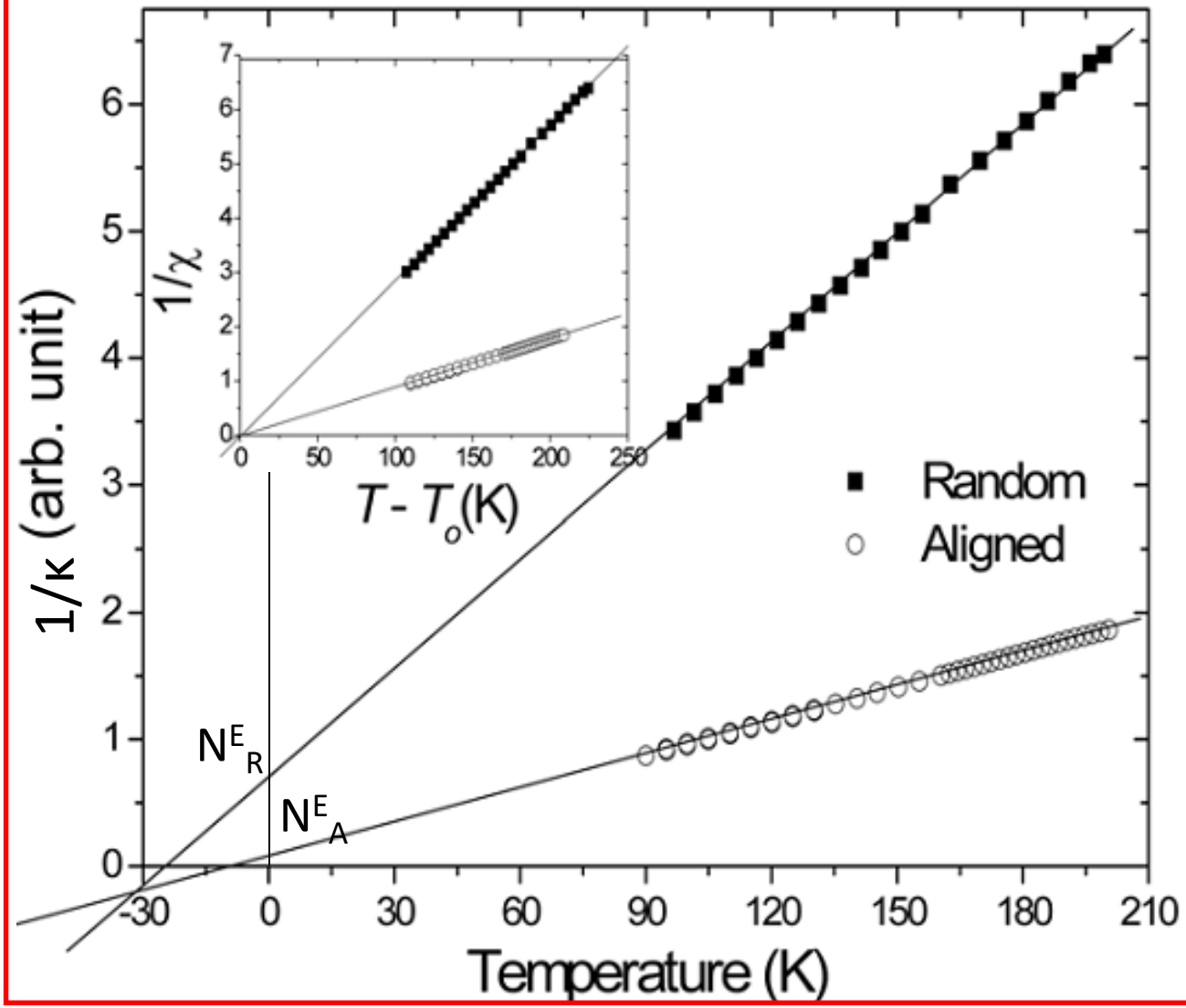

$$1/\kappa = 1/\chi + N^E$$

$$N^E_R > N^E_A$$

Menor energía magnetostática para ejes fáciles alineados

$$E_{me} = N^E V_s \mu_0 M^2/2$$

Magnetization behavior of ordered and high density Co nanowire arrays with varying aspect ratio

G. Kartopu,[1,a)] O. Yalçın,[2] M. Es-Souni,[1] and A. C. Başaran[3]

JOURNAL OF APPLIED PHYSICS **103**, 093915 (2008)

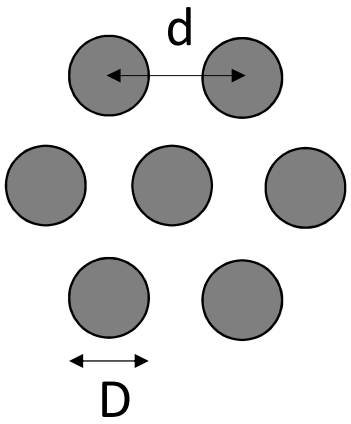

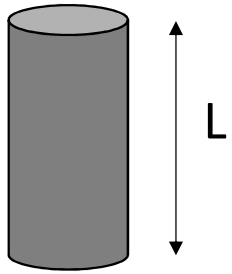

d = 105 nm

40 nm ≤ D ≤ 70 nm

200 nm ≤ L ≤ 10 µm

ϒ = d/D = 1/ρ

RA = L/D

5 ≤ RA ≤ 250

$$E_{\text{int}} = \frac{\mu_0 |\boldsymbol{\mu}_1||\boldsymbol{\mu}_2|}{4\pi r^3} S_2(\rho, m)$$

r = d

$$S_2(\rho,\tau) \approx \frac{1}{\tau^2}\left[\frac{2\tau^2\rho^2 - 1}{8(1+\tau^2\rho^2)^{5/2}} - \frac{2}{\rho^2\sqrt{1+\tau^2\rho^2}} + \frac{2}{\rho^2}{}_3F_2\left(\frac{1}{2},\frac{1}{2},\frac{2}{3};2,3;\rho^2\right)\right].$$

RA > 2

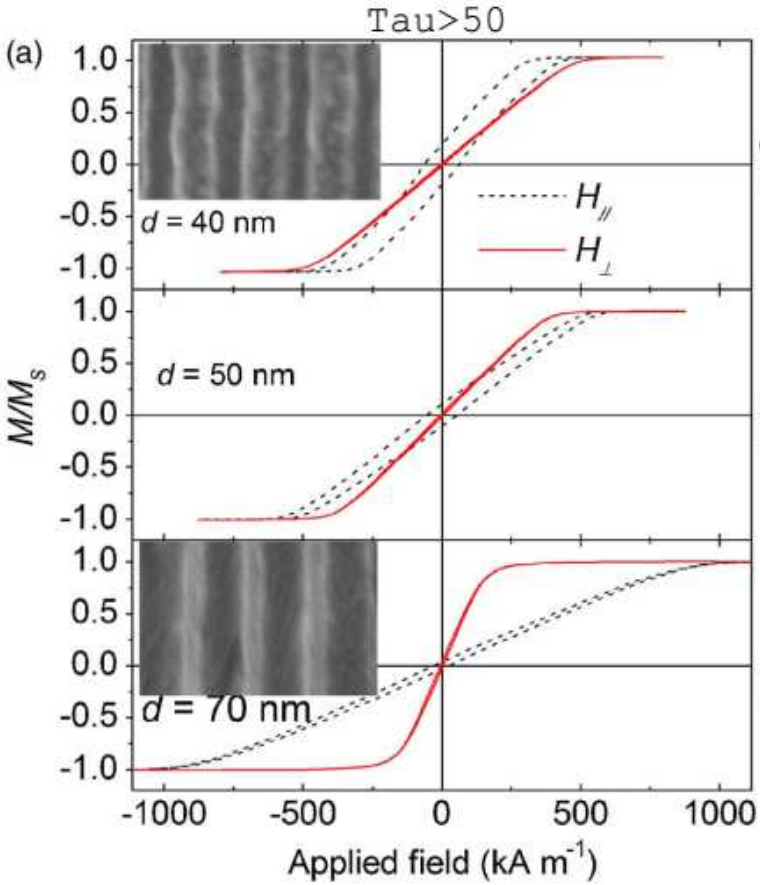

gamma=2.63
ro=0.381

gamma=2.1
ro=0.476

gamma=1.5
ro=0.667

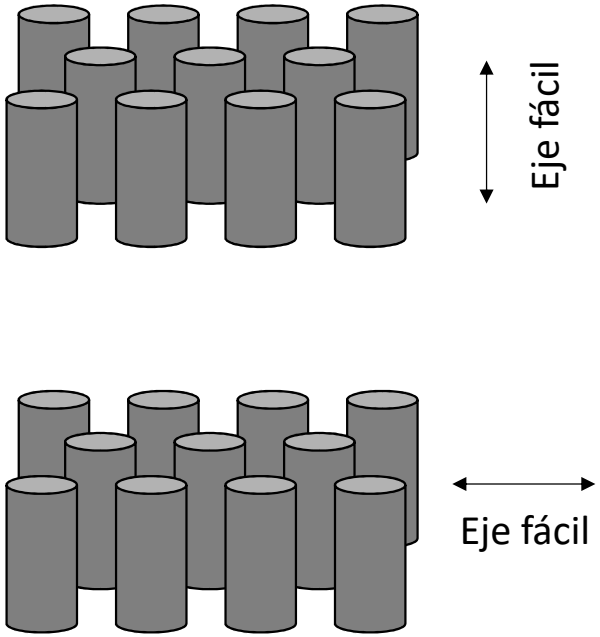

To sum up, it appears that a cooperative *reduction* of self- and macroscopic-demagnetization fields is the cause of observed magnetic behaviors with decreasing wire length L (or τ). Observations made in a small number of previous

Hexagonally ordered 100 nm period nickel nanowire arrays

K. Nielsch,[a] R. B. Wehrspohn, J. Barthel, J. Kirschner, and U. Gösel
S. F. Fischer and H. Kronmüller

Appl. Phys. Lett., Vol. 79, No. 9, 27 August 2001

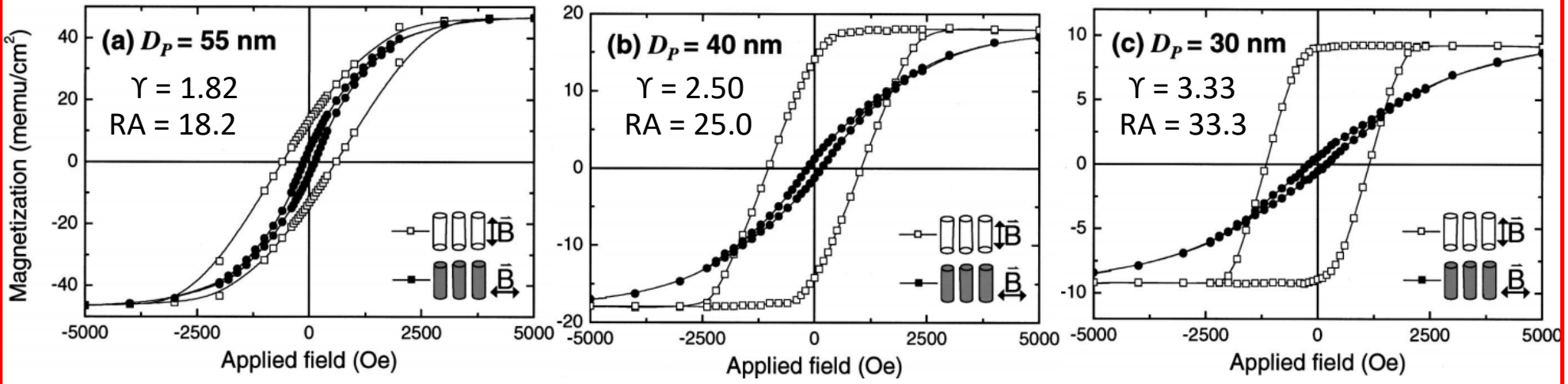

d = 100 nm

D =30, 40, 55 nm

L = 1 µm

AFM

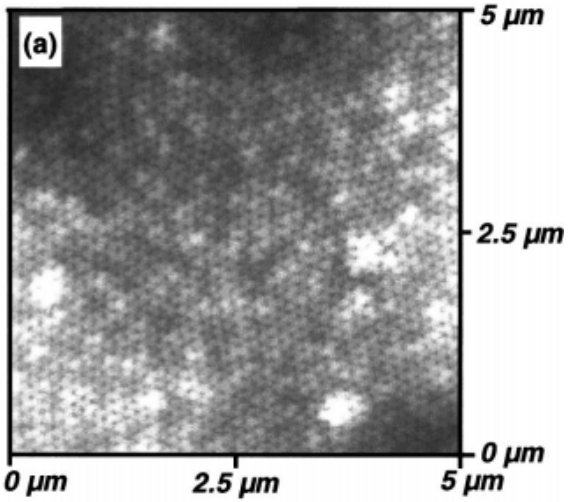

MFM

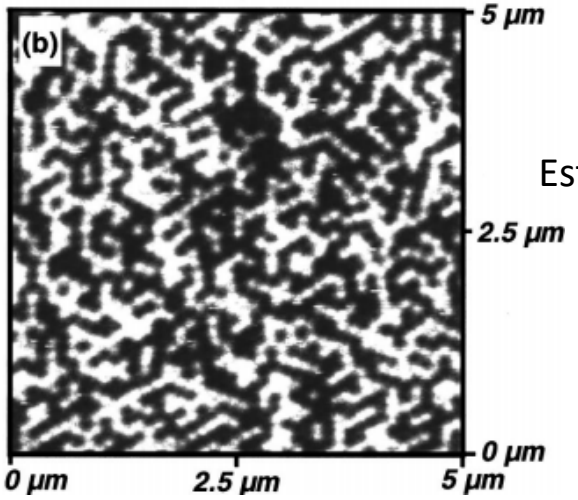

Estado desmagnetizado

Magnetic hysteresis in granular CuCo alloys

P Allia, M Coisson, P Tiberto, F Vinai and M Knobel J. Appl. Phys., Vol. 85, No. 8, 15 April 1999

Room-temperature hysteresis loops of granular $Cu_{100-x}Co_x$ alloys ($5 \leqslant x \leqslant 15$) obtained by planar flow casting in air and submitted to proper annealing treatments have been measured up to a field of 10 kOe by means of a vibrating sample magnetometer. In major loops ($|H_{vert}| = 10$ kOe), the reduced remanence-to-saturation ratio $m_r = M_r/M_s$ and the coercivity H_c measured on all studied materials appear to be related by an almost linear law of the type $m_r \approx 1/3\ (\mu H_c/kT)$, μ being the average magnetic moment on Co particles. A similar relation is also observed on minor symmetrical loops ($100\ \text{Oe} \leqslant |H_{vert}| \leqslant 9$ kOe). The observed results are accounted for by a model which considers the hysteresis as originating by magnetic interactions among nearly superparamagnetic Co particles.

¿Bloqueo o interacciones?

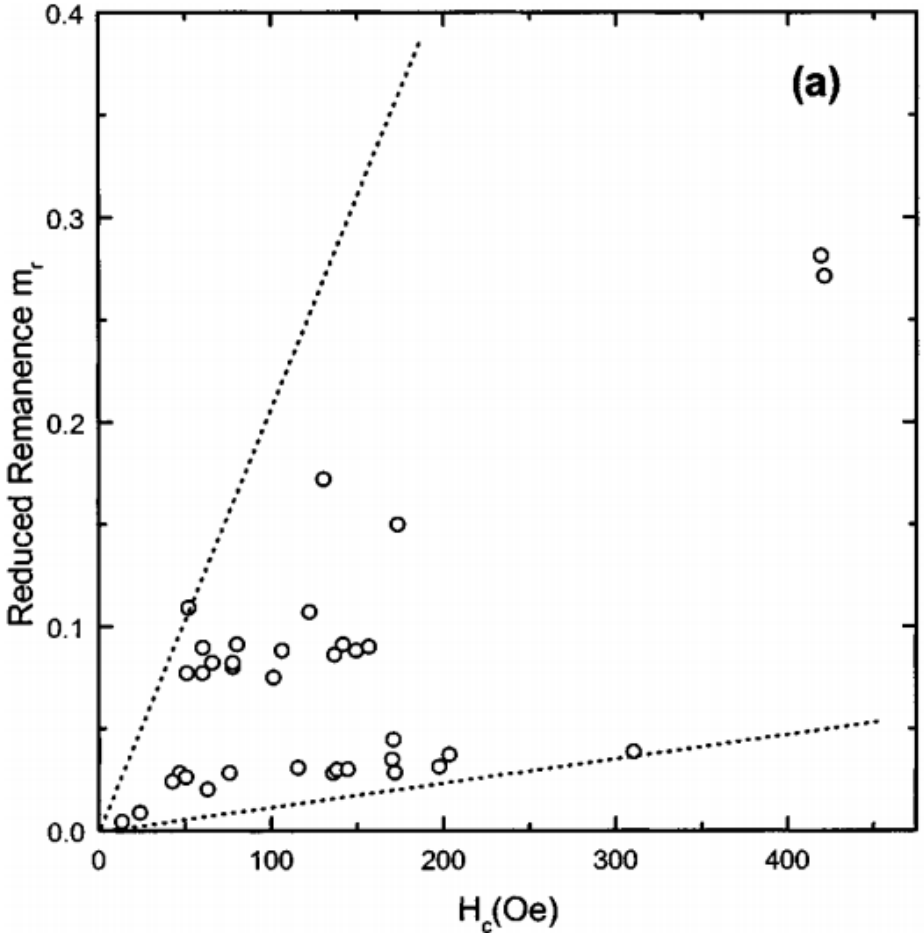

¿Bloqueo o interacciones?

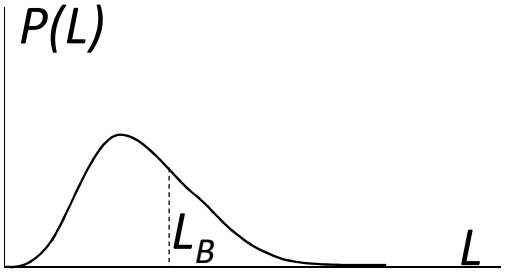

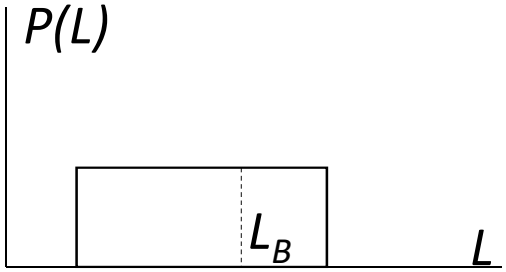

$$H_c = H_c^{\mathrm{MAX}} \int_{L_c}^{\infty} \left[1 - \left(\frac{L_c}{L} \right)^{1/2} \right] p(L)\,dL,$$

$$m_r = 0.5 \int_{L_c}^{\infty} p(L)\,dL,$$

$H^{MAX}{}_c = H_K = 2K/M_S$

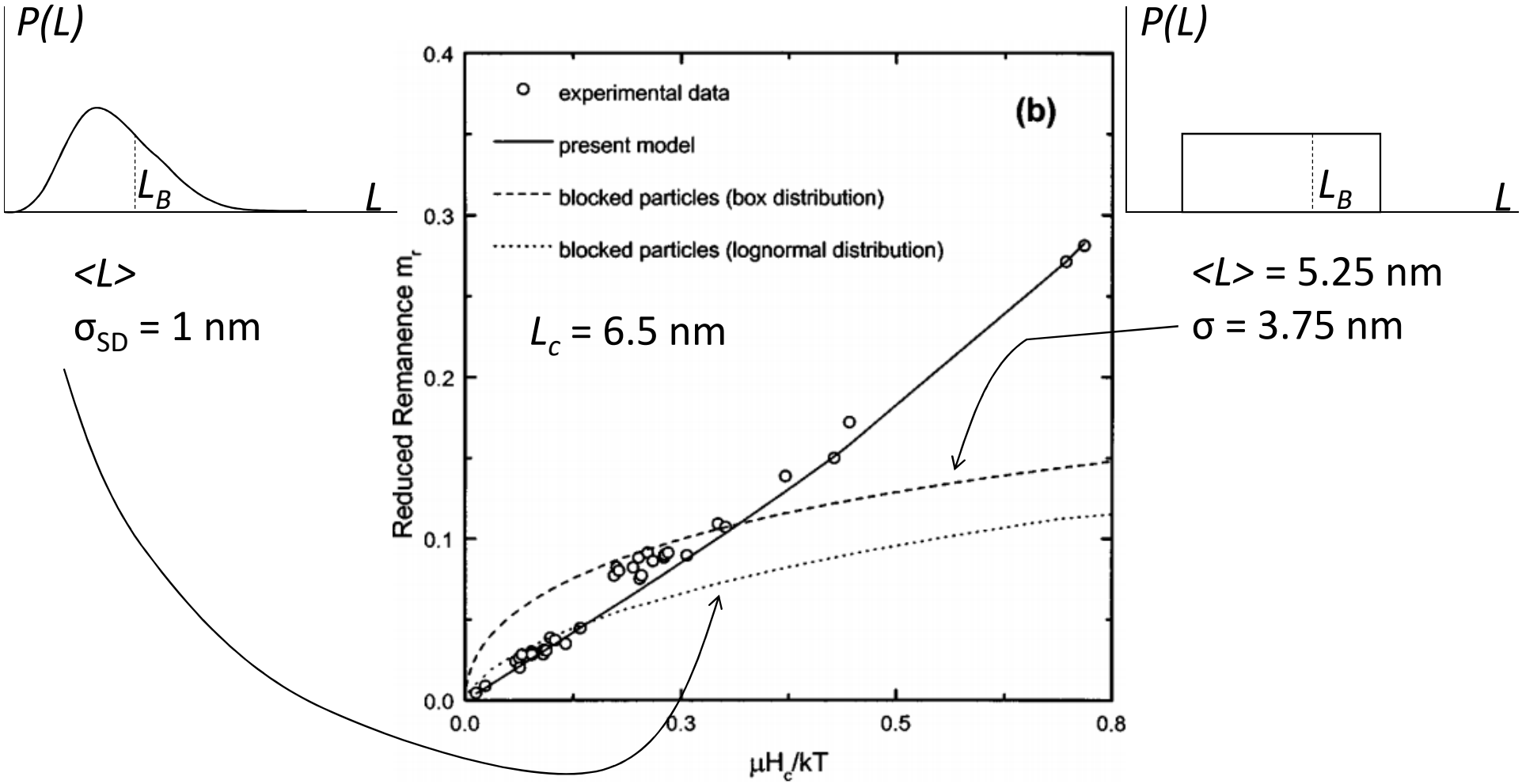
P(L)
L_B
L
<L>
σ_SD = 1 nm
experimental data
present model
blocked particles (box distribution)
blocked particles (lognormal distribution)
(b)
L_c = 6.5 nm
Reduced Remanence m_r
μH_c/kT
0.0
0.1
0.2
0.3
0.4
0.5
0.8
P(L)
L_B
L
<L> = 5.25 nm
σ = 3.75 nm

Modelo de campo medio

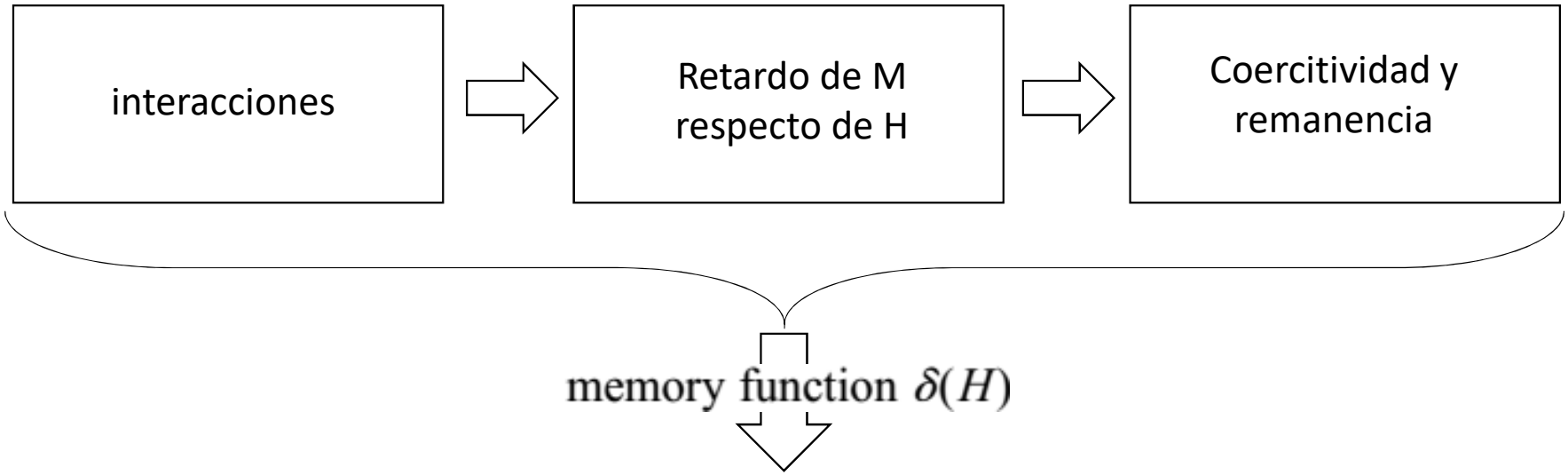

memory function $\delta(H)$

$$\delta(H) = \frac{\mu}{kT} H_{\text{int}}$$

$$H_{\text{int}} = \tilde{H}_0 [3(\langle u^2 \rangle - \overline{u}^2)]^{1/2}$$

$$\overline{u} = L(x)$$

$$\langle u^2 \rangle = 1 - 2L(x)/x$$

$$x = \mu H/kT$$

$H_{\text{int}}(H{=}0) = \tilde{H}_0$

$H_{\text{int}}(H \to \infty) = 0$

¿ $\begin{pmatrix} H_{\text{int}}(m=0) = \tilde{H}_0 \\ H_{\text{int}}(m=1) = 0, \end{pmatrix}$?

$$m_r = \frac{\frac{1}{3}\frac{\mu H_c}{kT}}{1 - \frac{3}{10}\left(\frac{\mu H_c}{kT}\right)^2} \sim \mu H_c/3kT$$

Correlación empírica

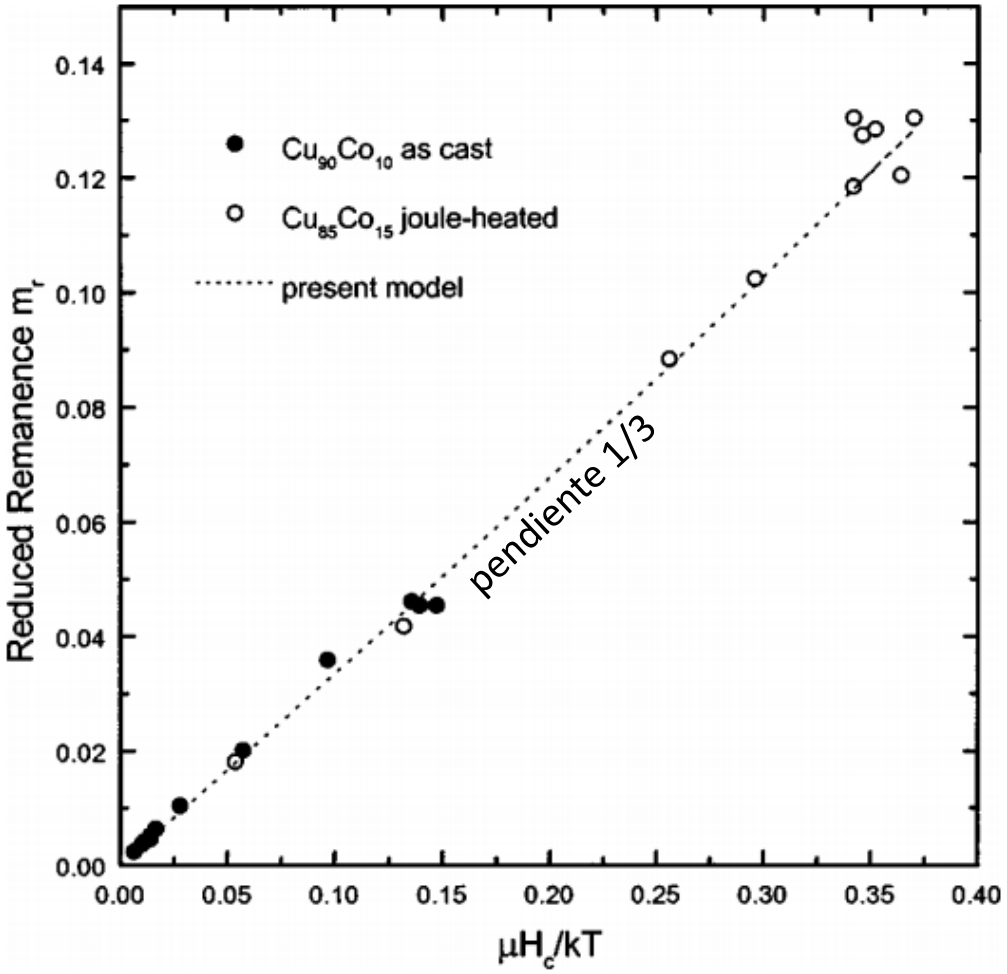

Algo que los autores no dicen…

$$m_r \sim \mu H_c / 3kT$$

$$\sqcap$$

$$m_r \sim M_r / M_S$$

$$\Downarrow$$

$$M_r \sim \mu M_S H_c / 3kT$$

$$\sqcap$$

$$M_S \sim \mu / V_{pp}$$

$$\Downarrow$$

$$\boxed{M_r / H_c \sim \mu^2 / V_{pp} 3kT = \chi_{rc}}$$

HYSTERETIC MAGNETISATION CURVES IN THE GRANULAR $Cu_{100-X}Co_X$ SYSTEM

P Allia, M Coisson, P Tiberto, and F Vinai

NanoStructured Materials, Vol. 11, No. 6, pp. 757–767, 1999

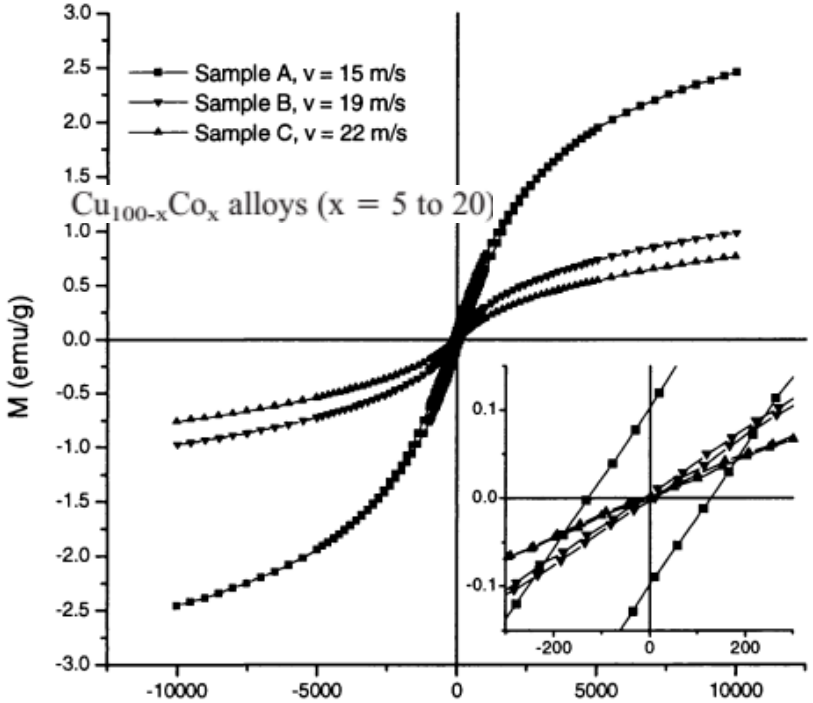

1. In the inset, the region close to the coercive field value is highlighted. All curves display both superparamagnetic and ferromagnetic features. The small area of measured loops and the unsaturating behaviour of the curves indicate a superparamagnetic behaviour. On the other hand, the ferromagnetic behaviour is evidenced by the non-zero values of remanence and coercivity (vanishingly small in the $Cu_{95}Co_5$ samples prepared with high quenching rate). These curves clearly indicate that the starting material is not an ideal solid solution of Co in Cu. The segregation of more Co particles improves the

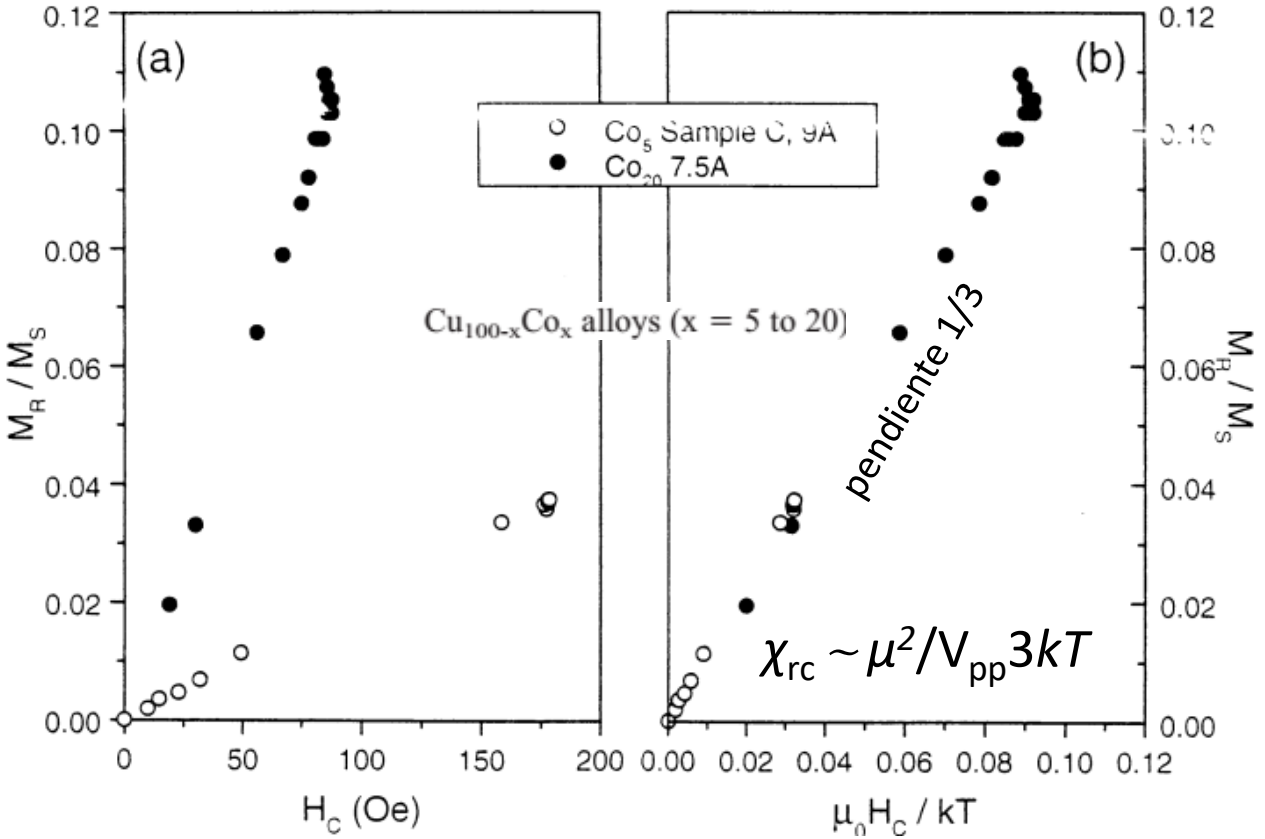

H_c ranging between 50 and 350 Oe and reduced remanence M_r/M_s ranging between 0.05 and 0.2 (M_S is the saturation magnetisation) [4]. These small values of both M_r/M_s and H_c lead one to consider hysteretic effects as truly minor and quite negligible, so that no efforts aimed to elucidate their nature

A Novel Representation of Hysteresis Loops

$$\sum = \frac{1}{2}[M_+(H) + M_-(H)] \qquad (1)$$

where $M_{\pm}$ refers to the upper (lower) loop branch, respectively. The function $\Sigma(H)$ is an odd function of H, taking the value $\Sigma = 0$ for $H = 0$; therefore, it is closely similar to an experimental anhysteretic curve, i.e., to the magnetisation curve obtained as the locus of the vertices of minor loops measured in sequence. As a matter of fact, the curve $\Sigma(H)$ turns out to be perfectly coincident (within the experimental errors, which are however very small in this case) with an anhysteretic curve obtained according to the above-mentioned experimental procedure. This result is reported in Figs. 7 and 8,

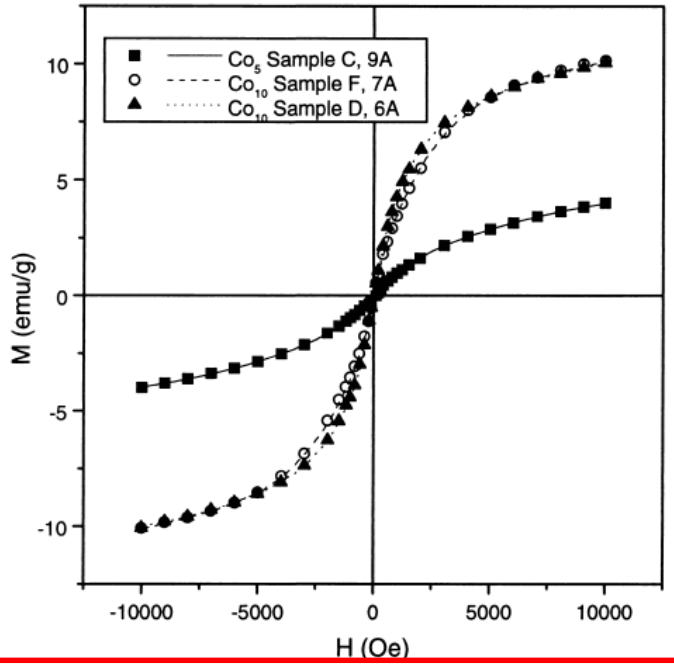

Curvas anhisteréticas

Líneas : Σ(H)
Símbolos: medidas tomadas de ciclos menores

Pueden analizarse con distribuciones de Langevin no desplazadas

On the other hand, the hysteretic character of these magnetisation curves is best evidenced by introducing another linear combination of the loops branches, i.e., the half-difference Δ:

$$\Delta = \frac{1}{2}[M_+(H) - M_-(H)] \qquad (2)$$

(1) Y (2) pueden reemplazarse por las cantidades normalizadas o reducidas

$$m = \frac{1}{2}[m_+(H) + m_-(H)]$$

$$\Delta_R = \frac{1}{2}[m_+(H) - m_-(H)]$$

$$m_{\pm} = M_{\pm}/M_s$$

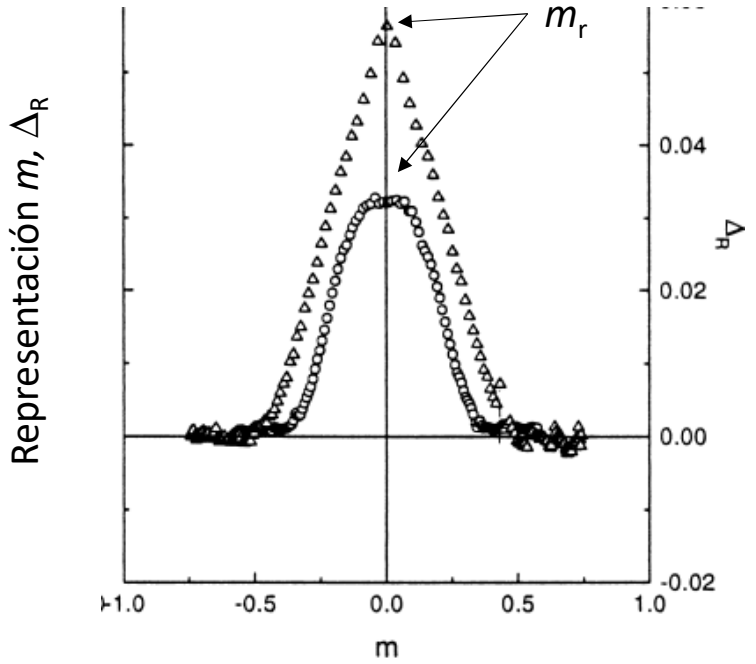

Magnetic hysteresis based on dipolar interactions in granular magnetic systems

P Allia, M Coisson, M Knobel, P Tiberto and F Vinai, 1999 PRB 60 12 207

The magnetic hysteresis of granular magnetic systems is investigated in the high-temperature limit ($T \gg$ blocking temperature of magnetic nanoparticles). Measurements of magnetization curves have been performed at room temperature on various samples of granular bimetallic alloys of the family $Cu_{100-x}Co_x$ ($x = 5-20$ at. %) obtained in ribbon form by planar flow casting in a controlled atmosphere, and submitted to different thermal treatments. The loop amplitude and shape, which are functions of sample composition and thermal history, are studied taking advantage of a novel method of graphical representation, particularly apt to emphasize the features of thin, elongated loops. The hysteresis is explained in terms of the effect of magnetic interactions of the dipolar type among magnetic-metal particles, acting to hinder the response of the system of moments to isothermal changes of the applied field. Such a property is accounted for in a mean-field scheme, by introducing a memory term in the argument of the Langevin function which describes the anhysteretic behavior of an assembly of noninteracting superparamagnetic particles. The rms field arising from the cumulative effect of dipolar interactions is linked by the theory to a measurable quantity, the reduced remanence of a major symmetric hysteresis loop. The theory's self-consistence and adequacy have been properly tested at room temperature on all examined systems. The agreement with experimental results is always striking, indicating that at high temperatures the magnetic hysteresis of granular systems is dominated by interparticle, rather than single-particle, effects. Dipolar interactions seem to fully determine the magnetic hysteresis in the high-temperature limit for low Co content ($x \leqslant 10$). For higher concentrations of magnetic metal, the experimental results indicate that additional hysteretic mechanisms have to be introduced. [S0163-1829(99)01037-1]

Representaciones

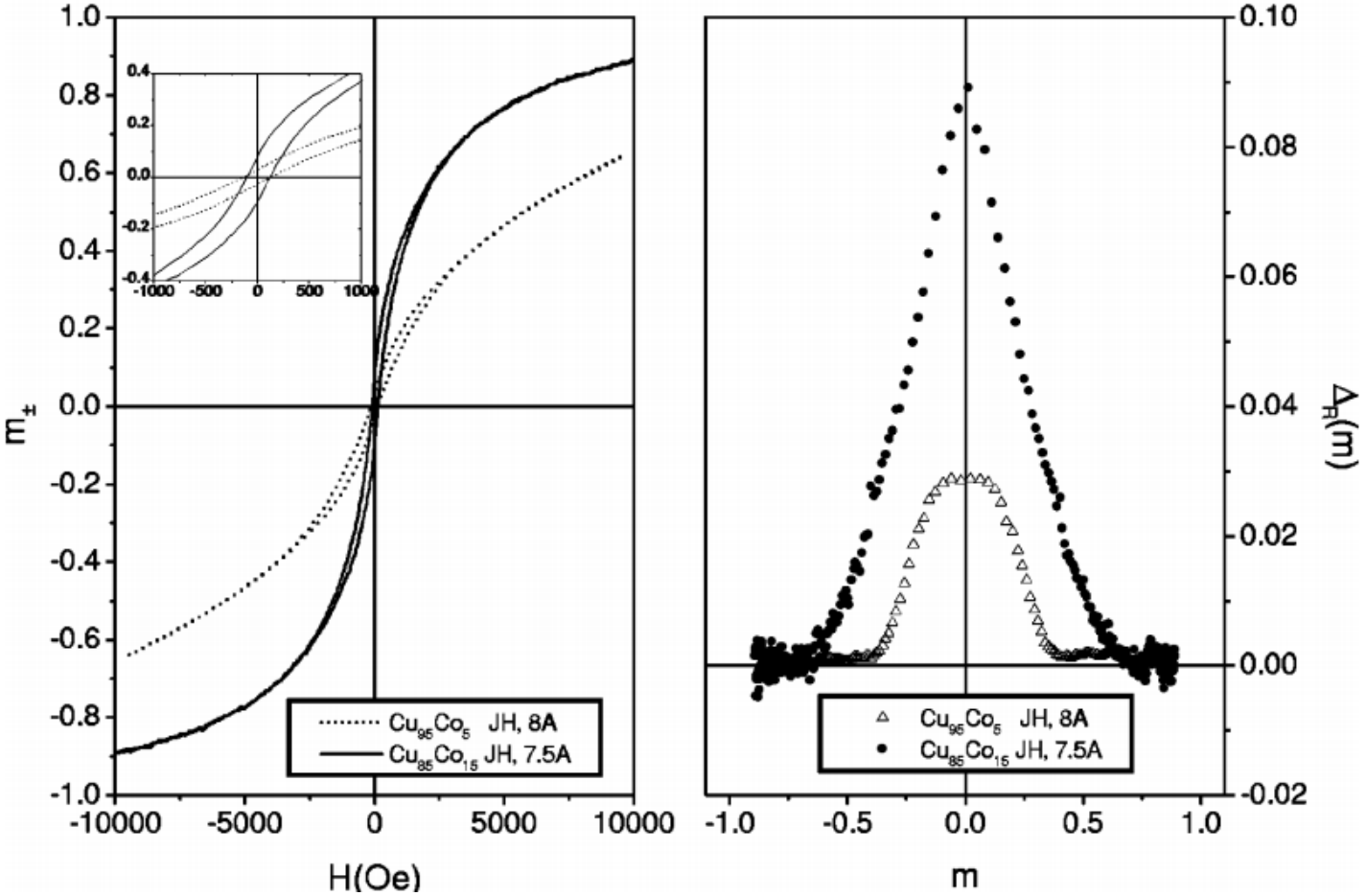

"memory function" $\delta(m, m_V)$

$$m_{\pm} = L\left(\frac{\mu H}{kT} \pm \delta(m_{\pm}, m_V)\right) \approx L\left(\frac{\mu H}{kT} \pm \delta(m, m_V)\right)$$

m es la magnetización reducida anhisterética

H_V campo vértice

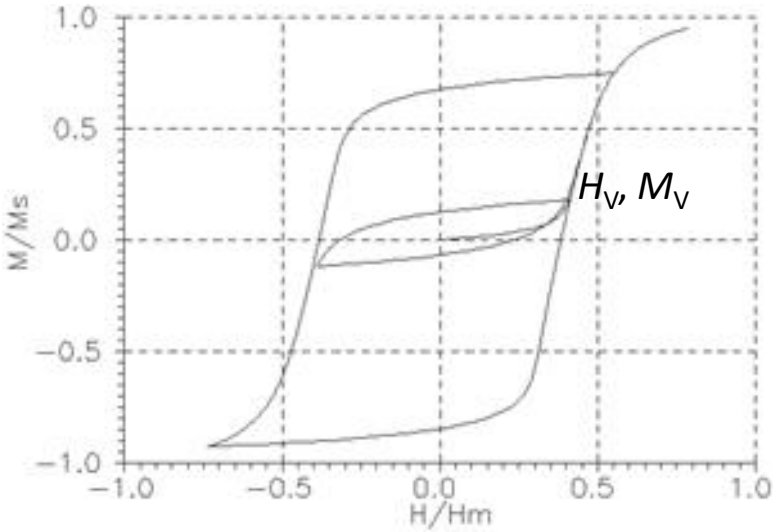

a) Se deben generar ciclos cerrados

b) δ debe ser mayor cuando los cambios de *m* con H son mayores

c) δ debe ser una función par de m, y hacerse cero cuando $H \rightarrow \pm\infty$ y $m \rightarrow \pm 1$

$$\delta(m, m_V) = \delta(m) - \delta(m_V), \quad |m| < |m_V|, \quad \delta(m) = 3\frac{dm}{dH}\Phi(m)$$

efecto de las Int. Dip.

$x = \mu H/kT$

$m = L(x) = u$

$dm/dH = (\mu/kT)\, dL(x)/dx = u'\,(\mu/kT) \rightarrow 3(dm/dH)_{H=0} = \mu/kT$

Componente z del campo dipolar en el sitio i

$$H_{iz}(t)=\sum_i A_{ij}\mu_{zj}(t)=\mu\sum_i A_{ij}u_j(t) \qquad A_{ij}=(3cos^2\theta_{ij}-1)/r_{ij}^3$$

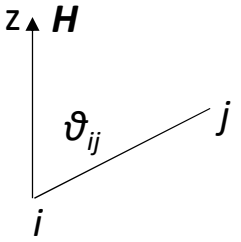

definimos

$$\Phi(m)\equiv\langle H_{zi}^2\rangle^{1/2}=\left(\sum_{jk} A_{ij}A_{ik}\langle u_j u_k\rangle\right)^{1/2}\mu$$

Raíz del campo cuadrático medio

$$\Phi(m)=\sqrt{3}\tilde{H}_o(\langle u^2\rangle-\langle u\rangle^2)^{1/2}$$
$$\equiv\sqrt{3}\tilde{H}_o(\langle u^2\rangle-m^2)^{1/2},$$

$$\tilde{H}_o=\mu(\tfrac{1}{3}\Sigma_j A_{ij}^2)^{1/2} \qquad \langle u^2\rangle=1-\frac{2L\left(\frac{\mu H}{kT}\right)}{\frac{\mu H}{kT}}$$

$$\delta(m,m_V)=3\sqrt{3}\,\frac{\mu\tilde{H}_o}{kT}\{u'(\langle u^2\rangle-m^2)^{1/2}$$
$$-u'_V(\langle u^2\rangle_V-m_V^2)^{1/2}\}$$
$$=\frac{\mu\tilde{H}_o}{kT}[F(m)-F(m_V)],$$

$$F(m)=3\sqrt{3}u'(\langle u^2\rangle-m^2)^{1/2}$$

$$F(0)=1,\ F(1)=0$$

Función "cutoff"

$\mu\tilde{H}_o/kT$ ~ 0.1 a RT

Algunas reflexiones sobre este modelo:

* El modelo apunta a entender la aparición de coercitividad a causa de las interacciones entre partículas. Este es un problema importante vinculado a la modificación de la respuesta temporal de los momentos a una dada excitación. Tiene probablemente el mismo origen que la variación del tiempo de relajación de NP.

* Este modelo ignora el efecto de las interacciones dipolares sobre la susceptibilidad del conjunto de NPs. No tiene en cuenta, por ejemplo, efectos desmagnetizantes. Tengo la impresión de que introduce un error importante porque para desarrollar la idea del "cutoffe" se basa en que el campo dipolar producido por una distribución espacialmente aleatoria de momentos alineados (uij =1) es nulo.

The time-dependent dipolar field acting on the ith site is given by Eq. (4). When all magnetic moments are aligned ($u_j = 1$) and are randomly distributed in space, H_{iz} is identically zero[33]

$$H_{iz}(t) = \sum_j A_{ij}\mu_{zj}(t) = \mu \sum_j A_{ij}u_j(t), \qquad (4)$$

$$A_{ij} = (3\cos^2\theta_{ij} - 1)/r_{ij}^3$$

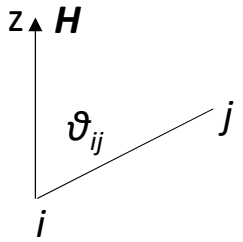

* Por otro lado un modelo de campo medio desmagnetizante que aproxime a **H**d como - **N**.**M** no da lugar a la aparición de coercitividad. Es posible que sea buena idea pensar en un modelo que combiene ambas Ideas, es decir, **H**d = - **N**.**M** $\pm$ **H**c F(σ_{SD}^2), donde el segundo término sea no nulo sólo en la vecindad de Hap = 0 pero tenga una justificación física correcta.

* Hay bastantes evidencias de que el procedimiento de efectuar la semisuma de las ramas de los valores experimentales de M vs. H para obtener una curva anhisterética

$$\Sigma = \frac{1}{2}[M_+(H) + M_-(H)]$$

es razonablemente correcto y posiblemente mejor que agregar al argumento de las funciones de equilibrio (Langevin, tanh) un término aditivo que describa la histéresis.

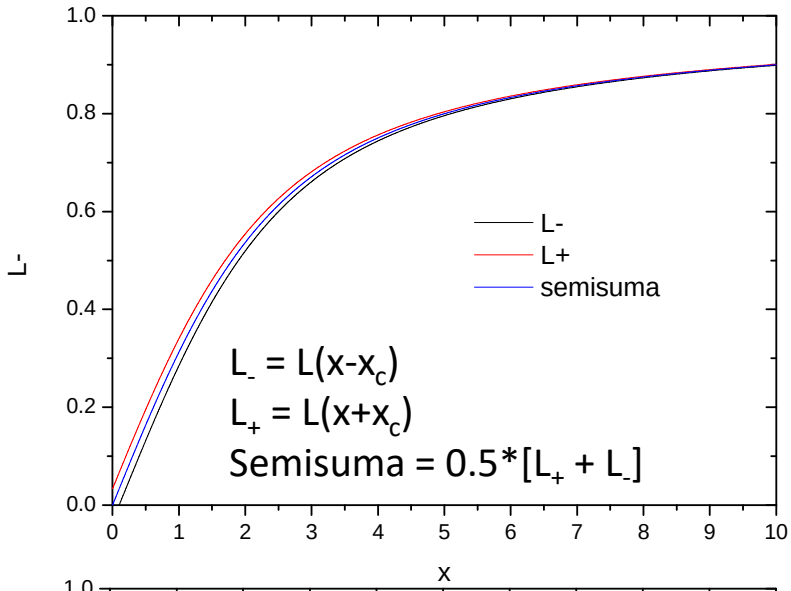
L-
L+
semisuma
$L_- = L(x-x_c)$
$L_+ = L(x+x_c)$
Semisuma = 0.5*[$L_+ + L_-$]
x

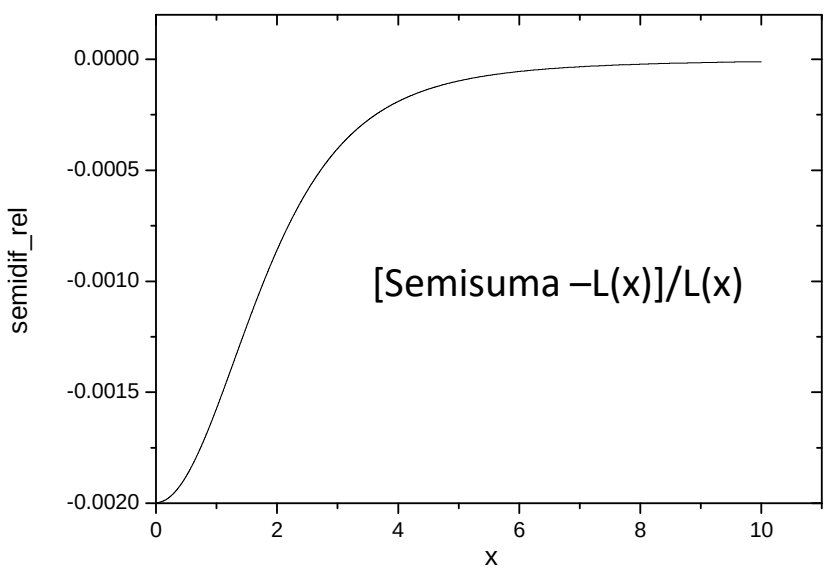
semidif_rel
[Semisuma –L(x)]/L(x)
x

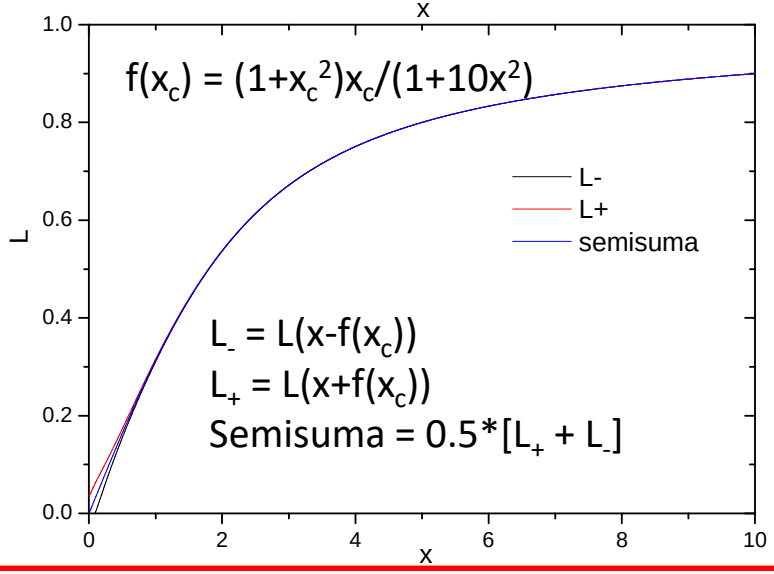
$f(x_c) = (1+x_c^2)x_c/(1+10x^2)$
L-
L+
semisuma
$L_- = L(x-f(x_c))$
$L_+ = L(x+f(x_c))$
Semisuma = 0.5*[$L_+ + L_-$]
L
x

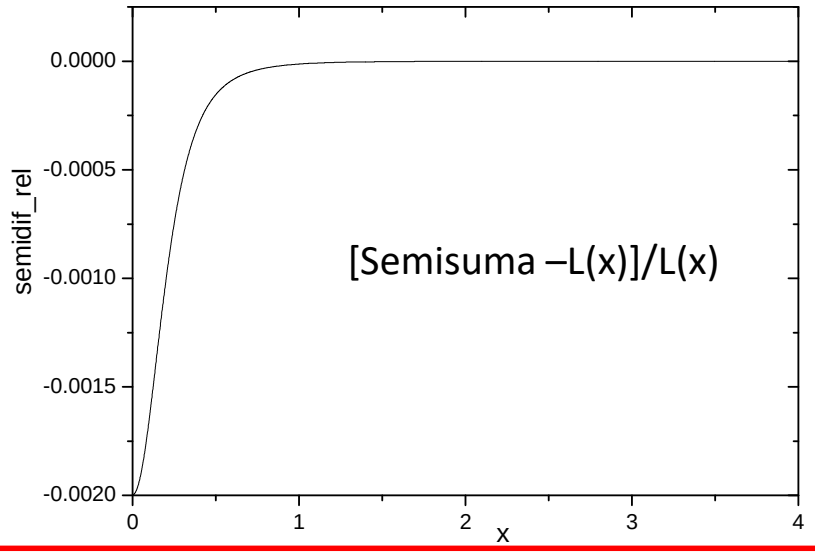
semidif_rel
[Semisuma –L(x)]/L(x)
x

The influence of a demagnetizing field on hysteresis losses in a dense assembly of superparamagnetic nanoparticles

S.A. Gudoshnikov [a,b,*], B.Ya. Liubimov [a], A.V. Popova [c], N.A. Usov [a,b]

Journal of Magnetism and Magnetic Materials 324 (2012) 3690–3694

below). The hysteresis loop measurements are carried out for magnetite nanoparticles with an averaged diameter $D=25$ nm in the frequency range $f=10$–150 kHz and for magnetic field amplitudes $H_0=100$–300 Oe. The results obtained demonstrate directly the dependence of the assembly hysteresis losses on the average demagnetizing factor of the whole sample. It is found that the SLP of the assembly diminishes approximately 4.5 times when the sample aspect ratio decreases from $L/d=11.4$ to $L/d\approx 1$, where L and d are the sample length and diameter, respectively. Evidently,

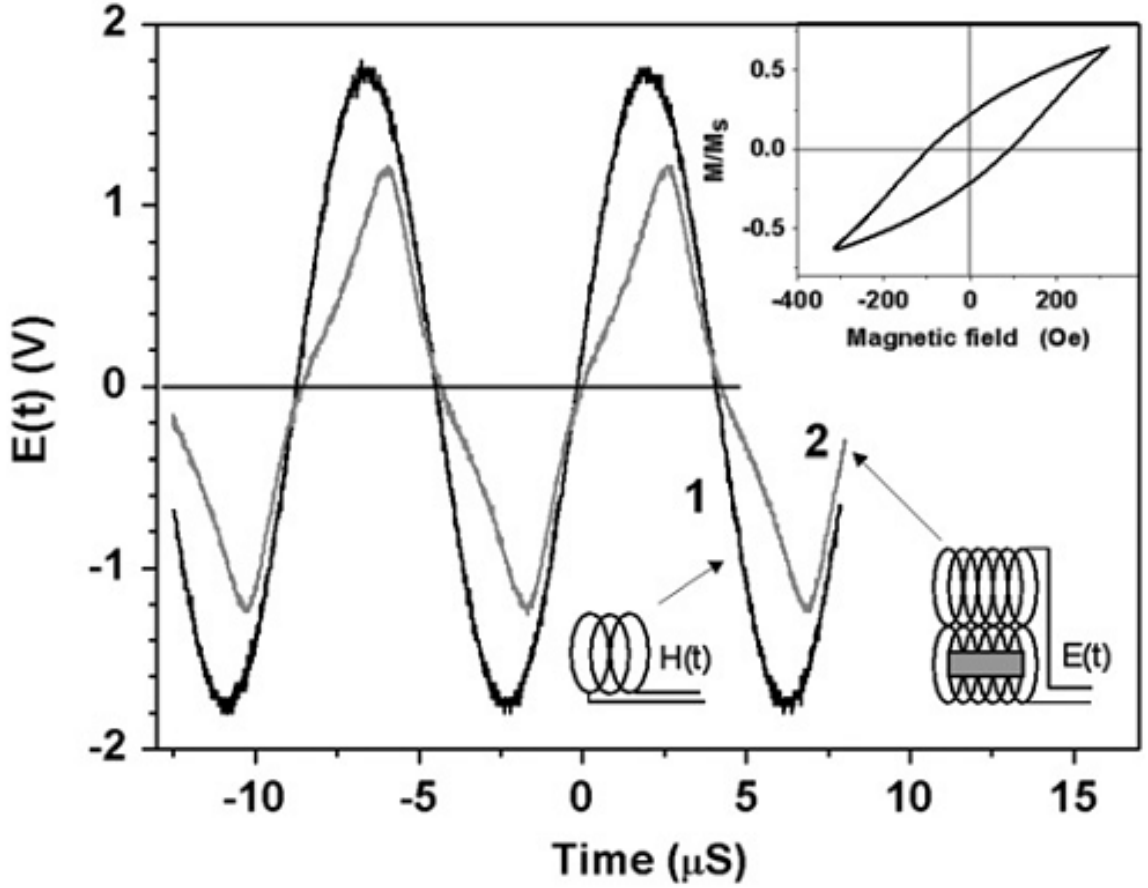

$f = 112$ kHz $H_0 = 280$ Oe $L/d = 5.9$

$$< MV > = \frac{cL_c}{4\pi N_c} \int E(t)dt$$

$$SLP = 10^{-7} \frac{f}{Q_m} \oint < MV > dH \ (W/g)$$

Magnetite nanoparticles were procured from Nanostructured & Amorphous Materials, Inc. [21]. The magnetite powder density was around 1 g/cm^3. The particles had nearly spherical shape and can be characterized by a log-normal size distribution with an average diameter $D=25$ nm and a dispersion $\sigma=0.3$. The powder x-ray diffraction confirmed that magnetite was the main crystalline phase. A quasistatic hysteresis loop of the assembly was zation of bulk magnetite, $M_s=80$ emu/g, is attributed to the presence of protected nonmagnetic layers at the particle surfaces.

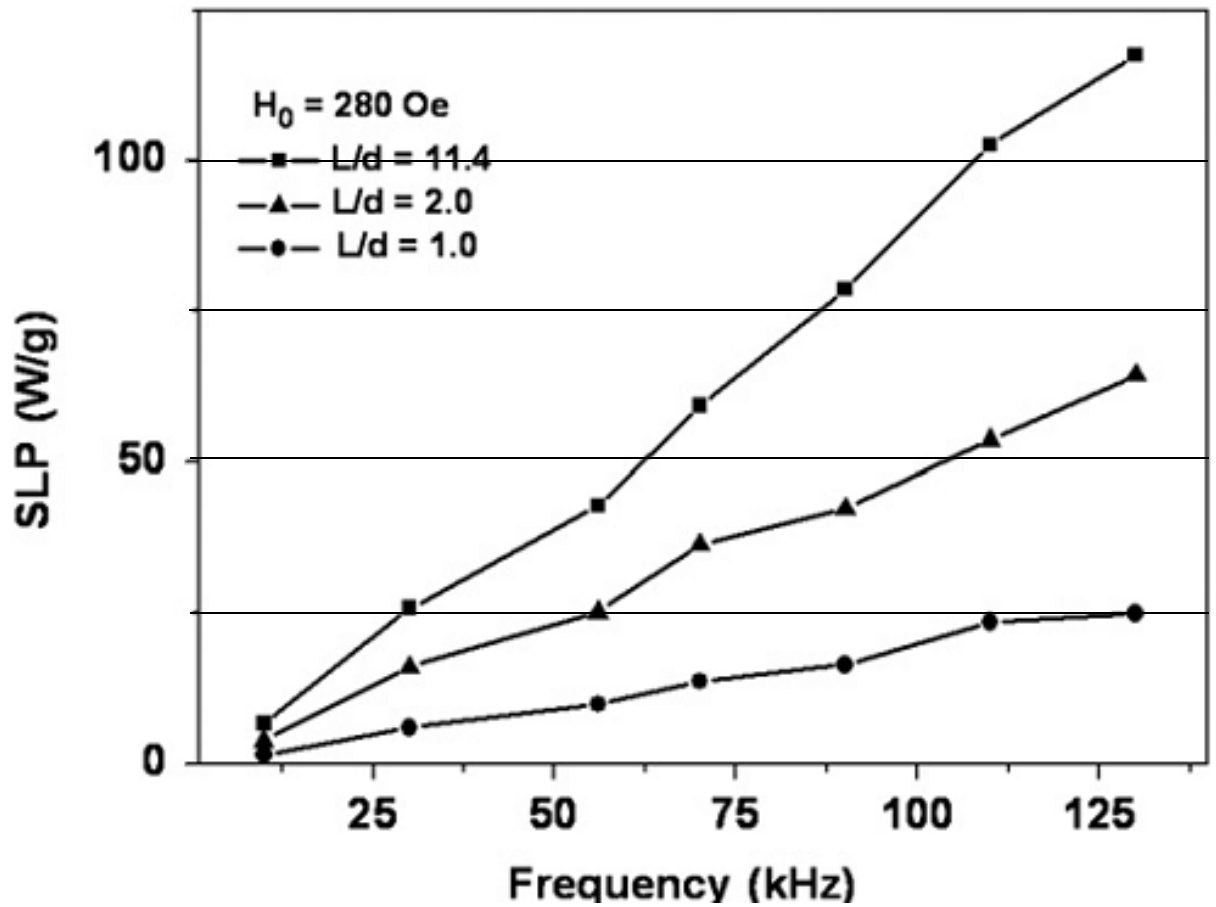
H_0 = 280 Oe
L/d = 11.4
L/d = 2.0
L/d = 1.0
SLP (W/g)
100
50
0
25
50
75
100
125
Frequency (kHz)

Interplay of dipolar interactions and grain-size distribution in the giant magnetoresistance of granular metals D. Kechrakos and K. N. Trohidou

PHYSICAL REVIEW B VOLUME 62, NUMBER 6 1 AUGUST 2000-II

At room temperature, which for most granular films is greater than the blocking temperature of the isolated particles, the magnetic configuration of the system is mainly ruled by the action of the magnetostatic interactions among the particles, while the effective anisotropy energy is of secondary importance.[21] The magnetostatic interactions tend to align the magnetic moments to form flux-closure loops and thus introduce short range ferromagnetic correlations in the ensemble of particles. In magnetic multilayers, the ferromag-

whole.[18,19] The Monte Carlo method used to obtain the magnetic structure and the thermal average of the conductivity is also presented in the same section. In Sec. III we present and discuss the numerical results for systems containing well separated particles (monodisperse) and systems containing clusters of coalesced particles (polydisperse). Finally, in Sec.

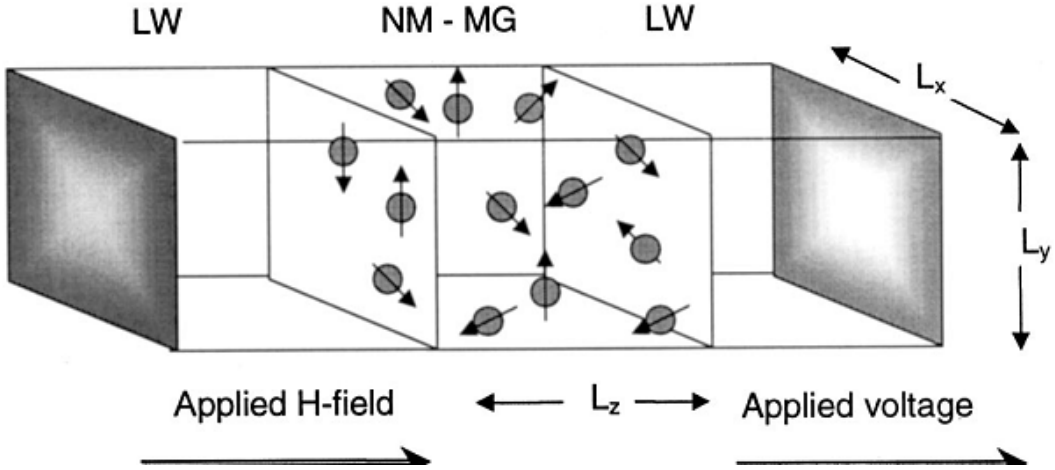

follows. We describe the magnetic granular system by an assembly of identical three dimensional classical spins (magnetic moments) located at random on the sites of a simple cubic lattice. The spins interact via dipolar magnetostatic forces. The total energy of the system reads

$$E=\sum_i \left[g \sum_j \frac{\hat{m}_i \cdot \hat{m}_j - 3(\hat{m}_i \cdot \hat{R}_{ij})(\hat{m}_j \cdot \hat{R}_{ij})}{R_{ij}^3} - h(\hat{m}_i \cdot \hat{H}) \right], \tag{6}$$

where m_i is the magnetic moment (spin) of ith particle, g is the dipolar strength, h is the Zeeman energy, and R_{ij} is the distance between particles i and j. Hats indicate unit vectors.

Dipolar interactions introduce an extra anisotropy to the system and consequently the assembly of dipolar interacting particle develops hysteretic behavior. One should therefore

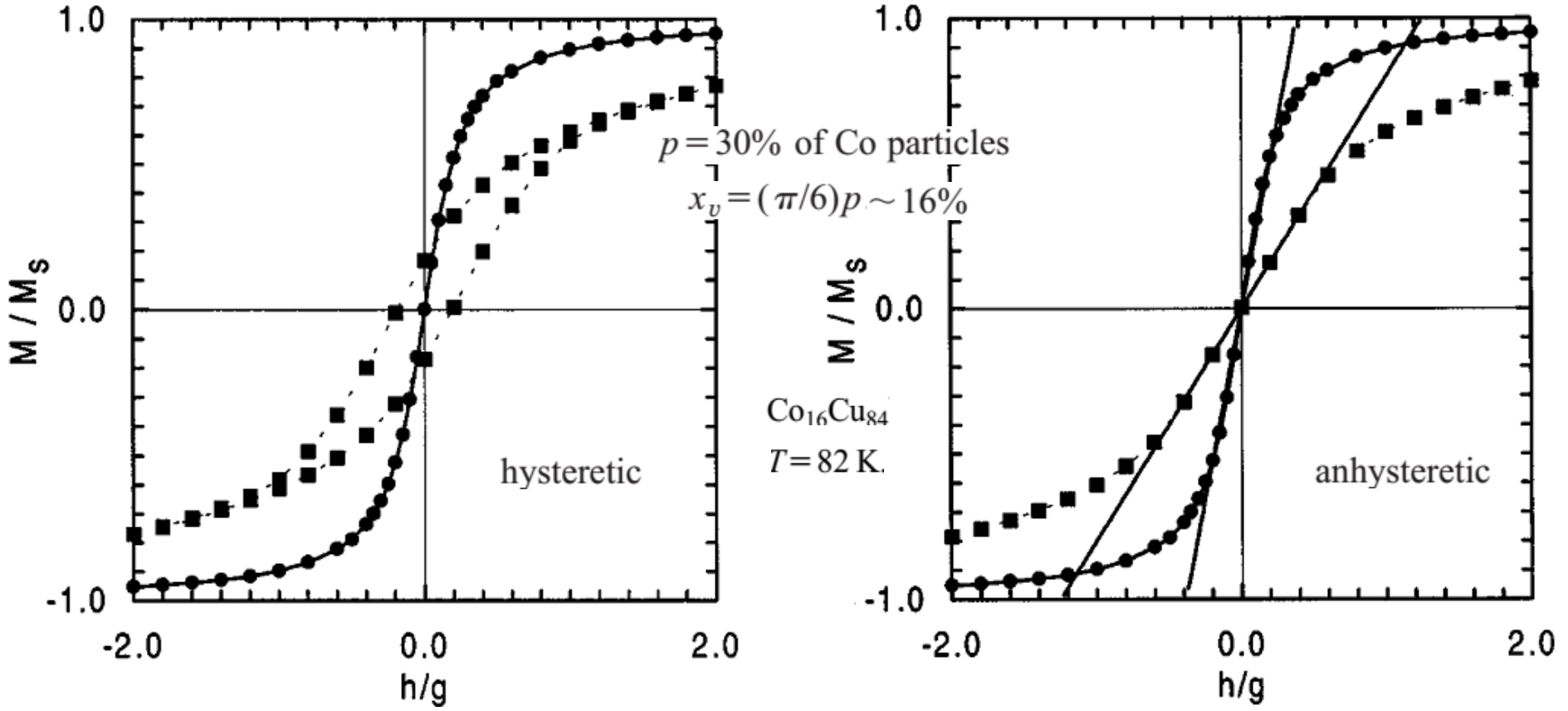

actions. A decrease of the initial susceptibility due to the presence of dipolar interactions is also observed (Fig. 3), from the value $x_0 \sim 9.3$ emu/Oe cm^3 for the noninteracting systems to the value $x_0 \sim 1.6$ emu/Oe cm^3 for the dipolar one.

Magnetic Nanoparticles Embedded in a Silicon Matrix

Petra Granitzer * and Klemens Rumpf *Materials* **2011**, *4*, 908-928; doi:10.3390/ma4050908

Abstract: This paper represents a short overview of nanocomposites consisting of magnetic nanoparticles incorporated into the pores of a porous silicon matrix by two different methods. On the one hand, nickel is electrochemically deposited whereas the nanoparticles are precipitated on the pore walls. The size of these particles is between 2 and 6 nm. These particles cover the pore walls and form a tube-like arrangement. On the other hand, rather well monodispersed iron oxide nanoparticles, of 5 and 8 nm respectively, are infiltrated into the pores. From their size the particles would be superparamagnetic if isolated but due to magnetic interactions between them, ordering of magnetic moments occurs below a blocking temperature and thus the composite system displays a ferromagnetic behavior. This transition temperature of the nanocomposite can be varied by changing the filling factor of the particles within the pores. Thus samples with

Formación de los poros

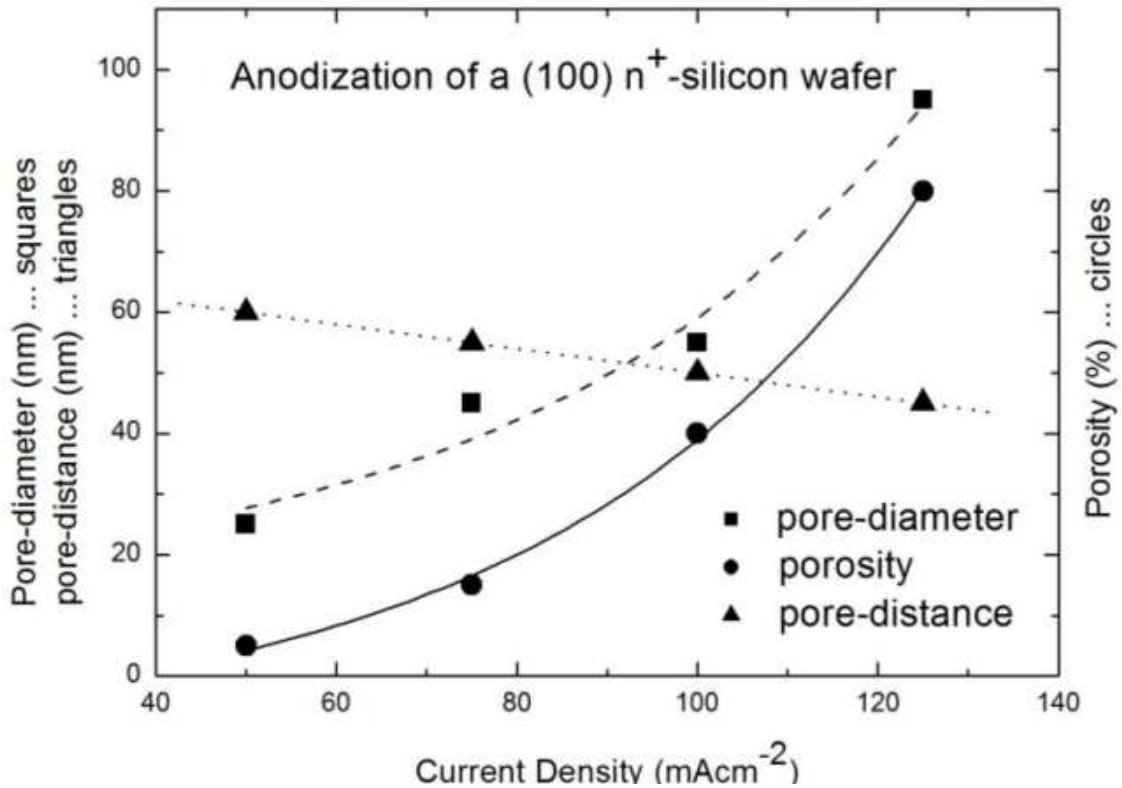

Cambio en susceptibilidad y bloqueo

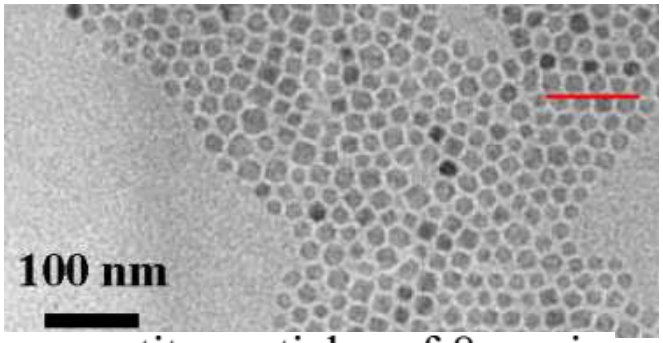

magnetite particles of 8 nm in size and an oleic acid coating of about 2 nm

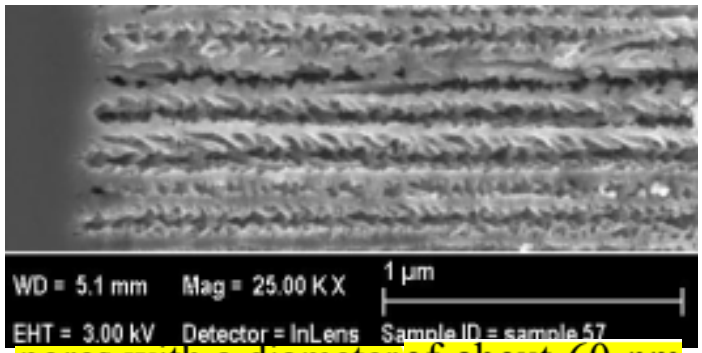

pores with a diameter of about 60 nm

Dpart=8nm
Dpore=40nm
t=4nm

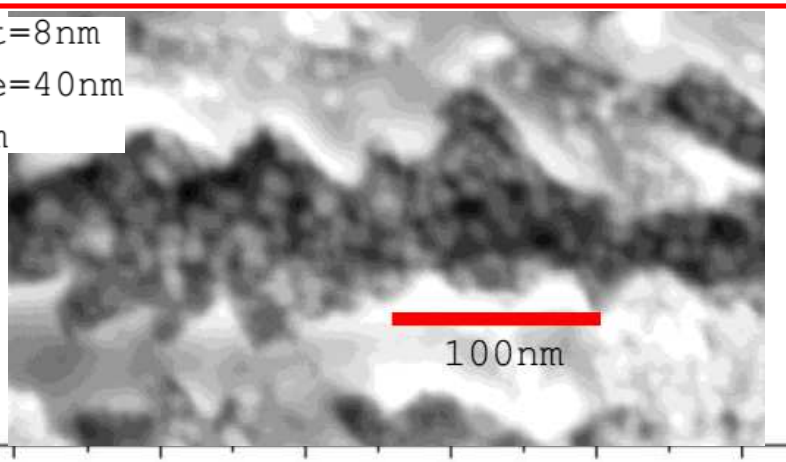

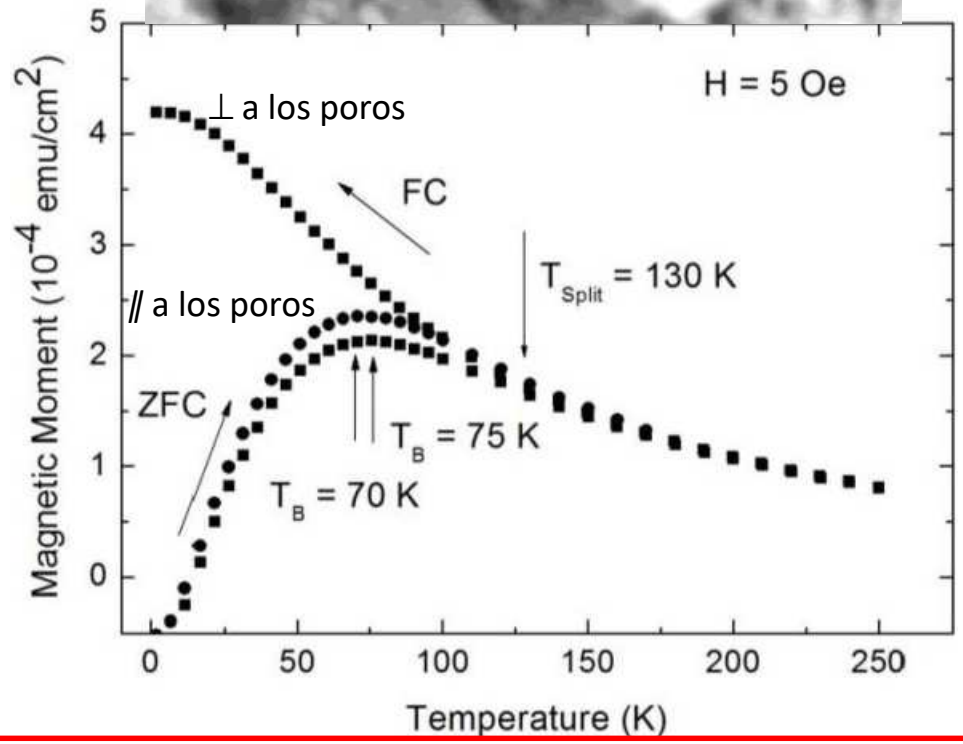

Cambio en susceptibilidad y bloqueo

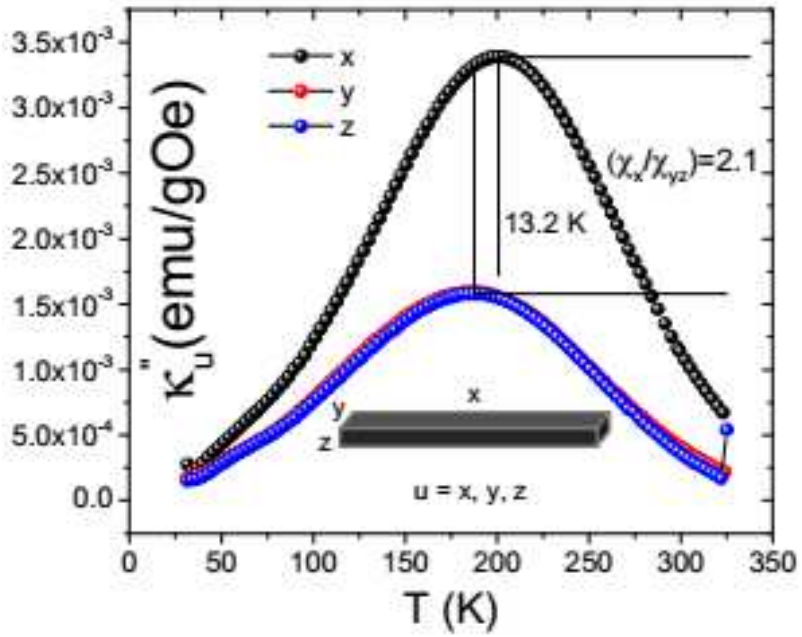

Size effects and interactions in $La_{0.7}Ca_{0.3}MnO_3$ nanoparticles

D.H. Manh[a,*], P.T. Phong[b], T.D. Thanh[a], D.N.H. Nam[a], L.V. Hong[a], N.X. Phuc[a]

Journal of Alloys and Compounds 509 (2011) 1373–1377

Table 1
Ordering temperature T_0, blocking temperature T_B and diameter values for all samples determined from Eqs. (4) and (5).

Samples	d_{total} (nm)	d_c (nm)	d_s (nm)	T_0 (K)	T_B (K)
S1	16	13	3	211.5	147
S2	35	31	4	247.9	138
S3	43	39	4	248.1	132
S4	73	68	6	248.9	116

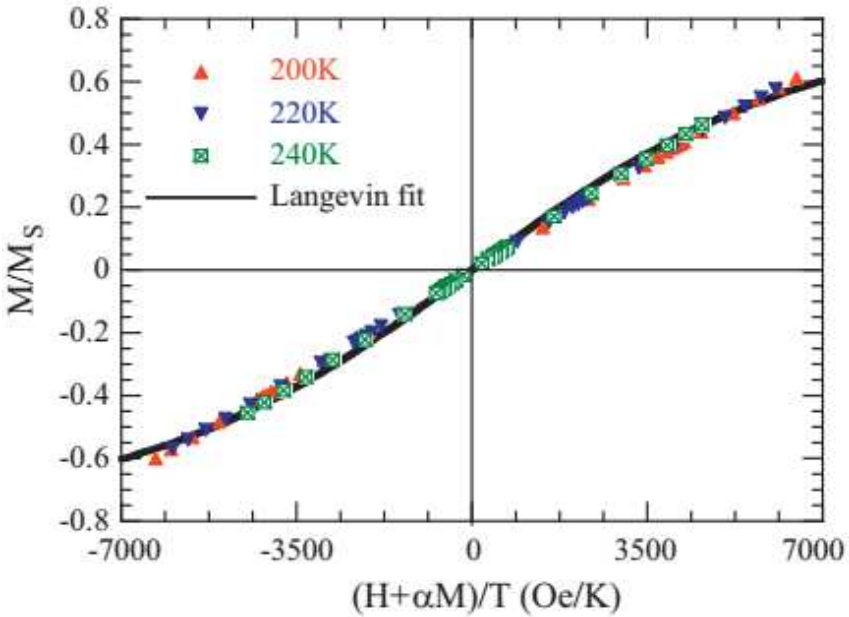

$$M(H,T) = M_S L\left(\frac{M_S \overline{m}[H_{ext} + \alpha M(H,T)]}{k_B T}\right)$$

masa media
De NP

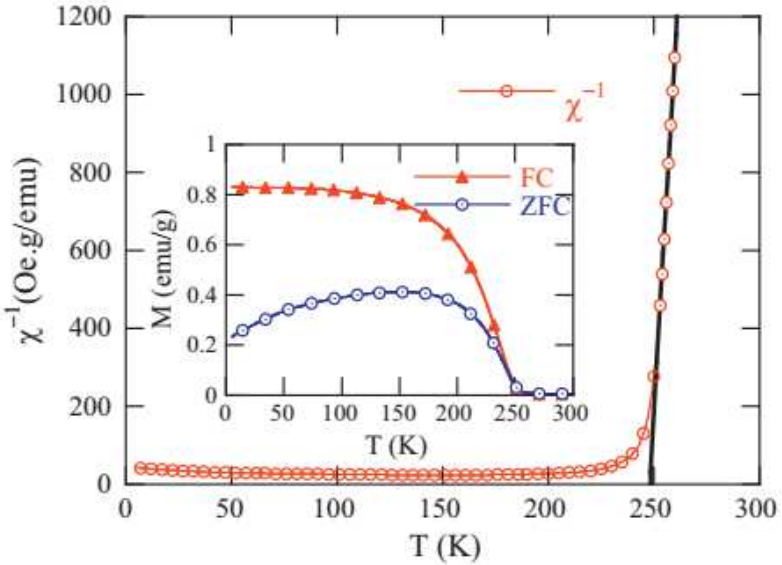

$$\begin{cases} \chi = \dfrac{M_S^2 \overline{m}}{3k_B(T - T_0)} \\ \dfrac{1}{\chi} = \dfrac{1}{C_S}(T - T_0) = \dfrac{1}{C_S}T - \alpha \\ C_S = \dfrac{M_S^2 \overline{m}}{3k_B} \end{cases}$$

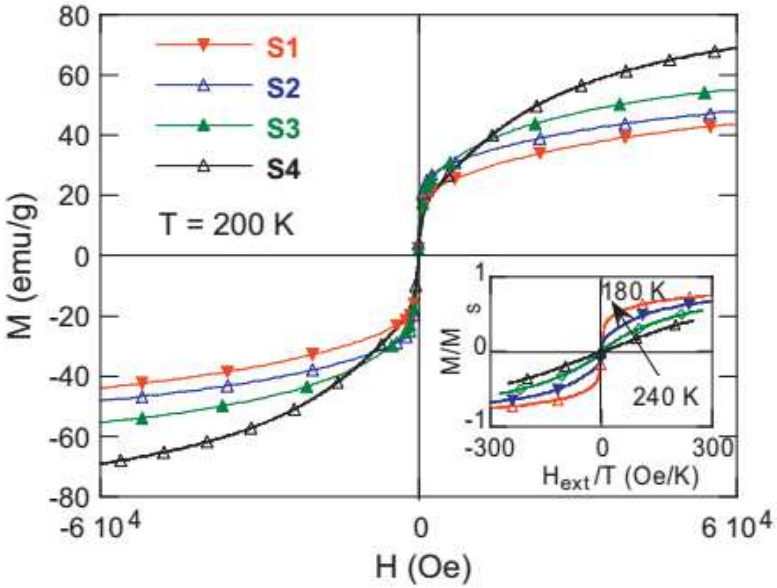

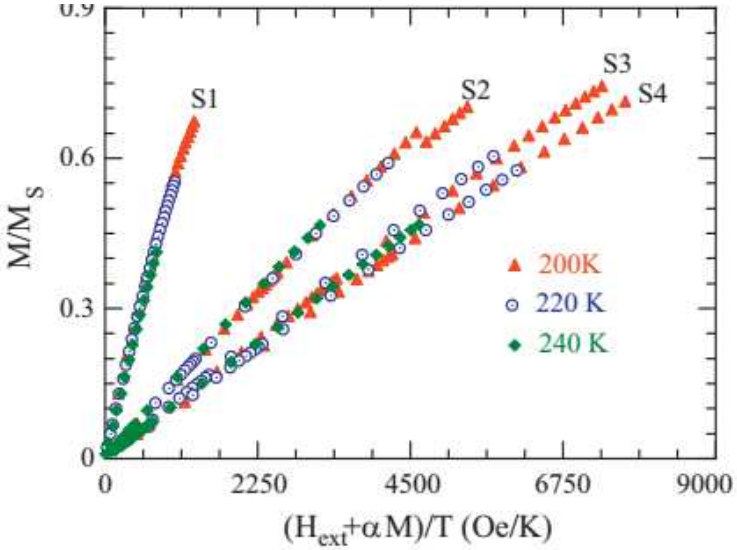

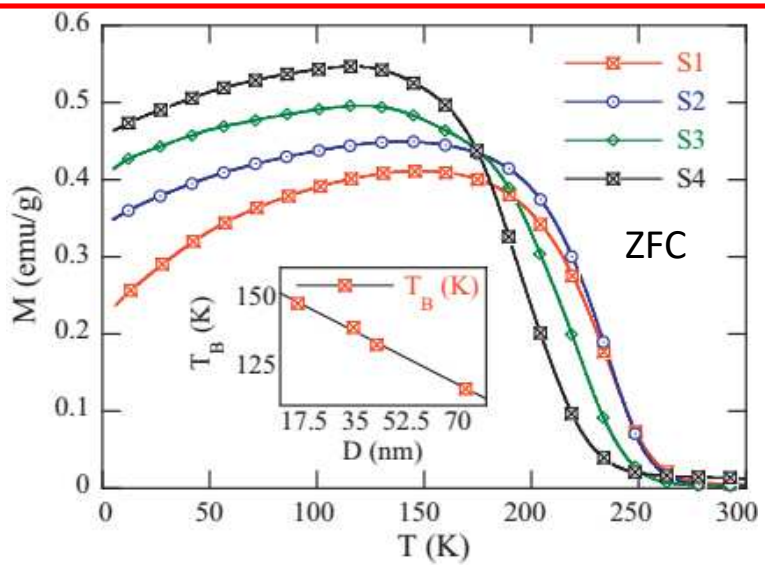

Some authors reported that the blocking temperature T_B decreases nomonotonically as the particle size decreases/or the milling time increases [13,18]. Morup [12] suggested that two magnetic regimes, governed by opposite dependencies of T_B, occurring due to interaction particles. In case of weak interaction, T_B signals the onset of a blocked state and T_B decreases as the interaction increase. In contrast, for strong interaction, a transition occurs from an SPM state to a collective state which shows most of the features of typical glassy behavior. In this case, T_B is associated with a freezing process and it increases with the interactions. The blocking temperature

Effective Demagnetizing Factors of Complicated Particle Mixtures

Ralph Skomski G. C. Hadjipanayis David J. Sellmyer

IEEE TRANSACTIONS ON MAGNETICS, VOL. 43, NO. 6, JUNE 2007

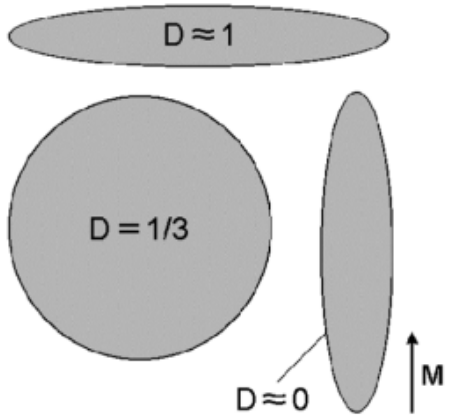

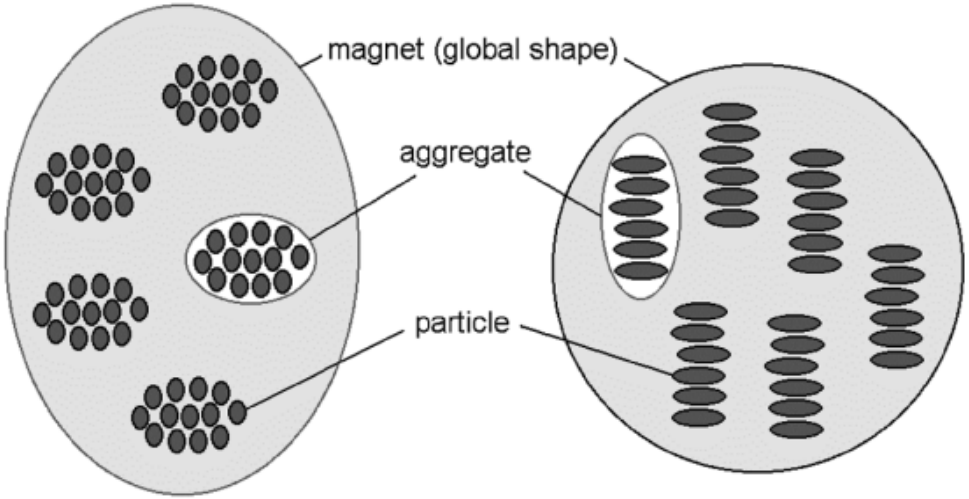

Partícula agregado global

$$D = D_{\mathrm{p}}(1 - f_{\mathrm{p}}) + D_{\mathrm{a}} f_{\mathrm{p}}(1 - f_{\mathrm{a}}) + D_{\mathrm{g}} f_{\mathrm{a}} f_{\mathrm{p}}$$

Configuration dependent demagnetizing field in assemblies of interacting magnetic particles

J M Martínez-Huerta[1], J De La Torre Medina[2], L Piraux[3] and A Encinas[1]

J. Phys.: Condens. Matter **25** (2013) 226003 (10pp)

nanowire samples

Material	Sample	Φ (nm)	P_N (%)	H_{eff} (kOe)	α_z (Oe)	P_m (%) experimental	M_s^* (emu cm^{-3})
Co	s1	39	4.8	7.65	400	4.63	1415
Co	s2	40	5.6	7.48	440	5.09	1406
Co	s3	30	3.9	7.57	240	2.91	1319
Co	s4	40	2.5	8.13	140	1.63	1360
Co	s5	30	3.9	7.77	362	4.08	1409
Co	s6	40	1.7	8.45	118	1.23	1396
Co	s7	30	4.2	7.68	370	2.85	1337
Co	s8	29	3.65	7.69	350	2.98	1343
NiFe	s9	30	3.46	4.64	140	3.19	816
NiFe	s10	40	3.4	4.45	180	3.58	792
NiFe	s11	35	8.8	5.62	580	7.87	1171
NiFe	s12	35	12	3.34	635	11.52	812
CoFe	s13	40	3.9	10.52	400	3.42	1868
CoFe	s14	29	5	10.24	640	5.23	1933
CoFe	s15	29	5	9.18	520	4.77	1706
CoFe	s16	18	10	8.45	1274	10.4	1953

diameter — FMR effective field — packing fraction P_m
packing fraction — dipolar interaction coefficient

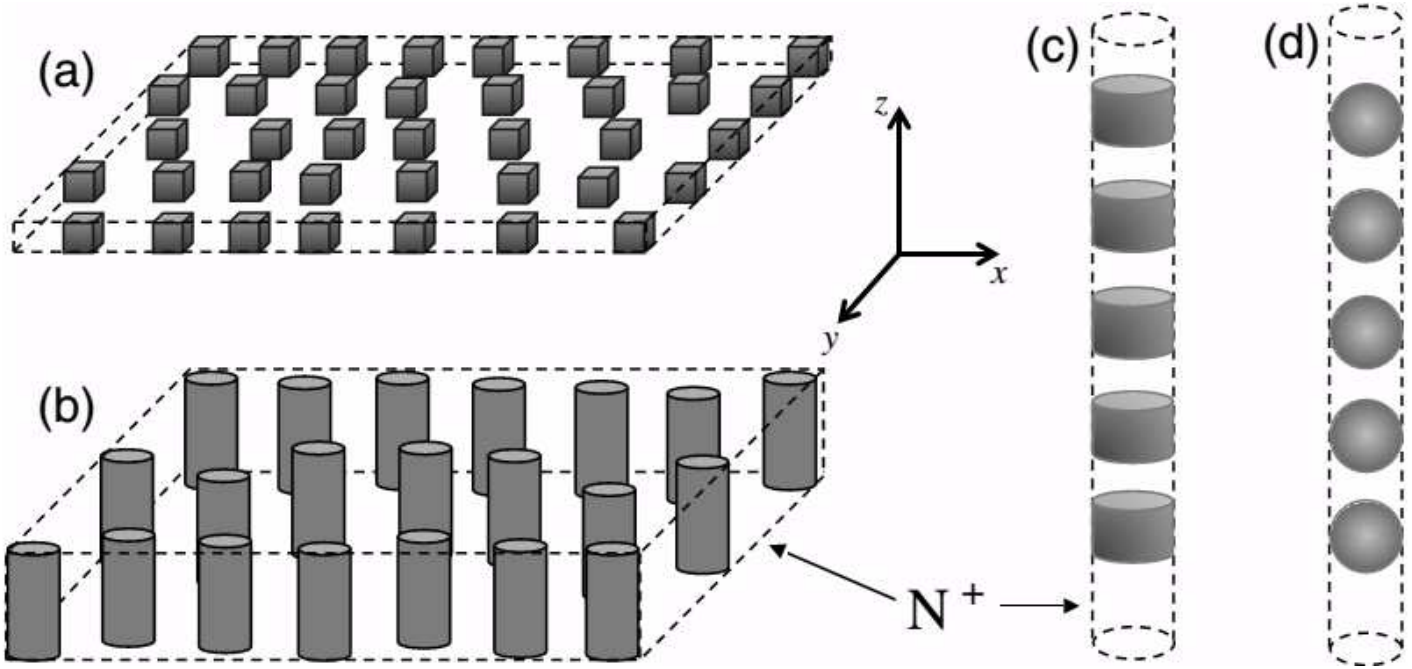
(a)
(b)
(c)
(d)
z
x
y
N +

energía

$$E = K_A \sin^2\theta + E_{int}$$

magnetostatic

$$K_A = K_{MC} + K_S + K_{ME}$$

Factores desmagnetizantes

packing fraction

inner demagnetizing factor

$$N_{eff} = N_T = (1 - P)N + PN^+$$

outer demagnetizing factor

$$N_T = N + (N^+ - N)P = N_{self} + N_{dip}$$

$$\mathrm{Tr}(N_T) = \mathrm{Tr}(N) + [\mathrm{Tr}(N^+) - \mathrm{Tr}(N)]P$$

$$\mathrm{Tr}(N_T) = 4\pi,$$
$$\mathrm{Tr}(N_{dip}) = 0.$$

Campo desmagnetizante en el estado saturado

$$H_T^{Di} = M_s N_i + (N_i^+ - N_i)M_s P \qquad H_{dip}^i = (N_i^+ - N_i)M_s P$$

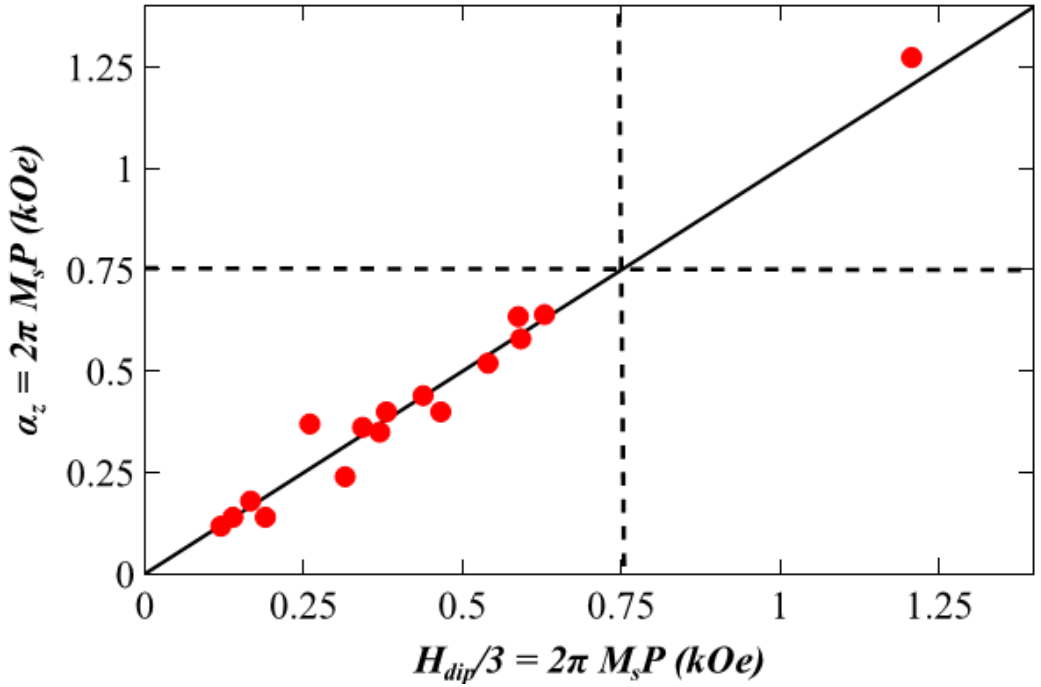

Figure 3. The easy axis component of the interaction field determined by magnetometry, $\alpha_z = 2\pi M_s P$, plotted as a function of $H_{dip}/3$, where $H_{dip} = 6\pi M_s P$ is the total interaction field measured by FMR in the saturated state, for all the nanowire samples listed in table 1.

FIN
(por ahora…)